Italian Journal of Agrometeorology
Rivista Italiana di Agrometeorologia

Anno 16 - n. 3 - Dicembre 2011

MODAMB - Environmental diagnostic model: description and application to a case study
Marianna Nardino, Federica Rossi, Teodoro Georgiadis pag. 5

Irregular Bearing and Climate in Olive
Guido Bongi, Claudio Ranocchia pag. 13

Influence of climate on durum wheat production and use of remote sensing and weather data to predict quality and quantity of harvests
Federico Guasconi, Anna Dalla Marta, Daniele Grifoni, Marco Mancini, Francesca Orlando, Simone Orlandini pag. 21

Comparison of phytophenological data: a proposal for converting between GFI and BBCH scales
Giovanna Puppi, Anna Letizia Zanotti pag. 29

Processing tomatoes under different irrigation regimes in Southern Italy: agronomic and economic assessments in a simulation case study
Michele Rinaldi, Pasquale Garofalo, Piero Rubino, Pasquale Steduto pag. 39

Periodico quadrimestrale dell'Associazione Italiana di Agrometeorologia (AIAM) - ISSN 2038-5625
Reg. Tribunale di Firenze n. 5221 del 4/12/2002

Editor in Chief (Direttore scientifico):
Simone Orlandini
Dipartimento di Scienze delle Produzioni Vegetali, del Suolo e dell'Ambiente, Agroforestale (DIPSA) - Università degli studi di Firenze Piazzale delle Cascine, 18 – 50144 Firenze (FI) Tel. +39 055 32 88 257 e-mail: simone.orlandini@unifi.it

Associate editor (Direttore scientifico aggiunto):
Luigi Mariani
Dipartimento di Produzione Vegetale – Università degli studi di Milano Via Celoria, 2 – 20133 Milano (MI)
Tel. +39 02 50 31 65 87 e-mail: luigi.mariani@unimi.it

Direttore responsabile:
Francesca Ventura
e-mail: francesca.ventura@unibo.it

Progetto grafico e Impaginazione:
Omega Graphics Snc - Bologna

Stampa:
LI.PE. Tipografia Persicetana, San Giovanni in Persiceto, Bologna, gennaio 2012

REDAZIONE,
ABBONAMENTI E PUBBLICITÀ
Pàtron Editore
Via Badini 12, 40057 Quarto Inferiore,
Granarolo dell'Emilia, Bologna
Tel. 051.767003 - Fax 051.768252
www.patroneditore.com
info@patroneditore.com

Presidente AIAM:
Federico Spanna
e-mail: federico.spanna@regione.piemonte.it

Consiglieri:
Marco Acutis, Roberto Confalonieri, Bruno Di Lena, Pierpaolo Duce, Simone Orlandini, Donatella Spano, Francesca Ventura

Revisori dei conti:
Giovanni Dal Monte, Vittorio Marletto, Luigi Pasotti

Segreteria AIAM:
Simone Falzoi, Emanuela Forni, Tiziana La Iacona, Mattia Sanna, Irene Vercellino
e-mail: segreteria@agrometeorologia.it

Sede operativa:
c/o Regione Piemonte – Settore Fitosanitario
Via Livorno, 60 – 10144 Torino Tel. 011-4324770, 4323706
Fax 011-4323710

Sede legale:
via Caproni, 8 - 50144 Firenze

***web:* www.agrometeorologia.it**
***e-mail:* ijagrometeorology@agrometeorologia.it**

ABBONAMENTI
Abbonamento € 40,00 (estero € 53,00)
Fascicoli arretrati € 15,00 (estero € 19,00)
Versamento sul c.c.p. n. 000016141400 intestato all'Editore
abbonamenti@patroneditore.com

La rivista è spedita gratuitamente ai soci AIAM. La quota associativa all'AIAM per il 2011 è fissata in € 60,00 per i soci singoli ed in € 300 per gli enti.

The presentation of this issue of Italian Journal of Agrometeorology (IJAm) gave me the inspiration, once again, to emphasize the broad range of arguments object of interest for the agrometeorological community. Crop protection, natural hazard, phenology, climate change, modeling, water management, remote sensing, yield quality and quantity represent a clear example of this, and furthermore, of the topical interest of our publications.

Agrometeorological studies are always inspired by the aim of giving concrete answers to the farmers and the potential group of end users and stakeholders. Studies try to give solution to problems and they are always updated to take into account that the modification of the environmental conditions determine both new needs for the farmers and the requirement of new solutions.

Recently many Italian regions were devastated by floods, following several months of drought. Summer was characterized by severe heat waves. At the same time the estimates of Carbon Dioxide Information Analysis Center (http://cdiac.ornl.gov/trends/emis/perlim_2009_2010_estimates.html) show that 2010 was by far a record year for CO_2 emissions from fossil-fuel combustion and cement manufacture. Globally 9,139 Teragrams of oxidized carbon (Tg-C) were emitted from these sources. I think that these data don't need any further comment, but they have to represent a stimulus for all of us to do our best to support agricultural sector to find sustainable solutions to the increasing number of problems that have to be solved day after day.

Simone Orlandini

OBIETTIVI

L'Italian Journal of Agrometeorology (Rivista Italiana di Agrometeorologia) si propone di pubblicare contributi scientifici originali, preferibilmente in lingua inglese ma anche italiana, riguardanti l'agrometeorologia, intesa come scienza che studia le interazioni dei fattori meteorologici e idrologici con l'ecosistema agricolo-forestale e con l'agricoltura intesa nel suo senso più ampio (comprendendo gli allevamenti e la pesca). Fra le aree tematiche di specifico interesse della rivista si segnalano: l'ecofisiologia, la fenologia, la crescita delle piante e la qualità e quantità della produzione, la fitopatologia, l'entomologia, le condizioni di benessere degli allevamenti, la fisica del terreno e l'idrologia, la micrometeorologia, la modellistica di simulazione e previsione, il telerilevamento, la pianificazione territoriale, i sistemi informativi geografici e le tecniche di spazializzazione, la strumentazione di misura di grandezze fisiche e biologiche, le tecniche di validazione di dati, l'agroclimatologia, la divulgazione in agricoltura e i servizi di supporto per gli operatori agricoli. La Rivista si avvale di un Comitato Scientifico, che è il garante della qualità delle pubblicazioni e che per tale scopo può avvalersi di referee esterni.

AIMS

The Italian Journal of Agrometeorology (Rivista Italiana di Agrometeorologia) publishes English or Italian written original papers about agrometeorology, that is the science which studies the interactions between meteorological, hydrological factors and the agro-forest ecosystem and with agriculture, including all the related themes (husbandry and fisheries). Among the main considered topics: ecophysiology, phenology, plant growth and quality and quantity of yield, animal comfort, phytopathology, entomology, soil physics and hydrology, micrometeorology, simulation and forecasting modelling, remote-sensing, landscape planning, geographical information system and spatialization techniques, instrumentation for physical and biological measurements, data validation techniques, agroclimatology, diffusion of information and support services for farmers. Submitted articles are reviewed by independent members of the Editorial Board or by other appropriate referee.

GUIDA PER GLI AUTORI

1. Il manoscritto inviato deve riferirsi a materiale originale, non pubblicato altrove, se non in fase strettamente preliminare.

2. Il manoscritto deve essere inviato esclusivamente via e-mail a: ijagrometeorology@agrometeorologia.it
La pubblicazione sull'Italian Journal of Agrometeorology (IJAm) è subordinata alla revisione ed all'approvazione del Comitato di Redazione, che potrà avvalersi del parere di revisori esterni per materie specifiche.

3. Sono accettati lavori per le tre sezioni della rivista: rassegne bibliografiche, lavori di ricerca, note tecniche.
L'articolo dovrà preferibilmente essere redatto in lingua inglese. Tutte le pagine e le righe del manoscritto devono essere numerate.

4. Occorre fornire Nome, Cognome, Posizione Accademico/ Professionale, ente di affiliazione, indirizzo, numero telefonico e indirizzo di posta elettronica degli Autori e indicare chiaramente l'Autore di riferimento per la corrispondenza con l'Editor.

5. Il riassunto (abstract) non deve superare le 12 righe e deve essere sia in lingua italiana sia in lingua inglese.
Le parole chiave (keywords) e il titolo devono essere sia in lingua italiana sia lingua inglese.

6. Come separatore decimale è necessario impiegare il punto e non la virgola (es. 4.33 e non 4,33).

7. Le figure, le tabelle, i grafici, le foto e le didascalie devono essere allegate salvandole in file diversi da quello del testo. Per una buona stampa, le immagini devono essere vettoriali o create a almeno 300 ppi/dpi.

8. Le didascalie di tutte le immagini, da predisporre sia in italiano che in inglese devono essere indicate come segue: Fig.x – Nome figura, Tab.x – Nome tabella. Nel testo invece devono essere citate come: (Fig.x), (Tab.x). La traduzione deve essere riportata in corsivo: Fig.x – Nome figura, Tab.x – Nome tabella.

9. Per gli autori stranieri, tutte le traduzioni in Italiano saranno a cura di AIAM.

10. Una versione definitiva ed impaginata dell'articolo pronto per la pubblicazione sarà inviata agli Autori, di norma una sola volta, per la segnalazione di eventuali correzioni tipografiche.

11. È prevista la stampa in quadricromia degli articoli solamente a carico degli Autori che richiederanno direttamente all'Editore un preventivo al seguente indirizzo:
Italian Journal of Agrometeorology
Pàtron Editor
Via Badini, 12
40057 Quarto Inferiore, Granarolo dell'Emilia (BO)
e-mail: periodici@patroneditore.com

12. Tutti i riferimenti citati nel testo devono essere riportati nel paragrafo "References/Bibliografia" e tutti i riferimenti presenti in "References/Bibliografia" devono essere citati nel testo.
Nel testo i cognomi degli Autori devono essere citati senza il nome e senza l'iniziale (es: "Rossi, 2003" e non "Federico Rossi, 2003" e nemmeno "F. Rossi, 2003").
Se nel testo viene citato un lavoro di due Autori, utilizzare la notazione "Bianchi and Rossi, 2003" (non utilizzare "&" tra i due nomi).Se nel testo viene citato un lavoro con più di due Autori, utilizzare la notazione "Bianchi *et al.*, 2003".
Per le riviste, le citazioni dovranno essere stese come segue:
Bianchi R., Colombo B., Ferretti N., 2003. Titolo dell'articolo. Nome della rivista, numero della rivista: pagine.
Per i libri:
Bianchi R., Colombo B., Ferretti N., 2003. Titolo del libro. Editore, Luogo, numero totale di pagine pp.
Può essere citato materiale "in stampa".
Non sono accettati riferimenti a lavori presentati in occasione di convegni, seminari e simili come poster o comunicazioni orali e non pubblicati nei relativi atti.

GUIDE FOR AUTHORS

1. Manuscript should refer to original researches, not yet published except in strictly preliminary form.

2. Manuscript should be submitted only by e-mail to ijagrometeorology@agrometeorologia.it.
Articles of original researches findings are published in Italian Journal of Agrometeorology (IJAm), subsequent to critical review and approval by the Editorial Board. External referees could be engaged for particular topics.

3. Three types of paper can be submitted: original paper, review, technical note.
Manuscript can be written in English or Italian. All pages and lines of the manuscript should be numbered.

4. First Name, Last Name, position, affiliation, mail address, telephone and fax number of all the Co-Authors are required. Corresponding Authors should be clearly identified.

5. The abstract should be no longer than 12 typed lines and should be written in both English and Italian.
Keywords and title should be written in both English and Italian.

6. Full stop, not comma, must be used as decimal mark (e.g. 4.33 and not 4,33).

7. Figures, tables, graphs, photos and relative captions should be attached in separate files. All images must be vector or at least 300 effective ppi/dpi to ensure quality reproduction.

8. Captions should be written both in English and Italian and should be written as: Fig.x – Caption title, Tab.x – Caption title. Images should be referred to in the text as (Fig.x), (Tab.x). The translation must be written in italic: Fig.x – Caption title, Tab.x – Caption title.

9. For foreign authors, all requested translations into Italian will be made by AIAM.

10. Proof of the paper (formatted according to the Journal style) will be sent to the Corresponding Author for proof reading just one time. Corrections can be made only to typographical errors.

11. Four colour printing of the article is available. Authors can demand an estimate of costs to the Editor:
Italian Journal of Agrometeorology
Pàtron Editor
Via Badini, 12
40057 Quarto Inferiore, Granarolo dell'Emilia (BO)
e-mail: periodici@patroneditore.com

12. All the references in the text must be reported in the "References" section and vice-versa. In the text, only the Author(s) last name must be present, without the name or the first letter of the name (e.g. "Rossi, 2003" and not "Federico Rossi, 2003" or "F. Rossi, 2003").
If two authors are present, refer to them as: "Bianchi and Rossi, 2003" in the text (do not use "&" between the surnames). If more than two Authors are present, refer to them as: "Bianchi et al., 2003" in the text.
For journals, references must be in the following form:
Bianchi R., Colombo B., Ferretti N., 2003. Title. Journal name, number: pages.
For books:
Bianchi R., Colombo B., Ferretti N., 2003. Book title. Publisher, publishing location, total number of pages pp.
Manuscripts "in press" can be cited.
Posters or oral presentation can not be cited if they are not published on the relative proceedings.

MODAMB - Environmental diagnostic model: description and application to a case study

Marianna Nardino[1], Federica Rossi[1], Teodoro Georgiadis[1]*

Abstract: *Late frost events in the Emilia-Romagna region can damage significantly the horticultural production. Modelling tools can be of great importance in addressing the proper explanation when in presence of damages to the cultures and to provide diagnosis of the evolution of the event. The diagnostic model MODAMB, here presented, was developed at IBIMET-CNR Institute* ad hoc *for the considered region to offer an interpretative tool to the agrometeorological services. In order to test the model, in this study a frost event really happened during the night of 17th March 2003 was analyzed.*
Keywords: *Micrometeorology, diagnostic environmental model, agrometeorology, late frost events.*

Riassunto: *Nella regione Emilia-Romagna gli eventi di gelate tardive possono seriamente danneggiare la produzione agricola. I nuovi strumenti di modellizzazione costituiscono un importante aiuto nella corretta descrizione degli eventi atmosferici che possono danneggiare le colture e nella determinazione della loro evoluzione temporale e spaziale.*
Il modello diagnostico MODAMB, qui presentato, è stato sviluppato, presso l'Istituto IBIMET-CNR, ad hoc per la regione considerata per offrire uno strumento interpretativo per i servizi agrometeorologici. Al fine di testare il modello, in questo studio è stato analizzato un evento di gelata tardiva realmente accaduto durante la notte del 17 marzo 2003.
Parole chiave: *Micrometeorologia, modello diagnostico ambientale, agrometeorologia, gelate tardive.*

1. INTRODUCTION

Spring frosts are often responsible of wide economic losses and serious injuries to fruit trees in Emilia-Romagna, which is Italy's leading area of high-value horticultural production.
In this region, the occurrence of strong advection frosts has been recorded in the winters 1929, 1956, 1985 and, more frequently, spring radiative freezing events are observed (Zinoni et al., 2002). The latter events are characterized by a clear sky, calm or very low wind speed, low dew point temperatures and air temperature falling below 0°C during the night although it was above 0°C during the day. This happens because the heat accumulated during the day is rapidly radiated to the atmosphere causing the establishment of temperature inversion. The depth of the inversion layer depends on the local atmospheric conditions (Rossi et al., 2002).
The frost risk assessment is an important operational application of meteorology in agriculture, since accurate frost forecasting may potentially reduce frost damage, providing farmers with the opportunity to make some counteractions against the frost events as a mitigation of adverse effects, but it is also of paramount importance to increase our knowledge in the diagnosis of the evolution of the frost episodes in order to adapt our strategies once understood the base mechanisms of occurrence in the territory.
The present work aims to improve the knowledge of the frost episodes evolution by the use of the diagnostic model MODAMB to simulate a real frost event and to test the effectiveness of the model performances in capturing the event.

2. MODEL DESCRIPTION

MODAMB (Environmental Diagnostic Model, bi-dimensional) has been developed by the Authors and it is a mass consistent diagnostic model suitable to reconstruct the main micrometeorological fields of a given region, starting from the standard meteorological data collected from the Meteorological Service stations.
The computation domain is represented by a rectangular box oriented in the West-East (x positive toward East) and South-North (y positive toward North) directions. The box is divided in a regular grid with cells of Δx and Δy dimension. Each grid cell is characterized by the position of its center, in UTM coordinates x_0 and y_0, relatively to the South-West point of the domain. The number of grid points in the two directions n_x and n_y completes the definition of the grid. Each micrometeorological field is calculated at the center of each cell. The 2D

* Corresponding Author e-mail: m.nardino@ibimet.cnr.it
[1] IBIMET CNR, Bologna
Received 26 April 2011 accepted 29 September 2011

domain is terrain-following, and these are the system coordinates:

$$\begin{cases} X = x \\ Y = y \\ \zeta = z - h_g \end{cases} \quad [1]$$

where h_g is the height above the sea level. The topography is given for each grid cell (i, j) (with i=1, 2, ……., nx+1 and j=1, 2, ……, ny+1) and its spatial variations throughout the domain are obtained through the estimates of slope and azimuth characteristic of each cell (Fu et al., 1995).
The reconstruction of 2D diagnosis is based on the available variables at once, in certain points of the computational domain where are present meteorological stations of a given regional network. In general, this network consists of measuring stations (Nstaz) each characterized by its geographic coordinates ($X_{station}$, $Y_{station}$). The purpose of the analysis system developed in MODAMB is to provide the reconstruction of the terrain-following of two-dimensional fields of several micrometeorological variables:

– air temperature;
– relative humidity;
– u e v wind speed components;
– global solar radiation;
– net radiation;
– cloud cover index;
– friction velocity;
– subsurface heat flux;
– sensible heat flux;
– latent heat flux;
– Monin-Obukhov length;
– PBL mixing height.

Since the computation domain is terrain following it is necessary to standardize all the data to a reference value: as far as air temperature is concerned its dependence on orography has been considered.
Following Malek (1997) for each meteorological station the potential temperature, which is a conservative quantity, (i.e. it is conserved for all dry adiabatic processes) was computed:

$$\theta_{X_{station},Y_{station}} = T(X_{station}, Y_{station}) + 0.0098 h_g \quad [2]$$

Applying this equation for each measurement point a set of standardized measurements of air temperature is made available. The interpolation of potential temperature at all the cells centers is based on a weighted mean where the different weights were determined using a variant of the method of Cressman (Sozzi et al., 2002).
In this way the 2D field of potential temperature is completely defined and applying the [1] to the value of potential temperature obtained in each cell the corresponding air temperatures and thus the 2D field can be determined.
Similarly, as regards the determination of the relative humidity 2D field, it is necessary to establish a conservative quantity for this physical variable. This quantity is the mixing ratio as reported in Malek (1997) defined as:

$$r = \frac{0.622 \cdot e}{p - e} \quad [3]$$

where e is the vapor pressure (which is obtained from the saturated vapour pressure and relative humidity values) and p is the atmospheric pressure (Sozzi et al., 2002).
Obviosly, this interpolation does not take into account the physical processes as advection or vertical mixing of air masses.
As far as wind speed is concerned, the interpolation takes into account two important effects that greatly influence the wind field patterns: the topography and the change in surface roughness. The surface roughness can change drastically between two neighboring grid points due to different land use of the real domain. This change affects the surface stress and, consequently, the wind speed components. For instance, when the wind moves from a smooth to a rough surface, it slows down and the overall field changes according to the pattern reported in Figure 1. In the model this effect is accounted for following the methodology proposed by Elliot (1958). The effects due to topography is included using the theory of the inner layer and the terrain following coordinates as reported in Kaimal and Finningan (1994) (Figure 2).
All the micrometeorological fields are derived from the measurements and the interpolation of air temperature, wind speed and relative humidity by use of the parameterizations already verified by comparison against experimental data (Sozzi et al., 1999; Sozzi et al., 2001). This set of parameterizations was developed "ad hoc" for Emilia-Romagna, with coefficients computed specifically for the Po valley surfaces and for its regional atmospheric characteristics.

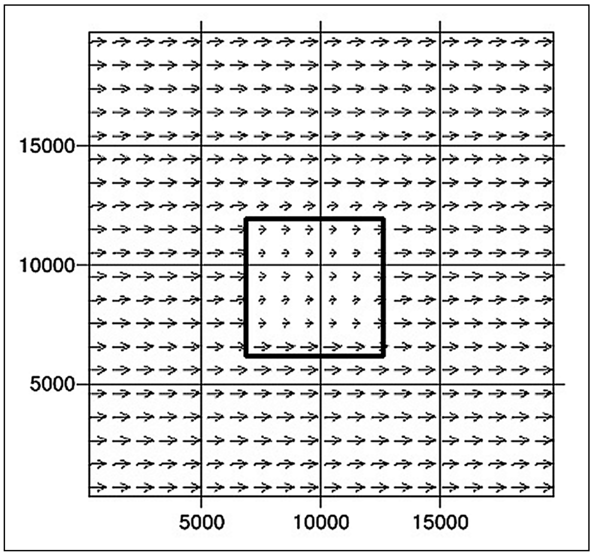

Fig. 1 - Bi-dimensional domain with surface roughness length change(the middle zone has a grater roughness) and relative perturbation of the wind field obtained with MODAMB model.
Fig. 1 - Dominio bi-dimensionale con un cambiamento della rugosità superficiale (la zona centrale ha una rugosità maggiore) e perturbazione relativa del vento ottenuta con il modello MODAMB.

The inputs of the model are consequently characterized by two data sets: the first based on the surface characteristics of the domain such as topography, albedo and roughness length. These quantities are fed to the model at each grid cell and can be retrieved directly from the land cover map. The second data set is represented by the meteorological data (temperature, relative humidity, wind speed and direction) of each available station. The outputs of the model for each grid point are the following variables: air temperature, relative humidity, U and V wind speed component, cloud fraction, global radiation, net radiation, soil heat flux, sensible heat flux, latent heat flux, friction velocity, and mixing height.

3. RESULTS AND DISCUSSION

In Figure 3 the 900-m grid spacing land cover input map is reported. It was used to initialize MODAMB. The whole computation domain is the Emilia-Romagna region, characterized by a wide flat area and by the Apennine hills located in the South part of the region. The land use (in LDAS code) shows a great area of irrigated crops, that represents the main agricultural production. From the land-use map both surface albedo and surface roughness length maps have been computed and are given as input into the model.
The frost event recorded during the night of 17th March 2003 was analyzed with MODAMB at two times of the day: midnight (before the event) and 4:00 a.m. (the recorded minimum temperature), both in GMT. The meteorological stations available for the analyses are reported in Figure 4 together with the topography of the region. For the analysis at 00:00 a.m. (Figure 4-a) 16 meteorological stations data were used, while at 4:00 a.m (Figure 4-b) data were available from 23 stations. Only the station simultaneously measuring air temperature, relative humidity, wind speed and wind direction have been considered.
In Figure 5 is reported a comparison of air

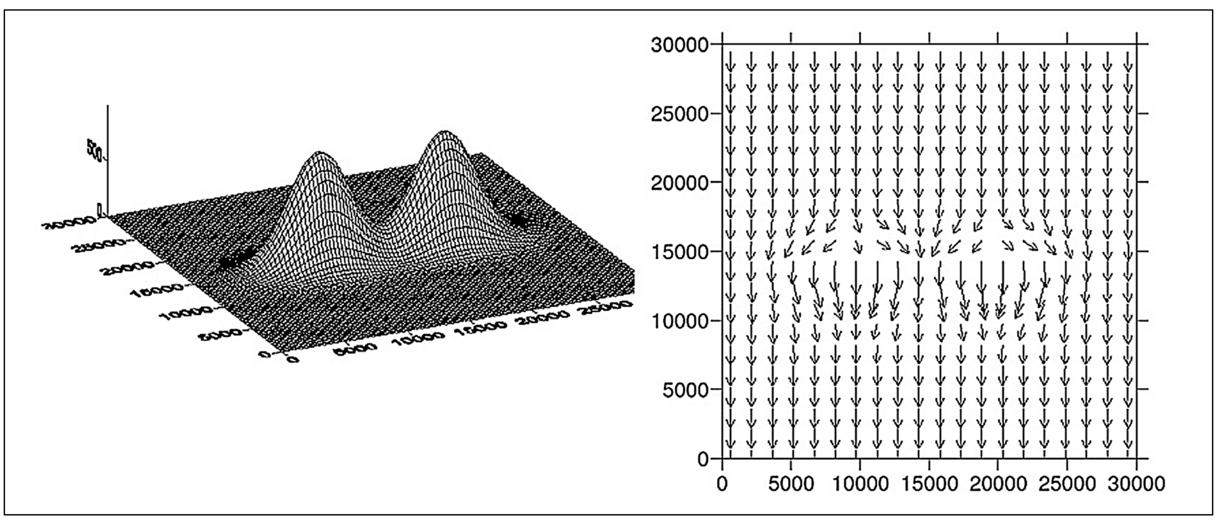

Fig. 2 - **Left:** topography change and **right**: relative perturbation of the wind field obtained with MODAMB model.
*Fig. 2 - **Sx**: cambiamento di topografia e **Dx**: relativa perturbazione del campo di vento ottenuta con MODAMB.*

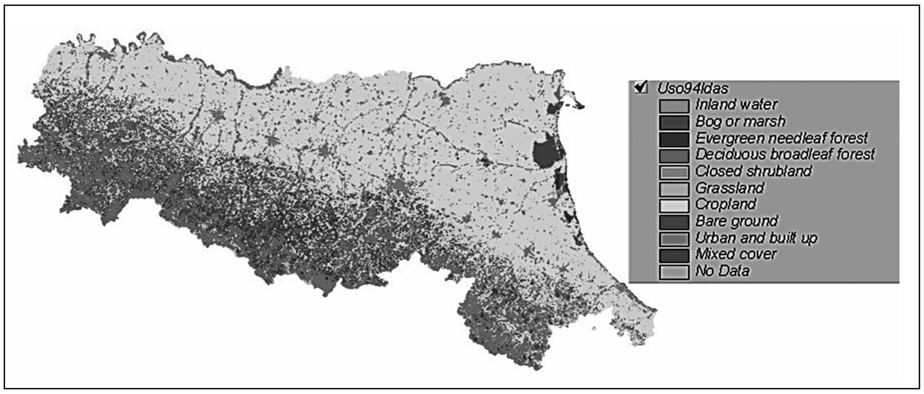

Fig. 3 - Land use in LDAS code of the Emilia Romagna region.
Fig. 3 - Uso del suolo in codice LDAS della regione Emilia Romagna.

temperature interpolation starting from 16 meteorological stations (Figure 5-a) and from 149 meteorological stations (Figure 5-b) in order to address the sensitivity of the geometrical interpolation to the number of stations and their average distance between each other. The Figure shows that the main features of the temperature field are well characterized also considering only 16 initial data and only some local spots do not appear. Furthermore, it was performed a numerical comparison to validate the goodness of model interpolation: Figure 6 shows the regression plot between the 149 meteorological data and the ones obtained by the model interpolation. The data are

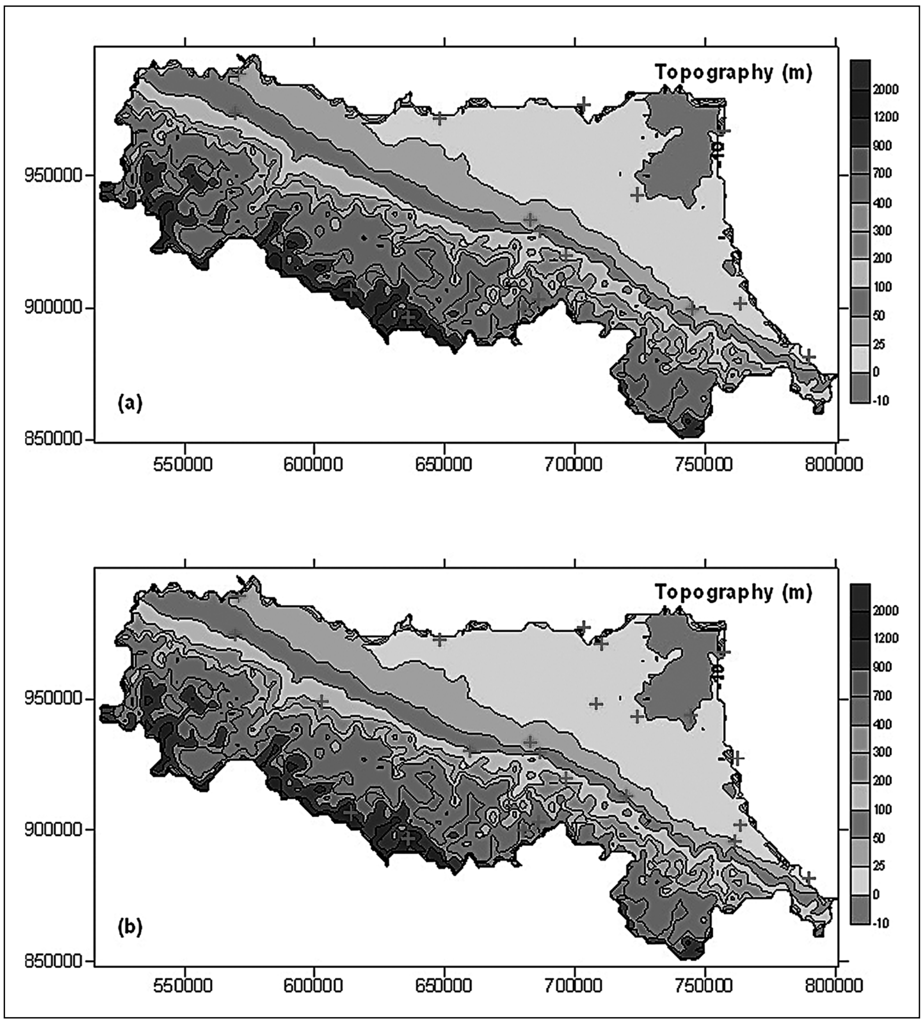

Fig. 4 - Spatial distribution of meteorological stations used to initialize the model at (a) 00:00 a.m. (16 stations) and (b) 4:00 a.m. (23 stations).
Fig. 4 - Distribuzione spaziale delle stazioni meteorologiche utilizzate per inizializzare il modello alle ore (a): 00:00 (16 stazioni) e (b): 4:00 (23 stazioni).

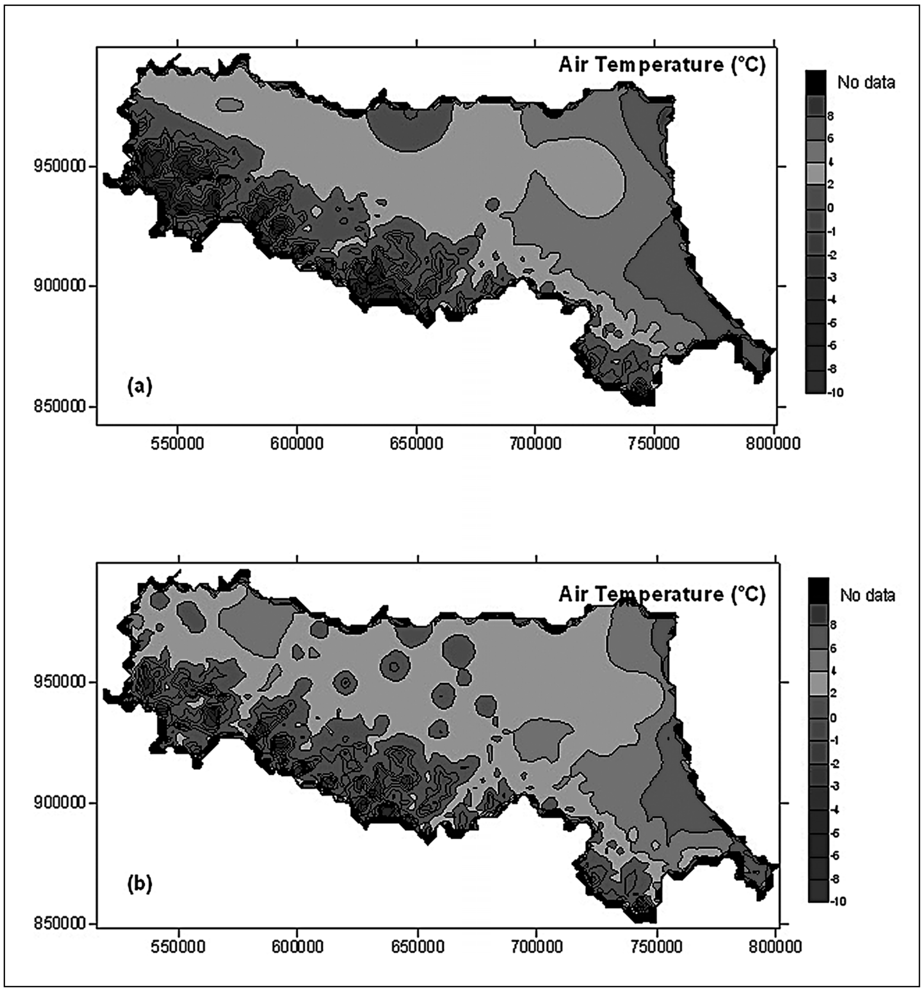

Fig. 5 - MODAMB interpolation of air temperature (in °C) obtained starting from (a) 16 and (b) 149 meteorological stations.
Fig. 5 - Interpolazione ottenuta attraverso MODAMB della Temperatura dell'aria (in °C) partendo da (a) 16 e (b) 149 stazioni meteorologiche.

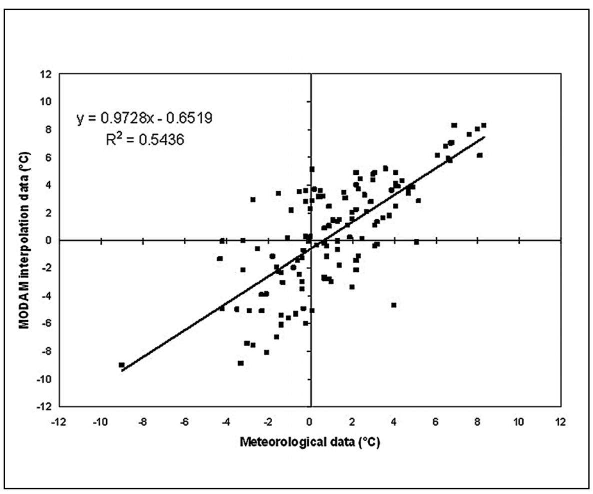

Fig. 6 - Scatter plot between air temperature recorded by meteorological station and the ones obtained by MODAMB interpolation.
Fig. 6 - Scatter plot tre la temperatura dell'aria registrata dalle stazioni meteorologiche e quelle ottenute dall'interpolazione effettuata con MODAMB.

scattered as indicated by the regression line value (R^2=0.54) but the best fit regression line is very close to 1:1 line. The root mean square error, representative of the size of a "typical" error, is equal to 0.63 °C, which can be considered acceptable for the purpose of the MODAMB application.

The analyses of the wind speed for the two different times are reported in Figure 7. For both hours the northern wind direction and the low wind speed intensities are typical of a radiative frost, and followed a cold air outbreak (not shown). By 4.00 am, the winds over the mountains and the foothills acquired a south-westerly component due to the drainage flow. This, along with radiative cooling, caused the temperature to decrease along the valley bottoms and the plain, as confirmed by the temperature analyses at the same times (Figure 8). The analyzed temperatures pattern are consistent with the climate minimum temperature during frost events shown in Figure 9 (data from ARPA-SIM Emilia Romagna Region). These data were obtained

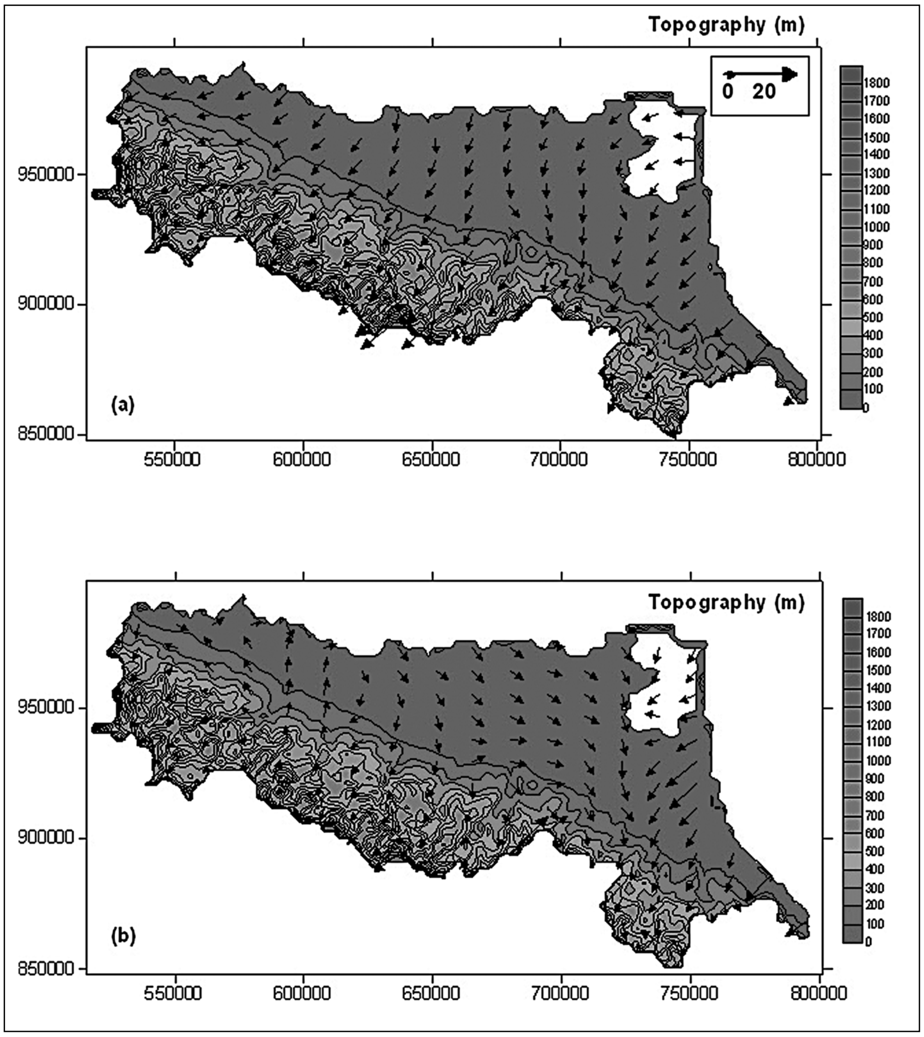

Fig. 7 - MODAMB analyses of the wind field at (a) 00:00 a.m. and (b) 4:00 a.m.
Fig. 7 - Analisi del campo di vento ottenuta con MODAMB alle ore (a) 00:00 e (b) 4:00.

by the application of a topoclimatic model as well explained in Zinoni et al., (2004).
The sensible heat flux, as computed by MODAMB, is reported in Figure 10 and shows a downward flux as we can expect thanks to the higher temperature within the surface layer, where the thermometer is located, than at skin surface. At lower temperature (Figure 10-b) the sensible heat flux decreases in absolute value because the temperature gradient decreases. The highest heat flux, in absolute value, is over the mountains. Moreover, the model MODAMB is suitable to reproduce the heat island due to the Bologna metropolitan area, because of the presence of meteorological stations in that area.

4. CONCLUSIONS

The results show that MODAMB can be a very useful tool for frost event analysis and more generally for agrometeorological applications (i.e. fire risk index, eco-physiology modeling, crop production, risk assessment).
This model can be hence a new instrument for the regional agrometeorological services in order to analyze and study micrometeorological events at small scale as required in this kind of environments.
Further studies are necessary to improve the application of a local diagnostic model to simulate events useful in agriculture mapping. The next step is to initialize a mesoscale forecast model (i.e. RAMS) with the Emilia Romagna land use and soil characteristics for forecast purposes and then to insert into MODAMB the output of RAMS to obtain a better local characterization of micrometeorological features of extreme events and to be able to give an early warning to the farmers.

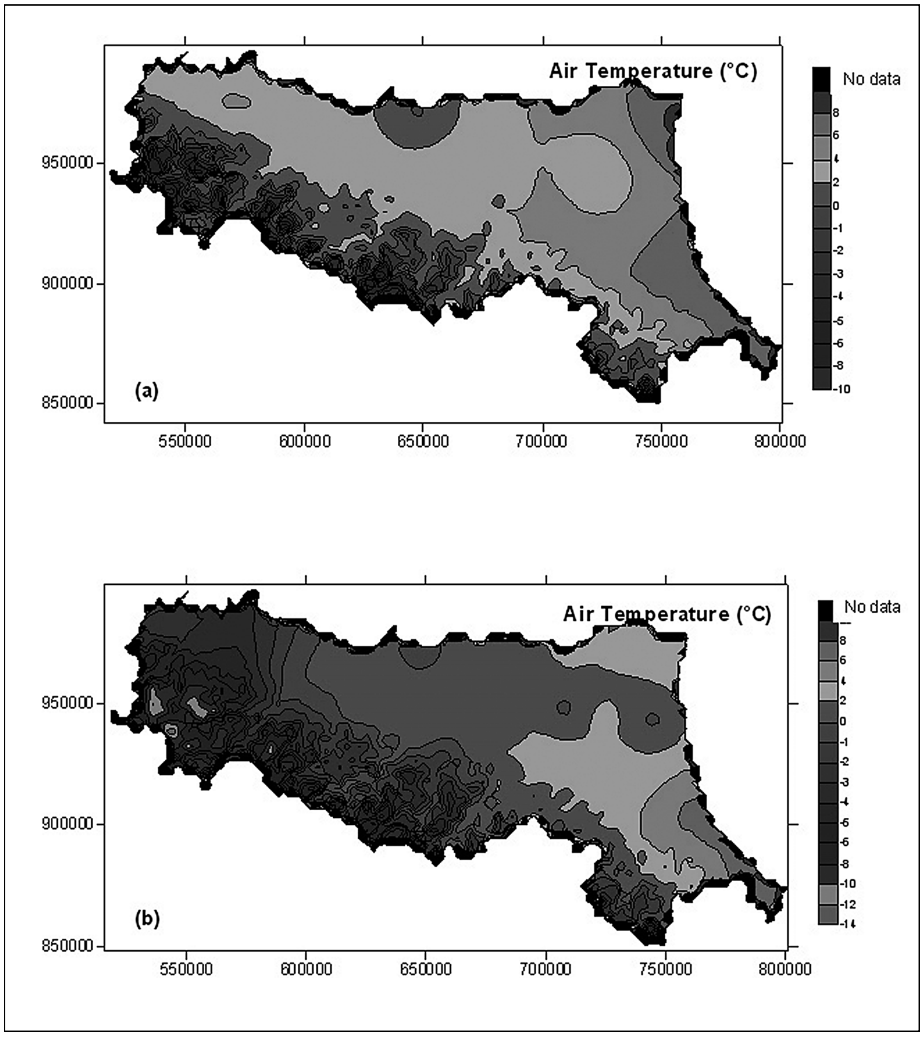

Fig. 8 - MODAMB analyses of the air temperature (in °C) at (a) 00:00 a.m. and (b) 4:00 a.m.
Fig. 8 - Analisi della temperatura dell'aria (in °C) ottenuta con MODAMB alle ore (a) 00:00 e (b) 4:00.

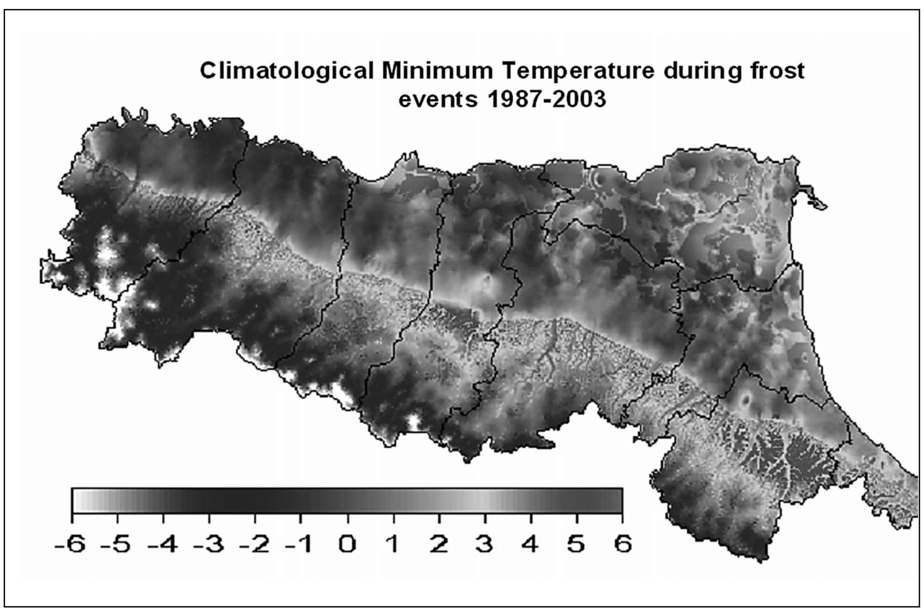

Fig. 9 - Climate minimum temperature (in °C) observed during frost event from 1987 to 2003. (Data and analysis from ARPA-SIM Emilia Romagna).
Fig. 9 - Temperatura minima climatica (in °C) osservata durante eventi di gelate tardive dal 1987 al 2003. (Dati e analisi ottenuti da ARPA-SIM Emilia Romagna).

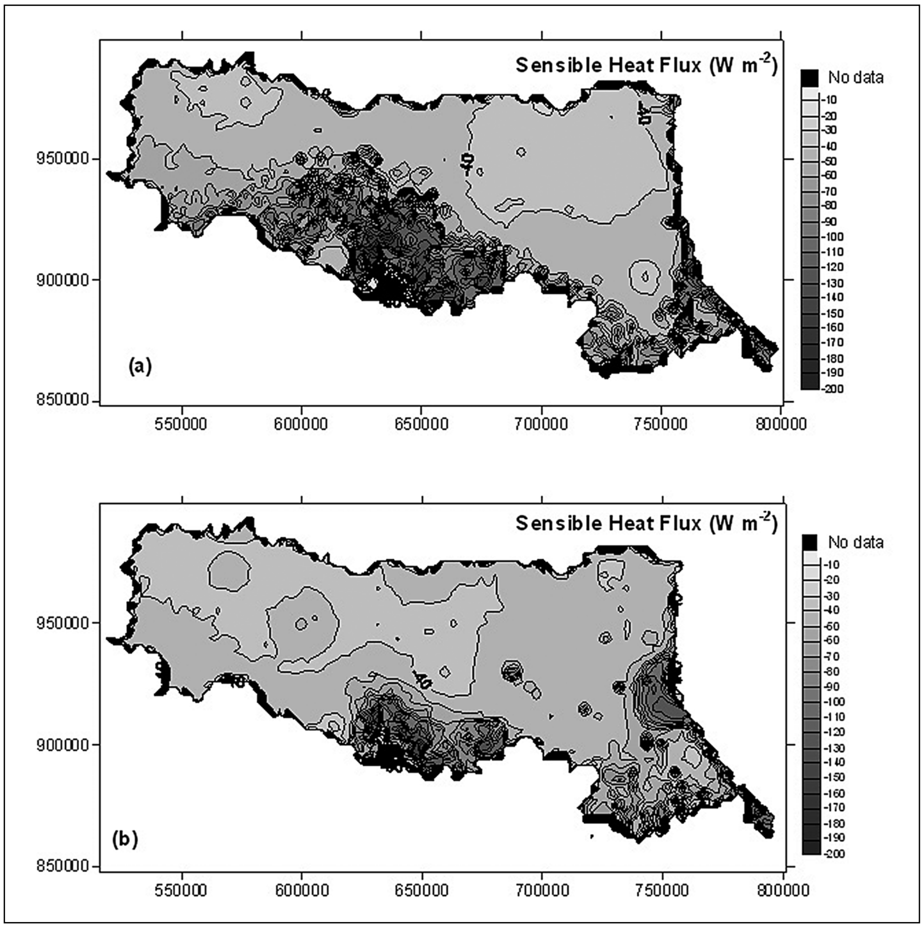

Fig. 10 - MODAMB sensible heat flux (in W m^{-2}) at (a) 00:00 a.m. and (b) 4:00 a.m.

Fig. 10 - Flusso di calore sensibile (in W m^{-2}) ottenuta con MODAMB alle ore (a) 00:00 e (b) 4:00.

ACKNOWLEDGEMENTS

The authors thanks the Emilia Romagna Idro-Meteorological Service for the meteorological station data and the minimum temperature climatic map.

REFERENCES

Elliot W.P. 1958. The growth of the atmosphere internal boundary layer. *Trans. Amer. Geophys. Union.* 39: 1048-1054.

Fu H., Tajchman S.J., Kochenderfer J.N., 1995. Topography and radiation exchange of a mountainous watershed. *J. Appl. Meteor*., 34, 890-901.

Kaimal J.C. and Finnigan J.J., 1994. Atmospheric Boundary Layer Flows: their structure and measurements. Oxford University Press, New York, USA.

Malek E. 1997. Evaluation of effective atmospheric emissivity and parameterizaion of cloud at local scale. Atmos. Res. 45: 41-54.

Rossi F., Facini O., Loreti S., Nardino M., Georgiadis T., Zinoni F., 2002. Meteorological and micrometeorological applications to frost monitoring in northern Italy orchards. *Chemistry and Physics of the Earth.* 27:1077-1089.

Sozzi R., Salcido A., Saldana Flores R. and Georgiadis T., 1999. Daytime net radiation parameterisation for Mexico City suburban areas. *Atmos. Res.* 50: 53-68.

Sozzi R., Rossi F. and Georgiadis T., 2001. Parameter estimation of surface layer turbulence from wind speed vertical profile. *Environ. Model. and Software*. 16: 73-85.

Sozzi R., Georgiadis T., Valentini M., 2002. Introduzione alla turbolenza atmosferica-concetti, stime e misure-Pitagora ed. (Bologna) pp. 525.

Zinoni F., Antolini G., Campisi T., Marletto V. and Rossi F., 2002. Characterization of Emilia Romagna in relation with late frost risk. *Chemistry and Physics of the Earth*. 27: 1091-1101.

Zinoni F., Antolini G., Marletto V., 2004. Valutazione del rischio da gelata tardiva. In Previsione e Difesa dalle gelate tardive, risultati finali del progetto DIsGELO, Notiziato Tecnico CRPV. 70: 29-48.

Irregular Bearing and Climate in Olive

Guido Bongi[1*], *Claudio Ranocchia*[1]

Abstract: *Long term yield records are important reference databases useful for calibration and validation of models for climate analysis. The evaluation of olive tree yields for Jaen province, the main production area in Spain, during a 21 years period of system stasis (constancy of variety and agro-techniques), revealed (a) a remarkable interaction between rainfall and previous year production with a significant non-additive term and (b) the fact that the previous year yield does not show any descriptive power of the current-year production. These evidences raise several questions about the rightness of alternate bearing as driving variable in olive orchard models, being the time series distributed in irregular fashion among conditions of Medium (M), Low (L) and High (H) fruit load.*
In the Jaen data set, the interaction between an aleatory factor (annual rainfall) and an equilibrium determined by two biological variables (flower fertilization and previous year shoot elongation) is statistically proved. These biological variables depend on the rainfall level. As a consequence, yield time series are not auto-correlated and yield modelling should measure productive efficiency at least in 3 classes of fruit load in order to avoid the risk of finding stochastic yield frequency. So the models of olive orchard production should record previous year fruit load, current year fruit load and water availability in order to describe up to 70% of the variance within IPCC fingerprint high confidence limits (i.e. above a probability level of 0.67).
Keywords: *Olea europea L., Fruit bearing, Production models, Water use efficiency.*

Riassunto: *Le serie produttive a lungo termine sono le basi di dati sulle quali supportare modelli e studi sull'impatto climatico. Nell'olivo la valutazione della produzione media ettariale del territorio di Jaen, principale provincia olivicola di Spagna, durante 21 anni di stasi del sistema (stessa varietà, stesse agrotecniche), ha rilevato una marcata interazione della produzione con la precipitazione annuale e la produzione dell'anno precedente, con un termine non-additivo significativo. Al contrario la produzione dell'anno precedente non ha nessuna capacità descrittiva se presa da sola. Queste evidenze pongono dei limiti al valore dell'alternanza a livello regionale come variabile guida nei modelli di previsione della produzione olivicola, essendo la serie temporale distribuita in modo assai irregolare fra le condizioni di media (M), bassa (L) ed alta (H) carica produttiva.*
Nel dataset di Jaen è statisticamente provata l'interazione tra un fattore aleatorio (la precipitazione annuale) ed un equilibrio biologico determinato dalla fertilizzazione dei fiori e dall'allungamento del germoglio. Queste variabili biologiche dipendono da un livello di pioggia determinato. Come risultato le serie produttive non sono autocorrelate ed i modelli produttivi dovrebbero ripartire le produzioni in almeno tre classi di carica fruttifera onde evitare il rischio di incorrere in una frequenza stocastica delle produzioni. In queste condizioni, note la produzione dell'anno precedente, lo stato di carica corrente e la disponibilità idrica è possibile stimare la produzione fino al 70% della varianza entro limiti accettabili nella fascia di confidenza alta dell'IPCC (al di sopra di un livello critico di probabilità di 0.67).
Parole chiave: *Olea europea L., Carica fruttifera, Modelli produttivi, Efficienza idrica.*

Abbreviations: H, M , L high, medium and low Fruit Load, LTE long term experiment, FL fruit load in kg ha-1 and RF annual rainfall in mm, IPCC Intergovernmental Panel on Climate Change.
Abbreviazioni: H, M, L alta, media e bassa produzione, LTE esperimento a lungo termine, FL produzione in kg/ha, IPCC Comitato Intergovernativo sui cambiamenti climatici.

INTRODUCTION

Time series of yearly mean yield in olive groves taken at farm or regional level show an high variability that has been defined as "alternate bearing" in a number of issues (Bongi *et al.* 1995, Loreti and Natali, 1991. Ben-Gal et al. 2011). This variability, testified for example by coefficients of variation often above 50%, is too high to achieve a mean separation into components (trend, seasonality, slow and fast variation and so on) so giving a strong limit to obtain predictive models of olive production.

A minimal area that could be related to gridded climatic models is much wider than a single orchard (0.5 by 0.5 degrees of lat long) or a parcel in an experiment, and climate impact studies require coherence in response linked to probabilities of a given set of driving variables in a range higher than 0.67 if the process is due to various possible causes (Parmesan and Yoe, 2003). This effects becomes a

* Corresponding Author e-mail: guido.bongi@cnr.it
[1] C.N.R.– Istituto per i Sistemi Agricoli e Forestali del Mediterraneo, Perugia
Received 11 June 2011 accepted 5 October 2011

'fingerprint' in IPCC schedules and high confidence range is limited to the interval over 0.67, accounting in this way the decimal proportion of cases that are in agreement with the variation in a subset of variables. With this boundary every model that predict below this probability limit is not important but can retain scientific value. In other practical activities a fingerprint coherence is perceived as "reliable" and this corresponds to model accepted in farm and olive mill catchment practices. We should however admit that possibly regional level studies are a summary of experiences and that the mean value for a single year represents a sort of meta-analysis, without knowing single year observational error. Above this limitation, economic trends are linked to entire regions for gross production and require coherence too.
Much more is known about the biology of olive in isolated field experiments where, in order to force the mean separation, strict sampling procedures are applied to parcels, but coherence with territorial scale behaviour of plant populations is not guaranteed. At design level the number of observations increases up to the inclusion of time series in parcels or the use of cumulative production as an extra variable.
At single shoot level, the notion of alternate bearing in analogy with AC current or pendulum periods is described by a regular fluctuation between statuses and a sequence H, L, H is sufficient to determine amplitude and phase of the variable. In olive tree studies the amplitude is reported as sensitivity to alternance and the period is assumed to be 2 years using H for high load and L for low fruit load cases. Caffeic acid–like substances and fruit shoot load with fruit bio-phenols have been suggested as a possible mechanism of alternate bearing acting at single shoot level (Lavee *et al*., 1986, Palese et al. 2010); this evidence was tested using substitution treatments in shoots. This qualitative description can be depicted in quantitative terms as a locus in a plot of current year production against the previous year one, with both X Y axes maximum coinciding with maximum production; the algorithm gives a zero in the year after a theoretical maximum was attained in X or Y, with all intermediates falling on a line with a slope -1. In this hypothesis the system may remain indefinitely in mean condition M until some perturbation occurs that triggers H or L condition.
Published experiments are often ranked by selecting an H, M or L condition (Dag *et al*., 2010) but the generalization of relationships like crop coefficients would require their relative frequency and a study of variability among fruit load classes (Ben-Gal *et al.*, 2011, D'Andria *et al.*, 2004, Pastore, 1940), even at single tree scale. The feasibility of experimental conditions measures the transition between experiments and trials. In terms of coherence this as a variable impact on actual rates of productive plantations. The sequence of states between different levels of fruit load is irregular and there is no grant about the stability of plot plant experiments when propagated at trial level. Is this sequence able to be apportioned to an algorithm like a line with slope -1? Is it possible to work out a stable predictor of olive production at regional level? Inherent instability of fertility in the shoot has also been proposed (Martin, 1990), but this would lead to an uniform distribution and to stochastic trends if propagated at higher level.
In this issue we test a reversed model at the lowest resolution spatial level in order to test production statistics in a region. Most of the uncertainty has been hypothesized to originate from random errors or systemic in-homogeneity but this possibility must be cleared using long term series. Farm and province scale studies include plantation age effects, with plantation to first productive crop interval, mature orchard duration and senescence, in succession of discrete steps, but their relative lengths vary upon treatments and determine treatments classes. Seldom olive cultivation areas are in steady state conditions for the variable effects of new plantations or product support incentives.

MATERIAL AND METHODS

This LTE (Long Term Experiment in the common meaning), is a time series from Andalusia, the major autonomous region of southern Iberian peninsula, in the province of Jaen described in Table 1, and was collected between 1945 and 1966 (Cantero de Andres, 1971). This case study coincided with a period of relative stasis of olive economy in Spain (Camilleri, 1984). The integration to a large area should buffer single orchard variations and show only synchronous

Whole area: 13496 Km^2
Mean location: 38 N and -3.5E
Olive area: 572627 ha (95% with Picual)
Landscape: hilly slopes
mean slope: 8 -15%
main cropping aspects: traditional, non intensive, rain fed, single-cultural olive

Tab. 1 - Jaen province main characters.
Tab. 1 - Principali caratteristiche della provincia di Jean.

sequences or a stable mean (Loreti and Natali, 1991, ex *Cantero de Andres ibidem*). For ease of reference in further studies the time series of olives yield (fresh fruits weight per hectare) and yearly rainfall (mm) are listed in Table 2.
Statistical analysis was used to test the existence of annual variability and auto-correlation with the previous year production D, in the hypothesis of a

Y	Kg	D	mm
1	1931	363	691.0
2	1965	1931	973.7
3	965	1965	762.1
4	988	965	420.3
5	638	988	354.6
6	2177	638	707.9
7	1500	2177	693.7
8	820	1500	338.2
9	1209	820	513.2
10	890	1209	660.9
11	1761	890	670.7
12	1897	1761	503.4
13	1159	1897	567.4
14	1863	1159	830.4
15	1886	1863	1032.2
16	1420	1886	757.1
17	1284	1420	747.8
18	3000	1284	1057.4
19	113	3000	737.5
20	784	113	588.7
21	2750	784	912.5

Tab. 2 - The series of 21 Years (Y) of consecutive production in Kg/ha (Kg) and annual rainfall in mm (mm). For statistical purposes D is the previous year production in the same units (rewritten from Cantero de Andres, 1971).
Tab. 2 - La serie di 21 anni di produzione consecutiva in Kg/ha (Kg) e la precipitazione annua in mm (mm). Per scopi statistici D è la produzione dell'anno precedente espressa in Kg (rielaborazione da Cantero de Andres, 1971).

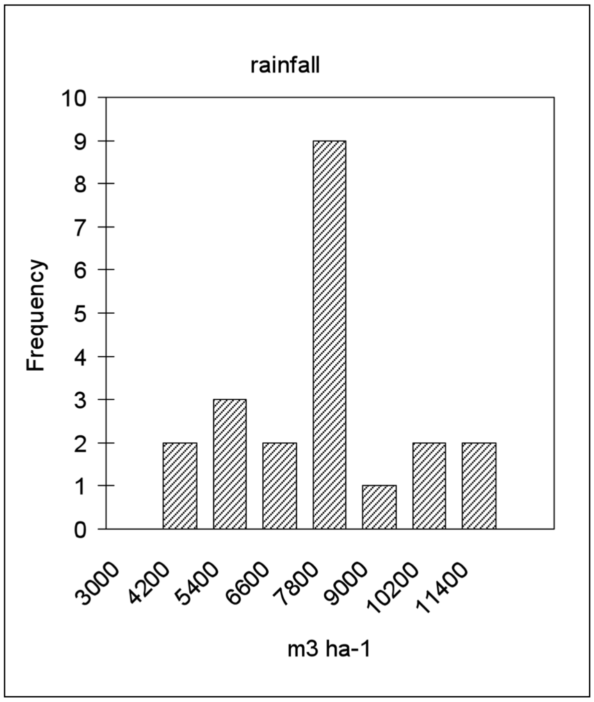

Fig. 1 - Distribution of rainfall in 21 Years in the province of Jaen. It was here considered in mm (mm, (m^3 ha-1)/10).
Fig. 1 - Distribuzione della pioggia nella serie di 21 anni a Jaen. In questo testo l'unità è in mm (mm, (m^3ha-1)/10).

strong effect of alternate bearing. Graphical functions and statistical tests from *lm* and *ts* functions of R version 2.7.0 package has been adopted (R Development Core Team, 2008).
The software library "*hsaur*" was also loaded in R to test multiple regression (Everitt and Thorton, 2006). To test interaction structure a model series was created using 0.25, 0.5 and 0.75 quantiles with the same grid spacing and numerosity of the original series and variance of internal classes was tested. Quantile separation was done using confidence intervals of subsets and Montecarlo generators driven by the standard deviation of the original subset. The paucity of data in their original ranking in H, L and M classes forbids the use of sub-subsets for calibration. The difference of cumulative rainfall sensitivity on different production classes was tested using R library "*gap*" (Zhao, 2007).

RESULTS

The stasis in the period offers an unique opportunity of a quite long series with regional smoothing effects on single site variations, but even in this condition the sequence of fruit bearing is markedly irregular. Sectioning the series in 3 quantiles for fruit production (i.e. high H, Medium M and low L), produced the sequence H, H, L, L, L, H, M, L, M, L, M, H, M, H, H, M, M, H, L, L, H. This series is not synchronous with previous year state nor with precipitation classes and it is hard to trust autocorrelation. The traditional view of a biennial bearing was tested with a model that takes into account only the effect of the previous year production. This model did not gave a significant output (adjusted R-squared of 0.007076 and high probability of null hypothesis – F statistic: 1.143 on 1 and 19 DF, p-value: 0.2985). If it is also considered that autocorrelation tests failed to find significance it is possible to reach the conclusion that the previous year charge is not an adequate predictor of olive charge time series. In Figure 3Tl we observe quite a random distribution below and above the locus of the theory of alternate bearing quantitative equilibrium (i.e. the line with slope -1). Parametric measures of fallacy are done by "sigma" in lm procedure of R and corresponds to the square root of estimated variance of random error, 689.2 kg on a mean tendency of 1420 kg ha-1. In coherence terms this would equal a wrong assignment in one case over 2 with this dataset.

The time series of the yearly rainfall for Jaen province shows a mean value of 780 mm, but production in fresh fruit per ha (kg) varies widely and the mean is not the most frequent datum but is far from an uniform distribution (Fig. 2). A linear

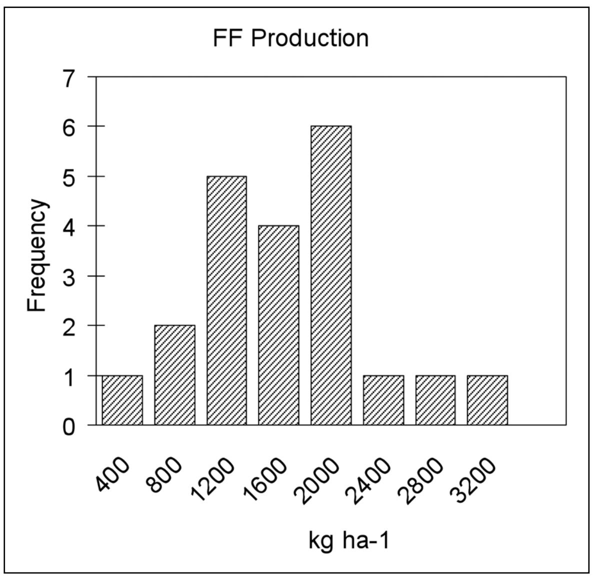

Fig. 2 - Frequency of Jaen province production in Kg ha-1 (fruit fresh production). The mean is not the mode and tails reveal system apparent stochastic boundaries.

Fig. 2 - Frequenza della capacità produttiva in frutti freschi di olivo della provincia di Jaen. La media non è la moda e si verifica una apparente stocasticità dei limiti.

Model	F	Pr(>F)	
0/2	20.524	0.00 0259	***
0/3	19.636	3.81 e -5	***
1/2	6.960	0.0167	*
2/3	9.792	0.001482	**
1/3	9.729	0.001525	**

Tab. 3 - Analysis of variance among production models in a partial contrast (/) matrix. The model of previous year production D on fresh fruit production (0) is compared (/) to different alternatives: the effect of rainfall (mm) (1), this last with previous year production D (2) and with model (3); model 3 is the case (2) with interaction D:mm. Variance within mm models is also considered; regression lines are significantly different but the main effect appears when the non additive term is added; missing comparisons are redundant and the *** in 0/- appears because model 0 (alternate bearing) does not converge so that any significant model would give an high probability of difference. The asterisks mean significance level at 5% (*), 1% (**) or 0.1% (***) of probability.

*Tab. 3 - Analisi della varianza tra i modelli presi in esame in matrice di contrasto (/). L'effetto della carica dell'anno precedente D sulla produzione è il caso (0) e la barra(/) indica il contrasto con la pioggia (1) sulla produzione, con la pioggia e con D (2), e con l'interazione D:mm (3) sulla stessa variabile. La varianza entro i modelli mm è esaminata; i modelli sono tra loro significativamente differenti, ma l'aumento principale avviene nel confronto con il modello con interazione. I casi mancanti sono ridondanti e il valore *** nei confronti 0/- è dovuto alla non convergenza del modello 0 (alternanza produttiva), in misura tale che ogni modello significativo avrebbe comunque una alta probabilità di differenza. Gli asterischi(*), (**) e (***) indicano 5%, 1% e 0.1% di probabilità dell'ipotesi nulla.*

model of rainfall effect on production is appropriate but describes 36% of the variance and is useless to describe production due to the large estimation error (F statistic was 12.61 on 1 and 19 DF, with a p-value: 0.002133 that is significant but deceptive, in the possibility of an high probability of missing representation ability near a critical border for coherence if we admit a perception that should require at least 2 cases right over 3 trials) (Fig. 3Tr). The significance of R2 was determined after testing the presence and stability of a zero production rain fall near to 300 mm; R2 is adequate after calibrating a zero production near 300 mm (thus having a response linear with intercept zero). With this correction the R2 measures the coefficient of determination, but the forecast error is too high to be useful. The sigma of this set is 562 kg per ha and the experimental rate of fallacy is about one case every 3.

The model with the inclusion of previous year

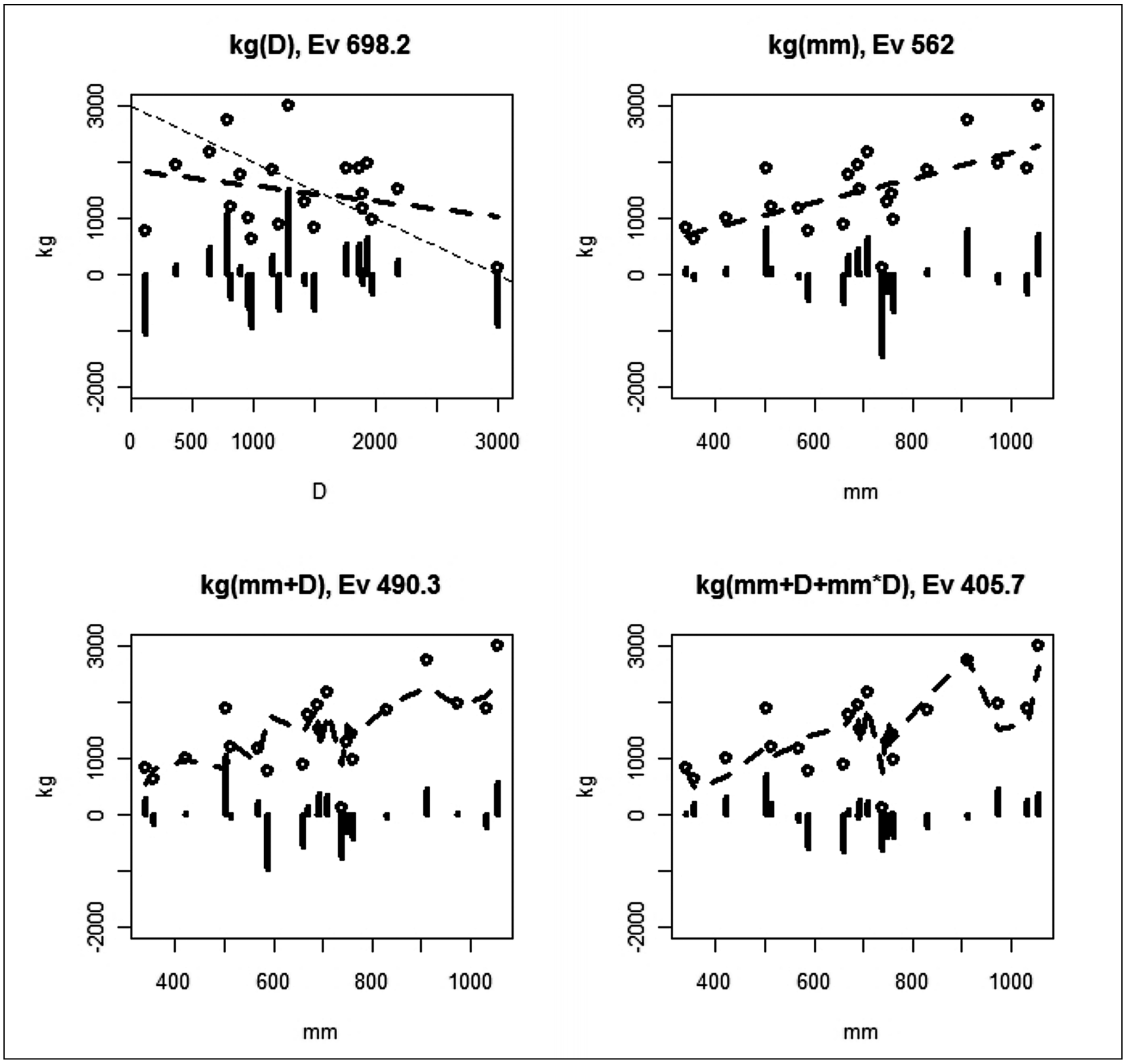

Fig. 3 - Top left (Tl) is testing the effect of alternate bearing D as an independent variable for production (kg); thin step line draws a theoretical line of perfect control, in all plots bars and tick line represent residuals and regression line. Top right (Tr) tests the effect of cumulative rainfall on kg without alternate bearing. Bottom left (Bl) is a bilinear hypothesis with both mm and D and Bottom right is the same with D*mm interaction. Ev stands for squared root of estimated variance of random error (sigma in R language).

Fig. 3 - Il grafico in alto a sinistra (Tl) misura l'effetto dell'alternanza (D) sulla produzione come variabile indipendente: la tratteggiata sottile rappresenta la linea teorica di perfetto controllo; in tutti i grafici le barre e le tratteggiate spesse rappresentano i residui e la regressione. Il quadro in alto a destra (Tr) prova l'effetto della pioggia cumulata sulla produzione senza l'alternanza di produzione. Il quadro in basso a sinistra (Bl) prova una regressione bilineare con D e mm e quello in basso a destra (Br) lo stesso modello con una componente non additiva. Ev rappresenta il valore della radice quadrata della varianza dell'errore casuale (sigma nel linguaggio R).

production, D showed a rise of R2 from 0.36 to 0.51 and the significant difference of models in the analysis of variance (anova, Table 3) was significant, thus meaning a better description (Tab. 2), in comparison with the single-year yield alone. This may lead to the conclusion that the D parameter alone has no mean separation power but cumulative rainfall of the year has such a power, and, within a given rainfall class, there is sensitivity to previous year fruit load. Residuals analysis then has an high chance of failure in production forecast also after this improvement (Fig 3Bl). The inclusion of an interactive term mm*D raised again R2 to 0.67 with a F-statistic of 14.55 on 3 and 17 Degrees of

Coefficients:	Estimate	Std.Error	t St.	Pr(>|t|)	
(Intercept)	-2.82 6e+03	1.091e+03	-2.59	0.019070	*
D	1.946e+00	7.920e -01	2.457	0.025076	*
mm	7.172e+00	1.597e+00	4.492	0.000321	***
D* mm	-3.412e -03	1.119e -03	-3.05	0.007263	**

Res.SE	DF	Mul.R2	R2	F val.	Pr(>F)
405.7	17	0.7197	0.6703	14.55	5.986e -05

Tab. 4 - Linear model of fresh fruit production with annual rainfall (mm) including the interaction (D*mm) as non additive term. signif. codes: 0 '***' 0.001 '**' 0.01 '*' 0.05.
*Tab. 4 - Modello lineare della produzione in frutto fresco con la pioggia annuale, includendo l'interazione (D*mm) come termine non additivo.*

freedom, with a p-value of 5.986e-05 with significant student t (Table 4, Fig. 3Br). This level of R2, being yield a collinear function only in this survey trial, whereas in orchard experiments it is covariate of many other independent variables, and subject to curvilinear relationships, is probably close to an optimum, considering a whole district and the lack of any other information. The relationship is finally adequate and satisfies the coherence with a fallacy of 1 case over 7 and a sigma of 405 kg ha-1. In the selected time series 3 years over 21 fail prevision test, but we must add many other aspects that were unreported, like years with frost or years with unexpected variation in fertility control due to heat shock or spring drought. It was evident however that a non-additive term, given by the interaction of rainfall with previous year production, produced a significant increase of prediction ability. The analysis of variance among models determined the significance of combinations including term D but only when it was included in multiple regressions with rainfall (Table 3).
The separation of production data in upper (H) medium (M) and lower (L) quantiles produced 3 different regression lines versus cumulative rainfall that well explain the non-additive effect. H status is more sensitive than the M or L to drought and an invariant locus exists near 880 mm (Fig. 4). To obtain a model suitable for production forecast in a given condition, the knowledge of this kind of behaviour is therefore required and more specifically the knowledge of LTE and 3 sensitivities. This LTE is only useful for the combination under study, that should hold as far extensive as rain-fed cultivation is concerned. This result highlights a structured response to the combination of 2 independent variables rather than a chaotic structure. The Chow test of regression slopes resulted highly significant (Tab 5) and the model has got enough sensitivity to partition residual variance and water sensitivity into secondary determinants for local effects.

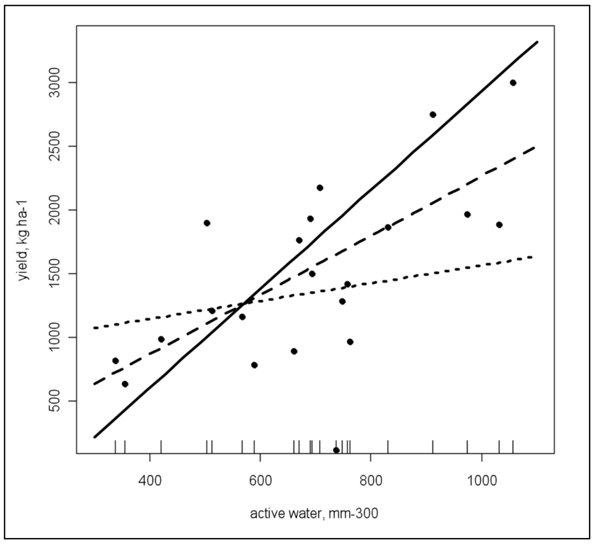

Fig. 4 - Annual rainfall and production of olives interact due to a varied sensitivity. The useful precipitation or active water is the actual level minus 300 mm m-2. Solid line depicts H status, step line M, and dot line L respectively. Rug plot on rainfall active fraction is a measure of uniformity.
Fig. 4 - Interazione tra carica e precipitazione utile (mm – 300) o acqua utile. La linea continua rappresenta l'anno di carica H, la linea a tratto breve l'anno di produzione media M e la linea punteggiata l'anno di scarica L. Il grafico a barre brevi indica la distribuzione della pioggia utile nella serie.

The diagram in figure 5 represents an hypothetical layout of the LTE multiple correlation. In water limited environments there was a tendency to fruit drop under water stress that diminished fruit

F value	DF 1	DF 2	Pr(>F)
7.501e+01	2	48	1.690175e-15

Tab. 5 - Chow test between H and L statuses. The coefficients of rainfall on production of olive orchard with low and high fruit load are physically different.
Tab. 5 - Test di Chow sui coefficienti idrici negli stati H e L. Questi coefficienti idrici dell'oliveto in condizioni contrastanti sono differenti fisicamente.

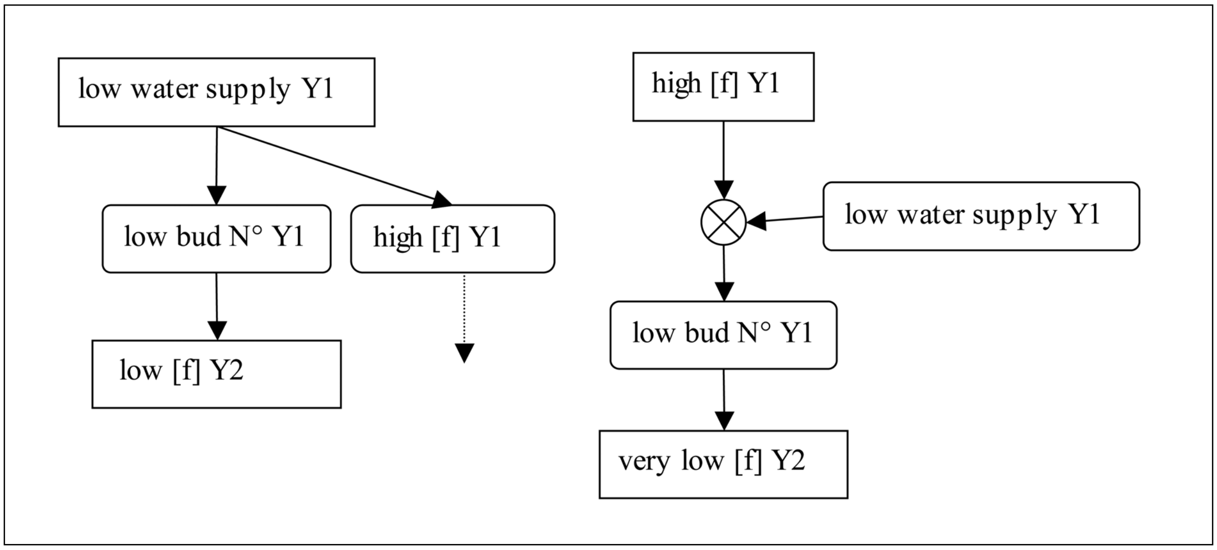

Fig. 5 - Diagrams of control in olive tree irregular bearing: the network on the left represents a feasible interpretation of LTE of Cantero de Andres (1971), where the dotted arrow is for fruit natural drop that follows water stress. It is also depicted the current biologist view in which the fruit concentration [f] should have exerted the main control on next year loading, the [f] Y2.

Fig. 5 - Schemi di controllo della irregolarità di carica nell'olivo: la struttura a sinistra rappresenta una ipotesi realistica della LTE di Cantero de Andres (1971), nella quale la freccia punteggiata rappresenta la cascola di frutti dovuta allo stress idrico. È anche rappresentata a destra la opinione biologica corrente che prevede che la concentrazione di frutti eserciti il controllo principale sulla carica dell'anno successivo.

concentration, [f], in year 'one', Y1. The interactive term of [f] Y2 with [f] Y1 is due to the action of water limitation on bud number. The hormonal action scheme by some growth inhibitor released from fruits or from water stress signals (Lavee et al., 1984), that has been found on experiments with uniform twig samples, is depicted on the right diagram and would have produced a strong autocorrelation between [f] Y1 and next year load, and a possible effect of water supply as secondary cause if this framework was maintained at population level. In case the [f] should persist in order to affect bud number. Eventually the absence of this relationship in regional trends was probably an artefact due to unreliable sampling for shoot heterogeneity.

In the Jaen province time series this set of causes seems to be bound to non-additive effects of rainfall on fruit production. In reversed models one should expect better cumulative performance if a rain fed system is fluctuating between H M and L statuses than if it is maintained in M condition if coincides with yearly rainfall fluctuations.

CONCLUSION

The analysis of production series in Jaen converges to the limits of quantitative effects of fingerprints after a simple bilinear model taking into account the interaction of rainfall and previous year production. This can be due to the compensative effects of the large areas cumulative production but there is no evidence of stable mean. A status of mean M can result from a fifty-fifty of L and H areal distribution or from the prevalence of M; in this case M should prevail in frequency; however this time series has got a low frequency of M and this supports the idea of a synchronicity across the area, without memory effects.

Alternate bearing in olive using single shoot experiments is a wrong argument to describe irregular bearing and this attribution mistake is possibly originating by a confusion of causes between small scale experiments and regional trends. A comparison scheme with biologist's current opinion can clarify this model as seen in comparison with substitution experiments.

This is a first contribution to the analysis of statistical stability of olive fruit production, but many other clues, like rain seasonality, plantation density and varietal effects require further analysis.

ACKNOWLEDGEMENT

The activity has been made possible by project Agriscenari, a grant MIPAAF after D.M. 8608/7303/2008.

BIBLIOGRAPHY

Ben-Gal A., Yermiyahu U., Zipori I., Presnov E., Hanoch E., Dag A., 2011. The influence of bearing cycles on olive production response to irrigation. Irrig. Science 253-263.

Bongi G., Moscariello P., Rosati A., 1995. A quantitative description of olive productivity. Olea n. 23: 76.

Camilleri A., 1984. La Agricultura Española ante la CEE. Ed. Instituto de Estudios Económicos. Madrid, 800 p.

Cantero De Andres F., 1971, Etude de la relation entre la production oléicole obtenue dans la province de Jaen et la pluviométrie enregistrée durant l'année agricole, période october-mai et f'année civile avant chaque cueillette, in conference proceedings of III conferencia internacional de tecnicos oleicolas, Torremolinos, (Spain), 14th 19th june.

Dag A., Bustan A., Avni A., Erel R., Yermiyahu U., Riov J., Lavee S., Biennial Bearing in Olive – Physiological Background and Control, 2010 in congress proceedings The 28th International Horticultural Congress ISHS Lisboa Congress Centre (CCL) august 22-27 2010.

D'Andria R., Lavini A., Morelli G., Patumi M., Terenziani S., Calandrelli D., Fragnito F., 2004. Effects of water regimes on five pickling and double aptitude olive cultivars. J Hort.Sci. Biotechnol n.79: 18-25.

Everitt B.S. and Hothorn T., 2006, A Handbook of Statistical Analyses Using R' Chapman & Hall/CRC.

Lavee S., Harshemesh H., Avidan N., 1986. Endogenous control of alternate bearing. Olea n. 17: 61-66.

Loreti F., Natali S., 1991. Cure colturali al terreno – Irrigazione. L'Olivo "Frutticoltura anni '80". Reda: 93-118.

Martin G.C., 1990. Olive flower and fruit population dynamics. Acta Horticulturae n. 286: pag 141-152.

Milella A., Dettori S., 1986. Confronto fra tre coefficienti colturali per l'irrigazione dell'olivo da mensa. Ortofrutticoltura It. n. 70: 231-240.

Palese A.M., Vitale N., Favati F., Pietrafesa A., Celano G., Xiloyannis C., 2010. Effects of water deficit on the vegetative response, yeld and oil quality of olive trees grown under intensive cultivation. Scientia Horticulturae n. 125: 222-239.

Parmesan C. and Yohe G., 2003. A globally coherent fingerprint of climate change impacts across natural systems Nature 421, 37-42 (2 January 2003).

Pastore R., 1940. La potatura di produzione dell'Olivo in terra di Bari. In atti Convegno nazionale Olivicoltura Bari 1938. REDA Roma: 106-122.

R Development Core Team, 2008. R: A language and environment for statistical computing. R Foundation for Statistical Computing, Vienna, Austria. ISBN 3-900051-07-0, URL http://www.R-project.org).

Zhao J.H., 2007. gap: genetic analysis package. Journal of Statistical Software, 23(8): 1-18.

Influence of climate on durum wheat production and use of remote sensing and weather data to predict quality and quantity of harvests

Federico Guasconi[1], Anna Dalla Marta[1], Daniele Grifoni[2], Marco Mancini[3], Francesca Orlando[3], Simone Orlandini[1]*

Abstract: *Climate conditions severely affect crop production, influencing plant responses and harvest characteristics. For the growers of durum wheat (*Triticum turgidum *L.* var. durum*) an important aspect, in addition to yield, is the grain quality taking into account that it is closely related to the flour properties and therefore to the quality of resulting pasta. The study analyzes the influence of rainfall and temperatures on the winter durum wheat productions and the predictive role of meteorological and satellite indices at large scale (NDVI). Results show a significant negative correlation between precipitation and grain protein concentration. On the other hand, increasing temperatures were associated with grain protein accumulation, while negative correlations were found with kernel specific weight and yield. NDVI recorded during the crop cycle resulted descriptive of all productive variables, showing the suitability to be integrated with the weather information in a local forecasting system.*
Keywords: Triticum durum*, protein content, specific weight, meteorological information, NDVI.*

Riassunto: *Le condizioni climatiche hanno un notevole impatto sulle produzioni agrarie, influenzando la risposta della piante e le caratteristiche del raccolto. Per i coltivatori di frumento duro (*Triticum turgidum *L.* var. durum*) un importante aspetto, oltre alla resa, è la qualità della granella, in considerazione del fatto che questa è strettamente legata alle proprietà della farina e quindi alla qualità della pasta prodotta. Lo studio analizza l'influenza delle precipitazioni e della temperatura sulla produzione di grano duro ed il ruolo che può essere svolto da indici calcolati a partire da dati meteorologici e satellitari su vasta scala (NDVI), al fine di sviluppare un sistema di previsione della qualità e della quantità dei raccolti. I risultati mostrano una correlazione negativa tra le piogge e il contenuto proteico della granella. D'altra parte, temperature crescenti risultano associate ad un accumulo di proteine, mentre determinano una diminuzione del peso specifico e della resa. L'NDVI durante il ciclo colturale è risultato descrittivo di tutte le variabili produttive mostrando l'idoneità ad essere integrato con le informazioni meteorologiche in un sistema di previsione locale.*
Parole chiave: Triticum durum*, contenuto proteico, peso specifico, informazioni meteorologiche, NDVI.*

INTRODUCTION

Winter durum wheat (*Triticum turgidum* L. *var. durum*) production represents approximately 58% of the cultivated wheat in Italy, in contrast it only covers about 9% of the wheat production in European Union (Eurostat, 2009). The Italian winter durum wheat is grown over an area of about 1.3 million hectares with an average yearly production of about 3.5-4 million tons (Eurostat, 2009). This crop provides the raw material for the pasta industry, one of Italy's most renowned products. Val d'Orcia, in Tuscany region, is one of the most suitable areas of central Italy where the cultivation of durum wheat has entered the tradition and it is the basis of typical products (i.e. "Pici"). The qualitative parameters of pasta (i.e. yellow degree, transparency, consistency, good cooking behavior regarding elasticity, stickiness and resistance) are closely related to that of the flour used and therefore of the grains, particularly referring to protein content and gluten quality (Dexter and Matsuo, 1980).

Several researches show that weather conditions, during shooting, grain filling and grain ripening stages, are crucial in determining the quality of harvest for the common wheat (*Triticum aestivum* L.) (Ciaffi *et al.*, 1996) and the study of Dalla Marta *et al.* (2010) and Orlandini *et al.* (2010) on durum wheat highlights the influence of air temperature and rain on grain protein content. In northern Europe, where the climatic

[*] Corresponding Author e-mail: federico.guasconi@unifi.it
[1] DIPSA – Department of Plant, Soil and Environmental Science, University of Florence. Florence (Italy)
[2] CNR-IBIMET – Institute of Biometeorology. Florence (Italy)
[3] CIBIC – Interdepartmental Centre of Bioclimatology, University of Florence. Florence (Italy)
Received 10 September 2011 accepted 10 October 2011

conditions entail a prolonged grain filling stage, the grains have high specific weight but low proteins concentration; in contrast in the Mediterranean areas, where the grain filling stage is shorter, the harvests are characterized by lower yield but good protein content level. Many studies confirmed that the meteorological factors, such as air temperature (Pan *et al.*, 2006; Smith and Gooding, 1999) and rainfall, greatly affect the grains quantity. Nevertheless most of studies focus on common wheat and few works were performed on the impact of meteorological variables on winter durum wheat (Peltonen-Sainio *et al.*, 2010).

The NDVI (*Normalized Difference Vegetation Index*) is a remote sensing index that supply a descriptive value of crop status being related to the vegetation cover density. The maximum NDVI value corresponds to the period of maximum photosynthetic activity due to highest rate of biomass production (Anderson, 1992). Maximum NDVI in wheat was recorded between the end of vegetative growth and the flowering start (Whan *et al.*, 1991); after the flowering and during the grain maturity stage, NDVI values decrease as a consequence of a photosynthetic activity reduction (Connor *et al.*, 1992). Many researches on durum wheat highlight a close relationship between NDVI and the product characteristics (i.e. yield and grain protein content) (Broge and Lebance, 2001). Nevertheless the most of these studies detected NDVI values through optical remote-sensing instruments at ground level, without evaluating the reliability of satellite measurements at large scale. The relationship between NDVI and wheat yields or biomass is confirmed by many authors (Raun *et al.*, 1993; Labus *et al.*, 2002; Hansen *et al.*, 2002). On the other hand the scientific literature shows controversial results about NDVI predictive role for grain protein.

Hansen *et al*. (2002) evaluated NDVI as a predictor index of the common wheat harvests obtaining good performance for the yield, but unsatisfactory results for grain protein content. Similarly, Freeman *et al*. (2003) reported that NDVI provided a trusted estimate of durum wheat yield and nitrogen uptake by the epigean biomass, but no significant correlations were found with grain protein content. Therefore for wheat the prediction of grain quality from remote sensing remains a challenge.

The current work studies the relationship between satellite-based NDVI, meteorological variables, recorded by ground weather stations, and the qualitative and quantitative aspects of winter durum wheat harvests, in a large scale study performed in Val d'Orcia. The main objective is the evaluation of the possible use of indices derived both by remote sensing and meteorological data to predict the crop performance, in terms of yield and qualitative characteristics.

MATERIALS AND METHODS

Study area

The research was carried out in Val d'Orcia (Province of Siena, Tuscany, Central of Italy) characterized by a typical Mediterranean climate with an average yearly air temperature of 13.6°C and yearly cumulated rainfall of about 715 mm, mainly concentrated during winter and autumn. Val d'Orcia, extended for 668.62 km² of which 15% cultivated with winter durum wheat, is one of the main area for the high quality production necessary for pasta industry. The Val d'Orcia area was studied, with the support of ArcGIS 9.1 software, through orthophotos, soils and land use maps, excluding the urban centers and identifying a study area of 135 km² characterized by the predominance of arable land and clay loam soil.

Meteorological indices

The meteorological data were acquired by five ground weather stations, located within the Val d'Orcia, in order to accurately represent the mean meteorological conditions over the study area. The sum of active temperatures above 0°C (SAT), equation (1), and the sum of precipitation (SP), equation (2), were calculated, considering the growing season of the crop from November to June, over the period 1998-2009.

$$SAT = \sum_{01/11}^{30/06} (t_{md} \geq 0) \qquad (1)$$

$$SP = \sum_{01/11}^{30/06} P_{mm} \qquad (2)$$

where t_{md} is the average daily air temperature (°C) and P_{mm} is the daily cumulated precipitation (mm).

Remote sensing reflectance index

Normalized Difference Vegetation Index (NDVI) data for the period 1998-2009 were supplied by raster images freely available on website (www.free.vgt.vito.be). The images, with spatial resolution approximately 1 km x 1 km and processed with a time-step of 10-day, were acquired by the VEGETATION sensor (VGT) on board the SPOT satellite.

The images supply NDVI values, calculated following the equation (3) (Peñuelas and Filella, 1998) and computed to finally obtain maximum value composites (MVCs) on a 10-day basis (Holben, 1986).

With the support of ArcGIS 9.1 software a single NDVI value for each interval was calculated as the mean of all pixels within the study area.

$$NDVI = (R_{900} - R_{680}) / (R_{900} + R_{680}) \qquad (3)$$

where R_{900} is the reflectance in near infrared wavelength (900 nm) and R_{680} is the reflectance in red region (680 nm).

Productive variables

The qualitative and quantitative variables taken into account were: yield (Y), percentage of protein on grain dry matter (P), kernel specific weight (W) and total protein production (T), calculated as the percentage of P on Y.

Crop data were supplied by the Council for Research in Agriculture (CRA), by the Agricultural Consortium of Siena and by "Carletti" farm for a total of 20 farms placed in the study area.

The data series used for the analysis is represented by the mean of the grain protein content of the locations for the period 1999–2009. Wheat varieties used for this study had similar characteristics and no significant differences in grain protein content. During the period analyzed, nitrogen fertilization and crop management remained constant under the agreement between the farms and the Agricultural Consortium (fertilization plan: 160 kg/ha N, distributed in three times, and 90 kg/ha P_2O_5 at sowing).

Statistical analysis

Independent variables SP, SAT and NDVI and dependent variables Y, P, W and T were taken into account for the statistical analysis. The simple linear correlation between the meteorological indices and the dependent variables was calculated on a monthly and multi-monthly basis. In the same way, the correlation between NDVI and the dependent variables was calculated on a 10-day and multi 10-day basis taking into account the three monthly NDVI values related to first 10-day (I), second 10-day (II) and third 10-day (III). All possible combinations during the period November-June were investigated in order to identify the periods during which the meteorological variable show a significant effect on harvest and during which the NDVI is descriptive of the crop status.

Moreover two multi-regression analysis were carried-out, one taking into account all independent variables and one considering only the meteorological indices. The results were evaluated identifying for each month the independent variable or the combination of independent variables with higher predictive power on quality and quantity of harvest.

RESULTS

Grain protein content

P showed negative and positive correlation, respectively with SP and SAT. The single monthly SP was not significantly correlated, otherwise the multi-monthly analysis highlighted significant correlation, with highest r values for the periods November-May (r = -0.757) and November-April (r = -0.712) (Tab. 1). The single monthly SAT was correlated with P in April (r = 0.609) and the multi-monthly analysis showed correlations in the spring-early summer period involving the months from March to June, with highest r values in February-June (r = 0.684), January-June (r = 0.634) and February-May (r = 0.613) (Tab. 2). These results confirm the positive effect of temperature, mainly during the spring-summer months, on grain protein accumulation (Motzo *et al.*, 2007).

NDVI recorded from April to June was inversely correlated with P. The single 10-day analysis showed higher r value in the second 10-day of June and in the second half of May (r = -0.769); the early predictor period was found in the second 10-day of April (r = -0.667). The multi-10-day analysis indicated higher r value for the period from the second half of May to the second half of June (r = -0.798) (Tab. 3).

The multiple regression analysis indicated that the best predictive index of P was SP in the period from January to March. The multi-regression analysis showed SP and SAT as the best combination for the period April-June (Tab. 4).

Nov	Nov - Dec P_1	Nov - Jan $P_1 T_1$	Nov - Feb $P_2 T_1$	Nov - Mar $P_1 T_1$	Nov - Apr P_2	Nov - May P_2	Nov - Jun P_1
Dec T_1	Dec - Jan $Y_1 T_2$	Dec - Feb $P_1 T_2$	Dec - Mar $P_1 T_1$	Dec - Apr $P_1 T_1$	Dec - May P_1	Dec - Jun	
Jan T_1	Jan - Feb	Jan - Mar	Jan - Apr	Jan - May	Jan - Jun		
Feb	Feb - Mar	Feb - Apr	Feb - May	Feb - Jun			
Mar	Mar - Apr	Mar - May	Mar - Jun				
Apr	Apr - May	Apr - Jun					
May	May - Jun						
Jun							

Tab. 1 - Correlations, calculated on a monthly and multi-monthly basis, between sum of precipitation and harvest characteristics. Legend: P = protein percentage; W = specific weight; Y = yield; T = total protein; significance: $_1$ = $P \leq 0.05$; $_2$ = $P \leq 0.01$; $_3$ = $P \leq 0.001$; the positive correlations are highlighted in bold.
Tab. 1 - Correlazioni, calcolate su base mensile e multi-mensile, tra la somma delle precipitazioni e le caratteristiche del raccolto. Legenda: P = percentuale di proteine; W = peso specifico; Y = resa; T = proteine totali; significatività: $_1$ = $P \leq 0.05$; $_2$ = $P \leq 0.01$; $_3$ = $P \leq 0.001$; le correlazioni positive sono evidenziate in grassetto.

Kernel specific weight
There was not significant correlation between W and SP (Tab. 1), while the results showed negative correlation with SAT. The effect of temperature is evident during all crop cycle and since the early stages: higher *r* values were recorded in March-May (*r* = -0.924) and the early predictor period was December-March (*r* = -0.617) (Tab. 2). The results highlighted positive correlation between NDVI and W since April. On 10-day basis, the most significant correlation occurred in the second half of May (*r* = 0.757) as the multi 10-day analysis confirmed higher *r* value for the period 11 May -30 May (*r* = 0.791) (Tab. 3).
The multiple regression analysis indicated SAT as the earlier predictive index of W in March and the multi-regression between SP and SAT in April, May and June (Tab. 4).

Yield
The rainfall did not show significant effects on Y, while negative correlation was recorded with SAT during the most of growing cycle: higher *r* values were observed in May (*r* = -0.839) and in March-May (*r* = -0.820) (Tab. 2). Positive correlations were found between NDVI and Y in April, May and June: on 10-day basis, higher *r* values occurred in the second half of May (*r* = 0.636) and, on multi-10-day basis, in the periods 21 April to 10 June and (*r* = 0.733) from 21 to 30 May (*r* = 0.724) (Tab. 3). These results are supported by others studies that showed positive correlation between Y and plant biomass at flowering (Whan *et al.*, 1991; Anderson, 1992).
The multiple regression analysis indicated SP and SAT as the best predictor of Y, highlighting the relevance of winter rainfall and spring temperatures (Tab. 4).

Total protein production
Negative correlations between SP and T were found with high significant values in December-January (*r* = -0.803) and December-February (*r*= -0.736) (Tab. 1). Negative correlations were found also between STA and T with highly

significant values in May (r = -0.685) and in March-May (r = -0.587) (Tab. 2). NDVI showed negative correlation with T only in the second half of November (r = -0.636).

The multiple regression analysis indicated SP as the best predictor of T in March and April, and for the following months of May and June the multi-regression between SP and SAT, confirming the role of winter rainfall and spring temperatures.

DISCUSSION AND CONCLUSIONS

The best prediction of the productive variables was performed through the combined use of meteorological indices, nevertheless NDVI was able singularly to give predictive information on the quality and quantity of winter durum wheat harvest.

P resulted negatively correlated with winter precipitation and positively correlated with spring temperatures. W and Y were not significantly correlated with rainfall, but significant and negative correlations were found with spring temperatures. The NDVI was in agreement with the rainfall effect showing a negative correlation with P. On the other hand, NDVI and temperature had respectively positive and negative relationship with W and Y values.

Studies can explain the negative effect of rainfall on P: precipitation encourages the dilution of early nitrogen reserves by vegetative proliferation, it increases the leaching and other forms of soil nitrogen loss, it may augment soil moisture reserves so that leaf life is extended during grain growth favoring carbohydrate assimilation and translocation more than that of nitrogen (Smith and Gooding, 1999). Therefore NDVI, as index of the vegetation cover, probably was able to describe the N dilution effect that occurs corresponding to plant vegetative proliferation.

Temperature had a positive effect on growth, accelerating the cycle and then decreasing the grain filling duration (Wheeler *et al.*, 1996). The final grain size, and hence the dilution degree of accumulated nitrogen, is closely related to the length of time the crop stay green after flowering: higher temperatures shorten this period penalizing the total carbohydrate accumulation and furthering the protein concentration (Smith and Gooding, 1999). Furthermore with a higher temperature range, from emergency to earing stage, the fruit setting improves with higher number of ears and, therefore higher number of seeds characterized by smaller size and lower specific weight. Moreover, the temperature plays an important role on the water status of the plant increasing

	Nov - Dec	*Nov - Jan*	*Nov - Feb*	*Nov - Mar*	*Nov - Apr* W_1	*Nov - May* W_2Y_1	*Nov - Jun* W_2Y_1
Dec	*Dec - Jan*	*Dec - Feb*	*Dec - Mar* W_1	*Dec - Apr* W_1	*Dec - May* W_2Y_1	*Dec - Jun* W_3Y_1	
Jan	*Jan - Feb*	*Jan - Mar* W_1	*Jan - Apr* W_1	*Jan - May* W_2	*Jan - Jun* $P_1W_3Y_1$		
Feb	*Feb - Mar* W_1	*Feb - Apr* W_1	*Feb - May* $\mathbf{P}_1W_3$	*Feb - Jun* $\mathbf{P}_1W_3$			
Mar W_2	*Mar - Apr* $\mathbf{P}_1W_2$	*Mar - May* $W_3Y_2T_1$	*Mar - Jun* $\mathbf{P}_1W_3Y_2$				
Apr $\mathbf{P}_1$	*Apr - May* $\mathbf{P}_1W_2Y_2$	*Apr - Jun* W_1Y_1					
May $W_2Y_3T_1$	*May - Jun* W_1Y_1						
Jun							

Tab. 2 - Correlations, calculated on a monthly and multi-monthly basis, between SAT (sum of active temperature) and harvest characteristics. Legend: P = protein percentage; W = specific weight; Y = yield; T = total protein; significance: $_1$ = $P \leq 0.05$; $_2$ = $P \leq 0.01$; $_3$ = $P \leq 0.001$; the positive correlations are highlighted in bold.

Tab. 2 - Correlazioni, calcolate su base mensile e multi-mensile, tra SAT (somma delle temperature attive) e le caratteristiche del raccolto. Legenda: P = percentuale di proteine; W = peso specifico; Y = resa; T = proteine totali; significatività: $_1$ = $P \leq 0.05$; $_2$ = $P \leq 0.01$; $_3$ = $P \leq 0.001$; *le correlazioni positive sono evidenziate in grassetto.*

AprI	*AprI-AprII*	*AprI-AprIII*	*AprI-MayI*	*AprI-MayII*	*AprI-MayIII*	*AprI-JunI*	*AprI-JunII* $\mathbf{Y}_1$	*AprI-JunIII* $\mathbf{W}_1\mathbf{Y}_1$
AprII $\mathbf{P}_1$	*AprII-AprIII*	*AprII-MayI*	*AprII-MayII*	*AprII-MayIII*	*AprII-JunI* $\mathbf{W}_1\mathbf{Y}_1$	*AprII-JunII* $P_1\mathbf{W}_2\mathbf{Y}_1$	*AprII-JunIII* $P_1\mathbf{W}_1\mathbf{Y}_1$	
AprIII	*AprIII-MayI*	*AprIII-MayII*	*AprIII-MayIII* $\mathbf{W}_2\mathbf{Y}_1$	*AprIII-JunI* $\mathbf{W}_1\mathbf{Y}_2$	*AprIII-JunII* $P_1\mathbf{W}_2\mathbf{Y}_1$	*AprIII-JunIII* $P_2\mathbf{W}_2\mathbf{Y}_1$		
MayI	*MayI-MayII* $\mathbf{W}_1$	*MayI-MayIII* $\mathbf{W}_2\mathbf{Y}_1$	*MayI-JunI* $P_1\mathbf{W}_1\mathbf{Y}_1$	*MayI-JunII* $P_2\mathbf{W}_1\mathbf{Y}_1$	*MayI-JunIII* $P_2\mathbf{W}_1\mathbf{Y}_1$			
MayII	*MayII-MayIII* $P_1\mathbf{W}_2\mathbf{Y}_2$	*MayII-JunI* $P_2\mathbf{Y}_1$	*MayII-JunII* $P_2\mathbf{W}_1\mathbf{Y}_1$	*MayII-JunIII* $P_2\mathbf{W}_1\mathbf{Y}_1$				
MayIII $P_2\mathbf{W}_2\mathbf{Y}_1$	*MayIII-JunI* P_2	*MayIII-JunII* $P_1\mathbf{W}_1\mathbf{Y}_1$	*MayIII-JunIII* $P_2\mathbf{W}_1\mathbf{Y}_1$					
JunI P_1	*JunI-JunII* P_2	*JunI-JunIII* P_2						
JunII $P_2\mathbf{W}_1$	*JunII-JunIII* $P_2\mathbf{W}_1$							
JunIII $P_1\mathbf{Y}_1$								

Tab. 3 - Correlations, calculated on a 10-day and multi 10-day basis, between NDVI and the quali-quantitative variables of harvest. Legend: I = first 10-day of month; II = second 10-day of month; III = third 10-day of month; P = protein percentage; W = specific weight; Y = yield; T = total protein; significance: $_1$ = $P \leq 0.05$; $_2$ = $P \leq 0.01$; $_3$ = $P \leq 0.001$; the positive correlations are highlighted in bold.

Tab. 3 - Correlazioni, calcolate per decadi e per valori medi di più decadi, tra NDVI e le variabili quali-quantitative del raccolto. Legenda: I = prima decade del mese; II = seconda decade del mese; III = terza decade del mese; P = percentuale di proteine; W = peso specifico; Y = resa; T = proteine totali; significatività: $_1$ = $P \leq 0.05$; $_2$ = $P \leq 0.01$; $_3$ = $P \leq 0.001$; *le correlazioni positive sono evidenziate in grassetto.*

the transpiration rate and reducing the potential yield (Simane *et al.*, 1993).

T is negatively correlated with winter precipitation and spring temperatures, depending on both productive variables P and Y. These results indicate that the weather predominant effects consist of the negative impact of rainfall on P and of temperature on Y.

The empirical approach is a limitation to the extension of the study results to other climatic contexts. However, the acquired knowledge can be useful for the modeling applications integrated with the climatic seasonal forecast, in order to develop a winter durum wheat local forecast system able to supply information about the potential quality and quantity of harvest to cereal growers, technicians and pasta producers.

ACKNOWLEDGMENTS

The authors wish to thank Fondazione Monte dei Paschi di Siena and Consorzio Agrario di Siena for their support to this research. This work was awarded as the best degree thesis 2010 by Associazione Italiana di AgroMeteorologia.

REFERENCES

Anderson W.K., 1992. Increasing grain yield and water use of wheat in a rainfed Mediterranean-type environment. Australian Journal of Agricultural Research 43, 1-17.

Ciaffi M., Tozzi L., Borghi B., Corbellini M., Lafiandra D., 1996. Effect of heat shock during grain filling on the gluten protein composition of bread wheat. J. Cereal Sci. 24 (2), 91-100.

Connor D.J., Theiveyanathan S., Rimmington G.M., 1992. Development, growth, water use and yield of a Spring and a Winter wheat in response to time of sowing. Australian Journal of Agricultural Research 43, 493-516.

Dalla Marta A., Grifoni D., Mancini M., Zipoli G., Orlandini S., 2010. The influence of climate on durum wheat quality in Tuscany, Central Italy. International Journal of Biometeorology, 55:87-96.

Dexter J.E., Matsuo R.R., 1980. Relationship between durum wheat protein properties and pasta dough rheology and spaghetti contents quality. J.Agric.Food Chem., 28:899-902.

Month			*r*	S
November	P	SP_{nov}	-0.51	n.s.
	W	$NDVI_{novIII}$	-0.45	n.s.
	Y	$NDVI_{novIII}$	-0.59	n.s.
	T	$NDVI_{novIII}$	-0.64	*
December	P	$SP_{nov\text{-}dec}$	-0.59	n.s.
	W	$NDVI_{decI}$	-0.58	n.s.
	Y	$NDVI_{novIII}$	-0.59	n.s.
	T	SP_{dec}	-0.67	*
January	P	$SP_{nov\text{-}jan}$	-0.65	*
	W	$NDVI_{decI}$	-0.58	n.s.
	Y	$SP_{dec\text{-}jan}$	-0.59	n.s.
	T	$SP_{dec\text{-}jan}$	-0.80	**
February	P	$SP_{nov\text{-}feb}$	-0.71	*
	W	$NDVI_{decI}$	-0.58	n.s.
	Y	$SP_{dec\text{-}jan}$	-0.59	n.s.
	T	$SP_{dec\text{-}jan}$	-0.80	**
March	P	$SP_{nov\text{-}feb}$	-0.71	*
	W	SAT_{mar}	-0.75	**
	Y	$SP_{dec\text{-}jan}SAT_{mar}$	0.83	**
	T	$SP_{dec\text{-}jan}$	-0.80	**
April	P	$SP_{nov\text{-}apr}SAT_{apr}$	0.83	**
	W	$SP_{mar\text{-}apr}SAT_{mar\text{-}apr}$	0.88	**
	Y	$SP_{dec\text{-}jan}SAT_{mar\text{-}apr}$	0.91	***
	T	$SP_{dec\text{-}jan}$	-0.80	**
May	P	$SP_{nov\text{-}may}SAT_{feb\text{-}may}$	0.94	***
	W	$SP_{mar\text{-}apr}SAT_{mar\text{-}may}$	0.97	***
	Y	$SP_{dec\text{-}jan}SAT_{mar\text{-}may}$	0.94	***
	T	$SP_{dec\text{-}jan}SAT_{mar\text{-}may}$	0.93	***
June	P	$SP_{nov\text{-}may}SAT_{feb\text{-}may}$	0.94	***
	W	$SP_{mar\text{-}apr}SAT_{mar\text{-}may}$	0.97	***
	Y	$SP_{dec\text{-}jan}SAT_{mar\text{-}may}$	0.94	***
	T	$SP_{dec\text{-}jan}SAT_{mar\text{-}may}$	0.93	***

Tab. 4 - Best predictive indices in each month for quali-quantitative variables of winter durum wheat harvest. Legend: decI = first 10-day of month; decII = second 10-day of month; decIII = third 10-day of month; P = protein percentage; W = specific weight; Y = yield; T = total protein; r = coefficient of correlation; S = significance; n.s. = not significant; * = $P \leq 0.05$; ** = $P \leq 0.01$; *** = $P \leq 0.001$.

*Tab. 4 - I migliori indici predittivi in ciascun mese per le variabili quali-quantitative del raccolto del frumento duro . Legenda: decI = prima decade del mese; decII = seconda decade del mese; decIII = terza decade del mese; P = percentuale di proteine; W = peso specifico; Y = resa; T = proteine totali; r = coefficiente di correlazione; S = significatività; n.s. = non significativo; * = P≤0.05; ** = P≤0.01; *** = P≤0.001.*

Freeman K.W., Raun W.R., Johnson G.V., Mullen R.W., Stone M.L., Solie J.B., 2003. Late-Season Prediction of Wheat Grain Yield and Grain Protein. Communications in Soil Science and Plant Analisys. Vol. 34, n° 13 e 14, pp. 1837-1852.

Hansen P.M., Jørgensen J.R., Thomsen A., 2002. Predicting grain yield and protein content in winter wheat and spring barley using repeated canopy reflectance measurements and partial least squares regression. J. Agric. Sci. 139, 307-318.

Holben B.N., 1986. Characteristics of maximum-value composite images from temporal AVHRR data. Int. J. Remote Sens. 7, 1417-1434.

Labus M.P., Nielsen G.A., Lawrence R., Engel R., Long D.S., 2002. Wheat yield estimates using multi-temporal NDVI satellite imagery. Int. J. Remote Sens. 23 (20), 4169-4180.

Motzo R., Fois S., Giunta F., 2007. Protein content and gluten quality of durum wheat (*Triticum turgidum* subsp. *Durum*) as affected by sowing date. J Sci Food Agric 87:1480-1488

Orlandini S., Grifoni D., Natali F., Mancini M., Dalla Marta A., 2010. Impacts of climate change on Tuscany durum wheat quality. In: Advances in Environmental Modeling and Measurements (Eds. D.T. Mihailovic, B. Lalic). Nova Science Publishers Inc., New York (USA), 195-208.

Pan J., Zhu Y., Cao W., Dai T., Jiang D., 2006. Predicting the protein content of grain in winter wheat with meteorological and genotypic factors. Plant Prod. Sci. 9, 323-333.

Peltonen-Sainio P., Jauhiainen L., Trnka M., Olesen J. E., Calanca P., Eckersten H., Eitzinger J., Gobin A., Kersebaum C., Kozyra J., Kumar S., Dalla Marta A., Micale F., Schaap B., Seguin B., Skjelvåg A.O., Orlandini S., 2010. Coincidence of variation in yield and climate in Europe. Agriculture, Ecosystems and Environment 139, 483-489.

Peñuelas J., Filella I., 1998. Visible and near-infrared reflectance techniques for diagnosing plant physiological status. Trends Plant Sci. 3, 151-156.

Powlson D.S., Hart P.B.S., Poulton P.R., Johnston A.E., Jenkinson D.S., 1992. Influence of soil type, crop management and weather on the recovery of 15N-labelled fertilizer applied to winter wheat in spring. J. Agric. Sci (Cambrige). 118, 83-100.

Raun W.R., Solie J.B., Johnson G.V., Stone M.L., Lukina E.V., Thomason W.E., Schepers J.S.,

1993. In-season prediction of potential grain yield in winter wheat using canopy reflectance. Agron. J. 93, 130-138.

Schlehuber A.M., Tucker B.B., 1959. Factors affecting the protein content of wheat. Cereal Sci. Today 4, 240-242.

Simane B., Peacock J.M., Struik P.C., 1993. Differences in developmental plasticity and growth rate among drought-resistant and susceptible cultivars of durum wheat (*Triticum turgidum* L. var. *durum*). Plant Soil 157:155-166.

Smith G.P., Gooding M.J., 1999. Models of wheat grain quality considering climate, cultivar and nitrogen effects. Agric. For. Meteor. 94, 159-170.

Whan B.R., Carlton G.P., Anderson W.K., 1991. Potential for increasing early vigour and total biomass in spring wheat. I. Identification of genetic improvements. Australian Journal of Agricultural Research 42, 347-61.

Wheeler T.R., Batts G.R., Ellis R.H., Hadley P., Morison J.I.L., 1996. Growth and yield of winter wheat (Triticum aestivum) crops in response to CO_2 and temperature. J. Agric. Sci. (Cambridge) 127, 37-48.

Comparison of phytophenological data: a proposal for converting between GFI and BBCH scales

Giovanna Puppi[1], Anna Letizia Zanotti[1]*

Abstract: *Phenological scales used in the past were not standardized: in different countries different methods were followed and these are often still in use today: for example Italian Botanists usually make the phenological observations by means of the GFI key, adopted in 1993 by the Italian Phenological Gardens, or by Marcello's Key. The comparability of data collected with different methods is a serious problem, so, in the last 20 years the scientific community has directed significant efforts toward the standardization of sampling methods and phenological scales: in Europe, the BBCH scale (Meier, 1997) has been generally adopted. Although the BBCH and GFI scales have different structures, several stages are corresponding. We present a method for the conversion between BBCH and GFI scales, based on the numerical relationship between the codes of the respective stages: in the reproductive cycle the relation is well approximated by a sigmoid function, while in the leaf development, by a linear function. The presented method also allows the fractional values of the stages to be converted (e.g. the average value of a population).*
Keywords: *Phenological scales, BBCH, GFI, growth stages, flowering, leafing*

Riassunto: *I rilievi fenologici in campo si effettuano avvalendosi di protocolli e scale (chiavi) fenologiche, che in passato non erano standardizzati. In paesi e in ambienti scientifici diversi si sono affermate scale di rilievo diverse: ad esempio in Italia tra i botanici è in uso la chiave GFI adottata nel 1993 dai Giardini Fenologici Italiani, o la scala "Marcello". L'uso di chiavi diverse crea problemi di confrontabilità dei dati, così, negli ultimi 20 anni si è cercato di convergere verso una soluzione standard a livello internazionale, rappresentata dalla scala centesimale BBCH (Meier, 1997). La scala BBCH è costruita in modo diverso rispetto alla scala GFI, tuttavia è possibile trovare corrispondenze nella descrizione di alcuni stadi. Qui viene presentata una ipotesi di conversione numerica tra la chiave GFI e la BBCH, che si basa sulle relazioni tra i valori numerici degli stadi delle due scale: per il ciclo riproduttivo la relazione si può approssimare con una funzione sigmoide e per lo sviluppo fogliare con una retta. Questa soluzione permette di convertire non solo gli stadi principali della chiave GFI, ma anche i valori frazionari (ad es. valori medi su vari individui).*
Parole chiave: *Scale fenologiche, BBCH, GFI, stadi di sviluppo, fioritura, fogliazione*

INTRODUCTION

Phenology, "*the study of the timing of recurring biological events*", is today largely an applied science, related to agriculture, forestry, climatology, human health, biomonitoring, etc.

In the 1990s the interest in phenological research increased substantially, because many studies showed that the timing of life cycle events provide a good indicator for climate change impacts (Schwartz, 2003). The growing importance of phenology for climate monitoring is also visible in the 4th assessment report of the IPCC (2007) and WMO Commission for Climatology (2007) and moreover, in the guidelines of the WCRP (World Climate Research Programme) where recommended methods for undertaking phenological observations are stated (Koch, 2010).

This renewed interest in Phenology has increased the demand for long series of data and the international cooperation at continental level. In Europe a great amount of phenological data were recorded in the past, but with quite different histories and traditions of observations (Menzel, 2003; Nekovar *et al.*, 2008; Koch, 2010): the observation methods, the coding systems, the monitoring guidelines were different among countries, and thus we now have a large data set at a continental level, without the homogeneity necessary for many applications.

The plans for establishing a global phenological network were started in 1993 by the Phenology Study Group of the ISB (International Society for Biometeorology) and then in 1996 the Global Phenological Monitoring Program (GPM) was completed. A main objective of the GPM was to increase cooperation and to provide standard methods as a basis for communication and research (Bruns *et al.*, 2003).

In the last decade, European projects have been set up to facilitate the integration between networks

* Corresponding Author e-mail: giovanna.puppi@unibo.it
[1] Dipartimento di Biologia E.S, Università di Bologna
Received 26 July 2011 accepted 11 October 2011

and the creation of one single database (EPN over the 2001-2003 period; Cost Action 725 over the 2004-2009 period). In all the cited projects (GPM, EPN, COST 725, PEP 725) phenological phases are defined according to the BBCH code, which classifies the plant growth phases of a large number of species on the base of a standardized system.
The Biologische Bundesanstalt Bundessortenamt, Chemische Industrie BBCH scale (Meier, 1997) is an internationally recognized standard in the agricultural sector. All cultivated plants with economic importance have their appropriate scales. For other species, the general BBCH scale can be used. The principal scale, characterized by ten principal growth stages, forms the framework within which the individual scales are developed (Tab. 1). The secondary growth stages 1 to 9 correspond to the respective ordinal numbers or percentage values. For example stage 3 could represent: 3rd true leaf, 3rd tiller, 3rd node or 30% of the final length or size typical of the species or 30% of the flowers open. The combination of the principal and the secondary stages, results in the two-digit code: for some cases a three-digit scale is presented alongside the two-digit scale.
This involves the inclusion of the so-called mesostage between the principal and the secondary stage, which provides a further subdivision (Meier, 2001).

Codes of Principal Stages	Description
0	Germination/sprouting/bud development
1	Leaf development (main shoot)
2	Formation of side shoots/ tillering
3	Stem elongation or rosette growth/ shoot elongation (main shoot)
4	Development of harvestable vegetative plant parts or vegetatively propagated organs/ booting (main shoot)
5	Inflorescence emergence (main shoot)/ heading
6	Flowering (main shoot)
7	Development of fruit
8	Ripening or maturity of fruit and seeds
9	Senescence, beginning of dormancy

Tab. 1 - Principal growth stages of the BBCH scale.
Tab. 1 - Stadi principali della scala BBCH.

Phenological scales in Italy

In Italy, the oldest phenological networks dates from the end of 19th century (Puppi and Zanotti, 2009) and are mainly related to meteorological networks. The international network (Belgium, The Netherlands, Germany, France, Italy) directed by the Belgian astronomer Adolphe Quetelet from 1840 to 1870, had several collaborators in Italy and a number of Italian scientists followed its methods (Caruel, Serpieri and others). Quetelet's protocol, with detailed instructions for the observations, was printed in 1853 by the Royal Academy of Sciences (Demarée and Chuine, 2006; Demarée, 2009).
Some years later (1876-1884), in 4 provinces of Northern Italy (Vicenza, Venice, Padua, Bologna) a phenological network was organized and directed by A. Da Schio in the years 1876-1884: a few phenophases (First leaf extended, Flowering, First fruit ripening, Leaves fall) were observed in a large number of common species (102). In 1885 the network was enlarged to the entire nation (Ministero per l'Agricoltura, 1887) with agro-meteorological aims.
In the same period, the first European Phenological network, also including Northern Italy, was established under the direction of Egon Ihne (1883-1941). Several standard phenophases were observed: b= beginning of flowering; BO= beginning of leaf unfolding; f= first fruit ripe ; W=green wood (more than 50% of leaves completely opened); LV= autumn colouring (more than 50% of leaves changed, including those fallen). In all the above-mentioned cases, a limited set of developmental phases was considered: in fact the purpose of the observations, was to indentify the date of occurrence of selected phenophases, in order to compare different sites and years (for bio-meteorological purposes), rather than to describe the developmental rhythm of species (biological research).
The Italian Phenological Network started at the beginning of the 20th century (1922-1936) under the direction of the mathematician M. Minio and was later renewed (from 1953 to 1965) by the naturalist A. Marcello, one of the most important Italian phenologists.
Marcello conceived a new method to assess the flowering development (Marcello, 1935) using a set of 3 binary codes (+=present and 0=absent): the first code was referred to flower buds, the second to open flowers, the third to faded flowers. So, for instance, if a plant begins to flower, it is coded by the sequence ++0, because of the presence of flower buds and open flowers, at the same time with the absence of faded flowers; hence, if a plant is in full bloom it is coded by +++ (or 0+0), and if all the flowers are faded, the code is 00+ (end of flowering). The 7 stages of the Marcello's Key ($\overline{000}$,

+00, ++0, +++, 0++, 00+, 000), are sequential in time and cover the whole flowering development, from the beginning to the end. The attractiveness of the method lies in its simplicity: all the phases are easily individuated and every case can be classified unambiguously.
Marcello's Key had a great success in Italy: it was adopted in the Italian Phenological Network (1953-1965) and was largely utilised by many scientists even after the closing of the network.
After several decades, a similar approach was applied to fruit development by Arrigoni (1977).
In the mid '80s a new sequential key for describing vegetative development was proposed by a group of phenologists of the University of Bologna (Puppi *et al.*, 1985; Puppi, 1989).
This sequential key described all the vegetative stages of the cycle of plants and was inspired by previous European keys (Ellenberg, 1954, 1956; Dierschke, 1972).

The GFI scale

In 1982 the first Italian Phenological Garden was founded at S. Pietro Capofiume near Bologna, with the purpose to join the IPG (International Phenological Gardens) network. In the following years other Gardens were added and finally, in 1993, the network of the "Giardini Fenologici Italiani" (GFI) was officially set up (Malossini, 1993). Besides the phases required by the IPG (BO = beginning of leaf unfolding,, M= May shoot, J= St.John's sprout, LV= autumn colouring, BF= leaf fall, B= beginning of flowering, AB= full flowering, F= first fruit ripe) in the Italian Gardens complete observations of the plant cycles were made by means of two new scales, reproductive and vegetative, named GFI (Tab. 2): the reproductive scale, in 12 stages, was the combination of the Marcello's and Arrigoni's keys, while the vegetative one, in 14 stages, was derived from that of the Bologna group (Puppi, 1989). The GFI scales

Codes of stages	Description
R 1	Flower buds (or inflorescences) visible, but not developed (+00)
R 2	Flower buds ready to open, petals just visible (aments developed but immature) (+00)
R 3	Flower buds and open flowers (immature and pollinating aments) (++0)
R 4	Full flowering: buds, open flowers and faded flowers (pollinating aments) (+++, 0+0)
R 5	Flower fading: open flowers together with withered ones; (pollinating and spent aments) (0++)
R 6	End of flowering: only withered flowers (spent aments) (00+)
R 7	Beginning of ovary growing (000)
R 8	Beginning of fruit development (size)
R 9	Fruits developed but mostly unripe
R10	Fruits mostly fully ripe
R11	Beginning of fruit fall and seeds dispersal
R12	Fruits spent or fallen; end of seeds dispersal
V 1	Bud dormancy
V 2	End of bud swelling
V 3	Bud breaking: swollen and opening buds with folded leaves
V 4	Open buds and first young leaves with unfolded blade
V 5	Young leaves unfolded, not yet full size
V 6	Young leaves unfolded together with leaves fully expanded
V 7	Leaves fully developed
V 8	Beginning of leaf discolouring
V 9	Leaves mostly discoloured
V10	Beginning of leaf dryness
V11	Leaves mostly dried up
V12	Beginning of leaf fall
V13	Leaves mostly fallen
V14	End of leaf fall, plants dormant

Tab. 2 - Growth stages of the GFI scale (Italian Phenological Gardens).
Tab. 2 - Stadi fenologici della scala GFI (Giardini Fenologici Italiani).

Italian Journal of Agrometeorology - 3/2011
Rivista Italiana di Agrometeorologia - 3/2011

Scheda osservazioni fenologiche – Angiosperme legnose – parte II

Giardino fenologico di…………………………………………………………………………………………
Specie……………………………… Varietà……………………………………… Nome comune……………………………
Famiglia……………………………… Posizione……………………… Età……….. Provenienza……………………………
Osservazioni…………………………………………………………………………………………

Norme di rilevamento e note

Le rilevazioni fenologiche vanno effettuate su singoli individui di ciascuna specie con cadenza settimanale. Il rilevamento consiste nell'identificazione della fase fenologica (talora si verifica la compresenza di più fasi) in cui si trova l'individuo. Le fasi fenologiche (fenofasi) da rilevare sono indicate nella relativa chiave di rilevamento. Osservazioni: spazio riservato alle osservazioni che non rientrano nelle tipologie previste dagli altri settori della scheda: fitopatie (malattie fungine, attacchi di insetti, virosi, batteriosi, danni provocati dalla grandine, dal gelo, dal vento, dalle lepri, danni accidentali,ecc.), operazioni colturali (potatura, trattamenti antiparassitari, concimazioni, irrigazioni, diradamento, spollonatura, ecc.). Non vanno segnalate le normali cure del giardino come fresatura, zappatura, rasatura erba, ecc..

Chiave di rilevamento

V01 Gemme in riposo: le gemme non hanno ancora iniziato ad ingrossarsi	**R01 Boccioli e amenti presenti ma poco sviluppati:** i boccioli o gli amenti sono ben visibili ma non hanno ancora completato il loro sviluppo
V02 Gemme rigonfie prossime alla schiusura: le gemme sono rigonfie ma non lasciano ancora vedere le foglioline sottostanti	**R02 Boccioli prossimi alla schiusura, rigonfi, con petali visibili; amenti sviluppati ma immaturi:** i boccioli sono prossimi alla schiusura, è visibile il colore dei petali; gli amenti sono completamente sviluppati, quelli maschili hanno stami con antere intatte che non emettono polline
V03 Gemme rigonfie assieme a gemme aperte, con foglioline ripiegate: sono visibili le foglioline nelle prime gemme aperte; le foglioline non hanno ancora disteso il lembo	**R03 Boccioli rigonfi e fiori aperti; amenti immaturi e amenti maturi:** compresenza di boccioli nei quali è visibile il colore dei petali e fiori aperti; gli amenti sono completamente sviluppati: quelli maschili, in parte, emettono polline
V04 Gemme appena aperte assieme a foglioline a lembo disteso: le gemme sono quasi tutte aperte e hanno già emesso le prime foglioline; parte di esse hanno il lembo disteso	**R04 Piena fioritura: boccioli, fiori aperti, fiori sfioriti; amenti maturi:** fiori sbocciati, pistilli e stami pronti per l'impollinazione; amenti maturi: quelli maschili hanno antere aperte che emettono polline
V05 Foglie giovani a lembo disteso: le giovani foglie hanno spinato il lembo che inizialmente era ripiegato dentro le gemme	**R05 Inizio sfioritura: fiori aperti e fiori appassiti; amenti maturi e amenti sfioriti:** i fiori e gli amenti hanno quasi completato la fioritura
V06 Foglie giovani insieme a foglie adulte: alle giovani foglie con lembo aperto si accompagnano foglie completamente sviluppate	**R06 Completa sfioritura:** fiori appassiti; amenti sfioriti: la fioritura è stata completata e sulla pianta rimangono solo fiori appassiti o amenti sfioriti
V07 Foglie adulte: le foglie sono completamente sviluppate	**R07 Allegagione:** inizio ingrossamento ovari; gli ovari fecondati sono visibil e hanno iniziato a trasformarsi in frutti
V08 Inizio della decolorazione fogliare: le foglie assumono colorazioni diverse dal verde (es. virano dal rosso al giallo), per fenomeni di senescenza	**R08 Inizio fruttificazione:** sono visibili sia ovari ingrossati che frutti in fase di accrescimento
V09 Foglie prevalentemente decolorate: la maggior parte delle foglie ha cambiato colore	**R09 Frutti evidenti ma in prevalenza immaturi;** i frutti sono ben visibili, ma immaturi
V10 Inizio disseccamento foglie: le foglie, dopo aver mutato colore, iniziano a disseccarsi	**R10 Culmine della fruttificazione:** i frutti sono maturi e cambiano consistenza (intenerimento dei carnosi e indurimento dei secchi)
V11 Foglie prevalentemente disseccate: la maggior parte delle foglie è disseccata	**R11 Frutti in parte caduti, degenerati o secchi:** completata la maturazione i frutti sono in parte caduti, degenerati o secchi
V12 Inizio caduta foglie: alcune foglie sono cadute, la chioma è ancora folta	**R12 Presenza di soli frutti residui:** i frutti sono tutti caduti, degenerati o secchi
V13 Foglie prevalentemente cadute: la maggior parte delle foglie è caduta e la chioma è visibilmente diradata	
V14 Piante completamente spoglie: tutte le foglie sono cadute e la pianta è spoglia	

Fig. 1 - Survey form adopted by the Italian Phenological Gardens. Guidelines and phenological scales (Botarelli and Sacchetti 1998, page 13).
Fig. 1 - Scheda fenologica adottata dai Giardini Fenologici Italiani (II parte). Norme di rilevamento e scale fenologiche. (Botarelli e Sacchetti 1998, pag. 13).

(Malossini, 1993, Botarelli and Sacchetti, 1998), still adopted today in the Italian Phenological Gardens (Fig. 1), were widely utilized in Italy also in phenological research on wild plants (Zanotti and Puppi, 2000; Chiesura Lorenzoni, 2003; Zanotti *et al.*, 2003; Bianchi and Drigo, 2009, Delleani *et al.*, 2009; etc.).

AIMS

The aim of this study is to realize a framework of conversion between the BBCH and the "GFI-Angiosperme legnose" (woody Angiosperms) scales. The conversion is necessary to allow comparisons between Italian and European data, and to enhance the value of many decades of phenological observations.

METHODS

The method consists of four steps:

1) Investigation of all the reliable correspondences between GFI and BBCH phenophases on the basis of their descriptions.
2) Building of the numerical relationships between the codes of the two scales, approximating by the best-fit function the points identified in step 1.
3) Use of the functions found in step 2 in order to calculate the remaining correspondences.
4) Test of the correspondences found in step 3, comparing the definitions of the phases.

Despite GFI is a qualitative scale, and vice-versa the BBCH is mostly quantitative (Meier, 2001), the method described above should be enforceable, since the two scales have a substantial affinity. In fact, both the phenological scales are largely sequential, having a continual succession of phases over time. In other words, the growing stages are identified as progressive steps of one developmental process, which can be represented by a function (stages versus time). Therefore we suppose that the growing functions of BBCH and GFI are substantially similar and thus comparable.

In the curve fitting process we tested several mathematical function (linear, logarithmic, polynomial, sigmoid functions, etc.) by regression analysis, selecting the one that showed the best fit to the series of the data points.

RESULTS

First of all we analyzed the gross relation between the GFI phases and BBCH stages: from this preliminary analysis some BBCH principal growth stages (2, 3, 4) were set aside, because they are missing in the GFI key.

Then we analyzed separately the correspondences in:

a) Flower bud development, Flowering, Fruit development and ripening (BBCH= 5 to 8; GFI= R1 to R12)
b) Bud and leaf development (BBCH= 0 and 1; GFI= V1 to V6)
c) Senescence and leaf fall (BBCH= 9; GFI= V7 to V14)

The definitions of stages generally refer to the BBCH general scale (Meier, 2001), except for a few cases, where specific scales (Fruits: Pome fruits, Stone fruits, Currants, Grape) are considered.

a) Flower bud development, Flowering, Fruit development and ripening

After an accurate analysis of the definitions of reproductive stages, the following biunique correspondences were singled out:

GFI=R2 (*Flower buds ready to open (petals just visible)*) corresponds to BBCH=59 (*Inflorescence fully emerged, first flower petals visible (in petalled forms)*)

GFI=R4 (*Full flowering: buds, open flowers and faded flowers*) corresponds to BBCH=65 (*Full flowering: 50% of flowers open, first petals may be fallen*)

GFI=R5 (*Flower fading: open flowers together with withered ones*) corresponds to BBCH=67 (*Flower finishing: majority of petals fallen or dry*)

GFI=R6 (*End of flowering, only withered flowers*) corresponds to BBCH=69 (*End of flowering: fruit set visible*)

GFI=R7 (*Beginning of ovary growing*) could correspond to BBCH=71 (*Ovary growing, beginning of fruit growth* (see Stone Fruit and Currant scales))

GFI=R10 (*Fruits mostly fully ripe*) corresponds to BBCH=89 (*Fully ripe: fruit shows fully ripe colour, beginning of fruit abscission*)

The remaining GFI phases have a range of correspondence with several BBCH stages:

GFI=R1 corresponds to BBCH= 51 to 55
GFI=R3 corresponds to BBCH= 61 to 64
GFI=R8 corresponds to BBCH= 72 to 77(78)
GFI=R9 corresponds to BBCH= (78) 79 to 87

Note that R11 (*Beginning of fruit fall and seeds dispersal*) and R12 phases (*Fruits spent or fallen, end of seeds dispersal*) aren't represented in the BBCH scale: in these cases, following the BBCH guidelines, new three-digit codes could be proposed (for example R11=BBCH 895; R12= BBCH 899).

Afterward, we analysed the relationship between

the two scales, putting the numerical values of the corresponding stages in a graph (Fig. 2): the two scales appear to have a non-linear relationship and it seems justifiable to approximate the points by a sigmoid function.
We tested the logistic equation: $Y=K/(1+e^{(a-bx)})$, where x= BBCH stages, Y= GFI phases, K= upper asymptote, a= constant (distance from the origin), b= speed of variation.
The best fit function shows a very high value of correlation coefficient (R^2= 0.999 **): the values of parameters are: K=10.2 ; a= 11.98; b= 0.1787.
We then examined the GFI phases with uncertain correspondence (R1, R3, R8, R9): the estimated values in BBCH were calculated by the best fit equation (Tab. 3) and the reliability of the correspondences was checked. Therefore, the best fit logistic function seems to be adequate for calculating the correspondences of the reproductive stages.

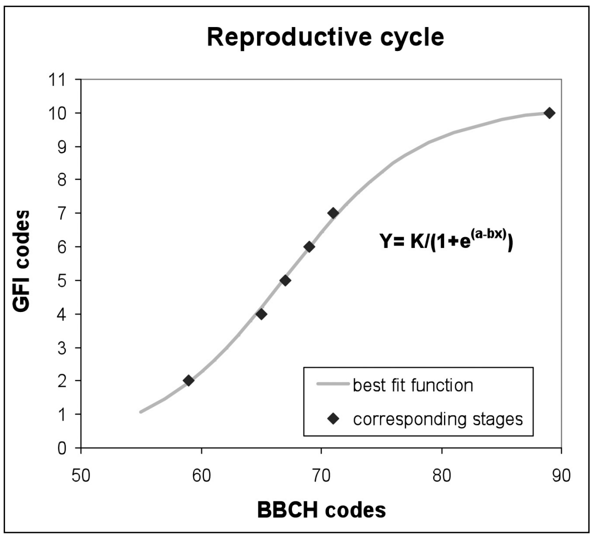

Fig. 2 - Relationship between the reproductive codes of BBCH and GFI. The points of the corresponding stages are approximated by a sigmoid function:
$Y= K/(1+e^{(a-bx)})$, where: X= BBCH stages, Y= GFI phases, K= upper asymptote, a= constant (distance from the origin), b= speed of variation.
The drawn line is the best fit function: the value of correlation coefficient is high and significant (R2= 0.9992 **); the values of the parameters are: K= 10.2; a=1198; b=0.1787.
Fig. 2 - Relazioni tra i codici numerici delle scale BBCH e GFI. I punti relativi agli stadi corrispondenti sono approssimati con una funzione sigmoide: $Y= K/(1+e^{(a-bx)})$, dove poniamo: X= stadi BBCH, Y= stadi GFI, K= asintoto superiore, a= costante (distanza dall'origine), b= velocità di variazione.
*La linea disegnata è quella della migliore funzione approssimante: il valore del coefficiente di correlazione è alto e significativo (R2= 0.9992 **); i valori dei parametri sono: K= 10.2; a= 11.98; b= 0.1787.*

GFI R codes	BBCH codes	BBCH estimated values
2	59	59
4	65	65
5	67	67
6	69	69
7	71	71
10	89	89
1		55
3		62
8		74
9		78

Tab. 3 - GFI-BBCH conversion table of the reproductive cycle. Recognized correspondences between stages are reported in the first and second columns: the correspondences of the last four GFI codes are undefined. The BBCH values in the third column are calculated by the best fit function of figure 2.
Tab. 3 - Tabella di conversione GFI-BBCH per il ciclo riproduttivo. Nella seconda colonna sono riportati gli stadi BBCH riconosciuti come esattamente corrispondenti a stadi GFI: mancano le corrispondenze delle ultime quattro fasi GFI, in quanto non chiaramente definite. Nella terza colonna sono riportati i valori di BBCH calcolati con la funzione di figura 2.

b) Bud and leaf development

The same procedure was applied also to the beginning of the vegetative cycle, from "*Winter dormancy*" to "*First leaves fully expanded*".
The following biunique correspondences were found:
GFI=V1 (*Bud dormancy*) corresponds to BBCH=00 (*Winter dormancy*)
GFI=V2 (*End of bud swelling*) corresponds to BBCH=03 (*End of bud swelling*)
GFI=V4 (*Open buds and first leaves with unfolded blade*) corresponds to BBCH=11 (*First leaf, leaf pair, or whorls, unfolded*)
GFI=V6 (*Young leaves unfolded together with leaves fully expanded*) corresponds to BBCH=19 (*first leaves fully expanded* (see BBCH for Fruits))
while the remaining GFI phases have a range of correspondence with several stages:
GFI=V3 (*Bud breaking: swollen and open buds with folded leaves*) corresponds to BBCH=7 to 10
GFI=V5 (*Young leaves unfolded, not yet full size*) corresponds to BBCH=12 to 18.
In this case the relationship between the two scales appears to be linear, so it seems justifiable to approximate the points by a linear function (Fig. 3) as: Y=a+bX
The best fit equation shows a high value of

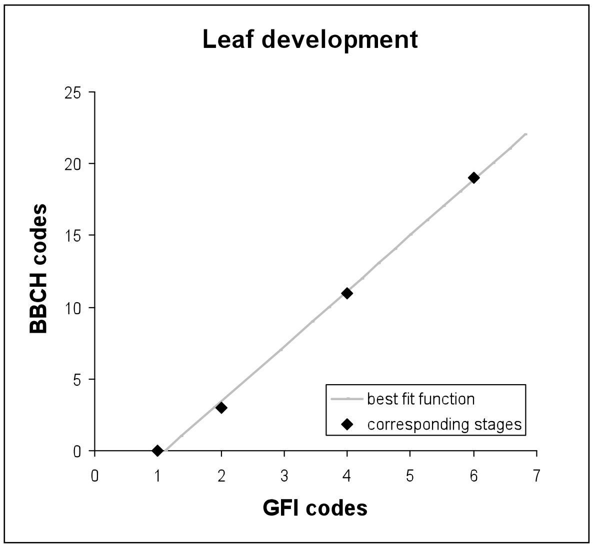

Fig. 3 - Relationship between GFI and BBCH codes of Leaf development. The points of the corresponding stages are approximated by a linear function. The value of correlation coefficient is high and significant (R2= 0.998 **): the values of parameters are: cost= - 4.254 and slope= 3.847.
*Fig. 3 - Relazioni tra i codici numerici delle scale BBCH e GFI dello sviluppo fogliare. I punti relativi agli stadi corrispondenti sono approssimati con una funzione lineare: il coefficiente di correlazione è alto e significativo (R2= 0.998 **): i valori dei parametri sono: intercetta= - 4.254; pendenza= 3.847.*

correlation coefficient (R^2= 0,998 **): the values of parameters are: a=-4,254 ; b=3,847.
We then examined the GFI phases with uncertain correspondence (R1, R3, R8, R9): the estimated values of BBCH were calculated by the best fit equation and the reliability of the correspondences was checked. The results are reported in Tab. 4.

c) Senescence and leaf fall
The numerical method could not be applied to the declining phases of the vegetative cycle, because the growing stages are not strictly sequential. To fix a precise sequentiality in leaf discolouring and falling is problematic because of the phenological differences between species: for example some trees become almost completely yellow (or red) before the beginning of leaf fall (*Ginkgo, Acer, Fagus, etc.*), while the foliage of others never become completely yellow because the beginning of discolouring is immediately followed by the start of leaf fall (*Sambucus*).
In the GFI, sequentiality is highly fragmented: V8-9 refer to leaf discolouring, V10-11 to leaf desiccation, and V12-13 to leaf fall, but it is well known that leaf desiccation and fall are alternative rather than sequential events. Moreover, even if V8

Vegetative cycle	GFI V codes	BBCH codes	BBCH estimated values
Leaf development	1	0	0
	2	3	3
	4	11	11
	6	19	19
	3		7
	5		15
Leaf senescence and fall	7	91	
	8	92	
	10 or 12	93	
	9	94	
	11 or 13	95	
	14	97	

Tab. 4 - GFI-BBCH conversion table of the Leaf development and senescence. Recognized correspondences between stages are reported in the first and second columns of data: the correspondences of the V3 and V5 GFI codes are undefined. The BBCH values in the third column of data are calculated by the best fit function of figure 3: the function cannot be applied to the last part of vegetative cycle (senescence).
Tab. 4 - Tabella di conversione GFI-BBCH per lo sviluppo e la senescenza fogliare. Nella seconda colonna di dati sono riportati gli stadi BBCH riconosciuti come esattamente corrispondenti a stadi GFI: mancano le corrispondenze delle ultime fasi GFI V3 e V5, in quanto non chiaramente definite. Nella terza colonna sono riportati i valori di BBCH calcolati con la funzione di figura 3: la funzione non è applicabile alla ultima parte del ciclo fogliare (senescenza).

(*Beginning of leaf discolouring*) always precedes V12 (*Beginning of leaf fall*), however in certain species, leaf fall (V12) can begin earlier than the discolouring of the majority of leaves (V9).
In the BBCH, sequentiality is almost achieved, but some phases are lacking or seem to be ambiguous. Moreover we notice that the second numbers of the code lose their quantitative meaning: only BBCH 95 maintains a link to the corresponding quantity "*50% of leaves fallen*".
The stage "*Beginning of leaf discolouring*" is lacking in the general scale, but is coded as 92 in the Fruit trees scales. The stage 93 is generally defined as "*Beginning of leaf fall*". The stage "*50% of leaves discoloured*" is lacking in the general scale, but in the Stone-fruit scale appears curiously coupled with leaf fall (BBCH 95); recently Bruns *et al.* (2003) proposed to use BBCH 94 for the stage "*50% of leaves discoloured*". Finally BBCH 97 is defined as "*end of leaf fall, above ground parts of plants dead or dormant*".
Nevertheless we found reasonable correspondences between the definitions of stages (Tab. 4):

- GFI V7 (*Leaves fully developed*) may correspond to BBCH 91 (*Foliage still fully green*)
- GFI V8 (*Beginning of leaf discolouring*) corresponds to BBCH 92
- GFI V9 (*Leaves mostly discoloured*) may be assigned to BBCH 94 (Bruns *et al.,* 2003)
- GFI V10 and V12 may be assigned to BBCH 93
- GFI V11 and V13 may be assigned to BBCH 95
- GFI V14 (*End of leaf fall, plants dormant*) corresponds to BBCH 97.

CONCLUSIONS

The numerical method for converting between GFI and BBCH scales here presented, is based on the sequential character of both the phenological keys and on their substantial affinity. The method is suitable for the larger part of the developmental cycle and shows several main advantages. First of all, the conversion of each stage is evaluated both singly, and considering the whole growing process. Then, having set up a rational and objective procedure, makes it possible to single out unambiguously the most uncertain correspondences between phases. Moreover, the use of mathematical functions enables the conversion even of the fractional GFI stages (derived from calculations of the average values of plant populations).
This method is inapplicable to the last part of the vegetative cycle, because the sequence of the senescence stages is based on different criteria in the two scales. In the latter case similar stages have to be compared and paired off singly, taking into consideration the phenological behaviour of the observed plant species or groups.
The importance of the conversion between GFI and BBCH scales is increased by the fact that the GFI includes older Italian keys (Marcello, etc.): in this way, a great amount of old phenological data, collected in the first part of the 20th century, could be compared with the European historical pheno-series.

ACKNOWLEDGMENTS

We would like to thank all the friends of the "Giardini Fenologici Italiani"and "Bioritmi e Fenologia" group for exchanging valuable opinions and field experiences: in particular we are grateful to Giovanna Aronne, Lucio Botarelli, Giovanni Dal Monte, Emanuele Eccel and Fabio Orlandi, for their precious suggestions and stimulating criticism.

REFERENCES

Arrigoni P.V., Lamioni S., Marconcini C., 1977. *Ricerche sinfenologiche in alcuni boschi della Toscana*. Webbia, 31:1-33.
Bianchi M., Drigo N., 2009. *Monitoraggio fenologico di Quercus.* Convegno IPHEN 2009, Fenologia vegetale, Roma 28 ottobre 2009. http://www.ucea.it/iphen/doc/iphen_2009.html
Botarelli L., Sacchetti V., (eds.), 1998. *Guida al Rilevamento dei Giardini Fenologici*. MiPA, Phenagri: 43 pp. http://www.phenagri.it/rprimopiano/manuali/Guida.pdf.
Bruns E., Chmielewski F.M., van Vliet A.J.H., 2003. *The Global Phenological Monitoring concept.* In Schwartz M.D.(ed.), *Phenology: an Integrative Environmental Science*. Tasks for Vegetation Science, vol.39. Kluwer, The Netherlands: 93-104.
Chiesura Lorenzoni F., 2003. *Specie guida fenologicamente predittive del comportamento delle colture.* Atti convegno nazionale "PHENAGRI: Fenologia per l'agricoltura" Roma, 5-6 dicembre 2002 UCEA, MiPAF: pp. 143-155.
Delleani D., Spanna F., Valfre' F., Caramiello R., Fossa V., Pelosini R., Loglisci N., 2009. *Il monitoraggio fenologico forestale in Piemonte*. Convegno IPHEN 2009, Fenologia vegetale, Roma 28 ottobre 2009. http://www.ucea.it/iphen/doc/iphen_2009.html
Demarée G.R., 2009. *The phenological observations and networking of Adolphe Quetelet at the Royal Observatory of Brussels*. Italian Journal of Agrometeorology 14(1):22-24.

Demarée G.R., Chuine I., 2006. *A concise history of the phenological observations at the Royal Meteorological Institute of Belgium*. In: Dazelios H., Tzortzios S. (eds.), *Proceedings* vol. III Phenology-Agroclimatology HAICTA, 20-23 September 2006. Volos.

Dierschke H., 1972. *Zur Aufnahme und Darstellung Phanologischer Erscheinnungen in Pflanzengesellschaften.* In: Tuxen R. (ed.), *Grundfragen und Methoden in der Pflanzengesellschaften.* Junk, Den Haag: 291-311.

Ellenberg, H., 1954. *Naturgemäße Anbauplanung, Melioration und Landespflege.* Landw. Pflanzensoziologie Bd. III. Verlag E. Ulmer, Stuttgart. 109 pp.

Ellenberg H., 1956. *Wuchsklimakarte von Sudwest-Deutschland*. Stuttgard.

IPCC, 2007. *Summary for policy makers. Climate change 2007: impacts, adaptations and vulnerability Working Group II contribution to the Intergovernmental Panel of Climate Change 4th assessment report.* Geneva.

Koch E., 2010. *Global Framework for Data Collection -Data Bases, Data availability, Future Networks, Online Databases*. In: Hudson I.L. and Keatley M.R. (eds.) *Phenological Research. Methods for Environmental and Climate Change Analysis*. Springer: 23-61.

Malossini A. (ed.), 1993. *Gruppo di Lavoro Nazionale per i Giardini Fenologici: Procedure per il rilevamento fenologico*. Regione Emilia Romagna, Bologna: 65 pp.

Marcello A., 1935. *Nuovi criteri per le osservazioni fitofenologiche.* N.Giorn. Bot. Ital. 42:543-56.

Meier U., 1997. *BBCH- Monograph Growth stages of plants.* Blackwell, Berlin und Wien: 622 pp.

Meier U. (ed.), 2001. *Growth stages of mono- and dicotyledonous plants,* BBCH - Monograph. 2 Edition, Federal Biological Research Centre for Agriculture and Forestry: 158 pp.

Menzel A., 2003. *Europe*. In: Schwartz M.D. (ed.). *Phenology: an Integrative Environmental Science*. Tasks for Vegetation Science, vol.39. Kluwer A.P., the Netherlands: 45-56.

Nekovář J., Koch E., Kubin E., *et al.* (eds.), 2008. *COST Action 725: The history and current status of plant phenology in Europe*. Finnish Forest Research Institut Muhos Research Unit COST Office Vammalan Kirjapaino Oy, Finland.

Puppi G.,1989. *Rilevamenti fenologici su piante della flora spontanea*. in Schirone B. (ed.), *Metodi di rilievo e rappresentazione degli stadi fenologici*. Quaderni metodologici n.12 IPRA. Grafica Tiburtina, Guidonia (Roma): 9-37.

Puppi G., Zanotti A.L., 2009. *Old phenological data on wild plants in Italy (XIX and early XIX century)*. Italian Journal of Agrometeorology, 14(1): 17-21.

Puppi Branzi G., Zanotti A.L., Speranza M., 1985. *Cartografia fenologica automatica nella collina bolognese*. Arch. Bot. Biogeogr. Ital. 61: 29-42.

Schwartz M.D. (ed.), 2003. *Phenology: an Integrative Environmental Science*. Tasks for Vegetation Science, vol. 39. Kluwer, The Netherlands: 521 pp.

WMO Commission for Climatology, 2007. *Expert team on climate monitoring*. http:// www.omm.urv.cat/ media/documents/WMOpdf.

Zanotti A.L., Puppi G., 2000. *Phenological surveys of allergenic species in the neighbourhood of Bologna (Italy)*. Aerobiologia. Vol. 16: 199-206.

Zanotti A.L., Puppi G., Zinoni F., Marletto V., 2003. *Mappe fenologiche a scala di dettaglio*. Atti convegno nazionale " PHENAGRI: Fenologia per l'agricoltura" Roma, 5-6 dicembre 2002, UCEA, MiPAF: pp. 118-124.

Processing tomatoes under different irrigation regimes in Southern Italy: agronomic and economic assessments in a simulation case study

Michele Rinaldi[1], Pasquale Garofalo[1], Piero Rubino[2], Pasquale Steduto[3]*

Abstract: *AQUACROP (Steduto et al., 2009; Raes et al., 2009) simulation model was calibrated and validated for processing tomatoes in Southern Italy (Capitanata Plain) and was subsequently used to evaluate the expected impact of different water irrigation regimes on yield, water use efficiency and net return.*
The simulated irrigation regimes were two: i) at fixed times (with seasonal water volumes of 170, 270, 370, 470 and 570 mm) and ii) using the soil water depletion criterion (refilling 30, 50 and 70 mm of soil water depletion). Cross calibration and validation, based on three years of experimental data (2002-2004), allowed to estimate crop parameters and their variation ranges, providing useful data which can be applied in similar environment conditions. The responses of the tomatoes in terms of plant biomass, fruit yield and water use efficiency were evaluated considering the mean values obtained from a long-term simulation. A simplified economic analysis, was performed to calculate the net return for each management scenario.
The greatest fresh fruit yield (123 t ha^{-1}) simulated by AQUACROP was obtained using an irrigation fixed time with 370 mm of seasonal water supply. About the same yield level was obtained with irrigation starting at 30 mm of soil water depletion, saving of about 70 mm of water.
The main advantage of soil water depletion criterion, apart from the low water loss in deep percolation, was the greater net income for farmers. Considering fixed irrigation turns, the net income oscillated between 1,280 € ha^{-1} and 3,420 € ha^{-1} for seasonal irrigation water amount equal to 170 and 570 mm, but with the highest income at 370 mm (4,011 € ha^{-1}). Oscillation in net income for irrigation based on water depletion, were contained in a smaller range (from 3,467 to 4,137 € ha^{-1}). Water use efficiency for total dry biomass and fruit yield was similar among the two water regimes, while the irrigation water use efficiency was heavily influenced by irrigation strategy, with higher values in the soil water depletion scenarios. The case study allowed us to estimate a list of crop parameters useful for the adoption of the AQUACROP model in similar conditions. The criterion of starting to apply irrigation at a level of soil water depletion of 30 mm proved to be effective for fruit yield (high average and low yearly variability) and the efficiency to convert the water available for the crop into biomass, reducing the water stress for the plants; moreover, it minimized water percolation in comparison to the fixed times application criterion.
Keywords: *AQUACROP model, net income, water cost, water productivity.*

Riassunto: *Il modello di simulazione AQUACROP (Steduto et al., 2009; Raes et al., 2009) è stato calibrato e validato per il pomodoro da industria nel Sud Italia (Piana di Capitanata) ed è stato, successivamente, usato per valutare l'impatto atteso di diversi regimi irrigui sulla produzione, efficienza d'uso dell'acqua e reddito netto.*
I regime irrigui simulati sono stati due: i) a turni fissi (con volume irrigui stagionali pari a 170, 270, 370, 470 e 570 mm) e ii) usando il criterio del ripristino del consumo idrico nel suolo (ripristinando 30, 50 e 70 mm di acqua persa dal suolo). Una calibrazione e validazione incrociata, basata su tre anni di dati sperimentali (2002-2004), ha permesso di stimare i parametri colturali e i loro range di variazione, fornendo utili dati che possono essere utilizzati in condizioni ambientali simili. Le risposte del pomodoro in termini di produzione di biomassa, produzione di frutti ed efficienza d'uso dell'acqua sono state valutate considerando le medie ottenute in una simulazione di lungo termine. Un'analisi economica semplificata è stata condotta per calcolare il reddito netto per ciascuno scenario agrotecnico.
La produzione più alta di frutti freschi (123 t ha^{-1}) simulata dal modello AQUACROP è stata ottenuta usando un turno irriguo fisso e con 370 mm di volume stagionale. Circa lo stesso livello produttivo è stato ottenuto con l'irrigazione che partiva dopo 30 mm di consumo idrico, risparmiando così 70 mm di acqua.
Il maggiore vantaggio del criterio del ripristino del consumo idrico del suolo, oltre alla minore incidenza dell'acqua persa per percolazione profonda, è il maggiore reddito netto per gli agricoltori. Considerando il regime a turni fissi, il reddito netto è variato tra 1,280 € ha^{-1} e 3,420 € ha^{-1} con i volumi irrigui stagionali tra 170 e 570 mm, ma con il reddito più elevato a 370 mm (4,011 € ha^{-1}). Oscillazioni del reddito netto per il regime irriguo basato sul criterio del consumo

[*] Corresponding author: michele.rinaldi@entecra.it
[1] CRA - Unità di Ricerca per i Sistemi Colturali degli Ambienti caldo-aridi, Bari (I)
[2] Università degli Studi di Bari, Facoltà di Agraria - Dipartimento di Scienze delle Produzioni Vegetali, Bari (I)
[3] FAO - Land and water division, Roma (I)
Received 26 July 2011 accepted 12 October 2011

idrico si sono osservate in un range più limitato (tra 3,467 e 4,137 € ha-1). L'efficienza d'uso dell'acqua per la resa in biomassa secca totale e per la resa in frutti è risultata similare tra i due regime irrigui, mentre la efficienza d'uso dell'acqua irrigua è stata pesantemente influenzata dalla strategia irrigua, con valori più alti negli scenari irrigui con il criterio del ripristino del consumo idrico. Il caso di studio ha permesso di stimare una serie di parametri colturali utili per l'adozione del modello AQUACROP in condizioni simili. Il criterio di partire con l'irrigazione ad un livello di consumo idrico nel suolo di 30 mm è apparso efficace per la produzione di frutti (media elevate e ridotta variabilità interannuale) e per l'efficienza nel convertire l'acqua disponibile per la coltura in biomassa, riducendo lo stress idrico per la pianta; inoltre, ha ridotto al minimo, rispetto allo scenario irriguo a turni fissi, l'acqua percolata e quindi persa, al di sotto delle radici.
Parole chiave*: modello AQUACROP, reddito netto, costo dell'acqua, productività dell'acqua.*

1. INTRODUCTION

In the Mediterranean environment water is a limiting factor for crop yield and this requires a careful evaluation of the method, time and amount of water supply in order to rationalize and preserve this resource, maximize crop yield and at the same time to ensure a suitable income for farmers.

Italy is one of the world's major producers of the processing tomato (*Lycopersicum esculentum* Mill.), with a production of 600,000 t in 2009 (ISTAT, 2009), amounting to 23% of world production (Faostat, 2009). In Italy, tomato production represents one of the most intensive uses of agricultural land in terms of water use and chemical input (Rinaldi et al., 2003). In particular, in Southern Italy, the use of water for this crop during its cycle was estimated to be about 800 mm with an irrigation water requirement of between 400 and 600 mm depending on climatic conditions (Rana et al., 2000), and with a production in terms of total plant dry biomass from 6 to 12 t ha^{-1} and fresh fruit yield from 80 to 160 t ha^{-1} (Rinaldi et al., 2007).

To obtain adequate fruit yield levels and maximize net income for farmers, it is necessary to improve water management to prevent water waste.

Indeed, a prolonged water deficit limits growth and reduces yield (Scholberg et al., 1997). Tomatoes require a constant and adequate supply of water, especially during flowering time (Waister and Hudson, 1970) to prevent a reduction in fruit growth and size. Furthermore, fluctuations in soil water content may induce physiological disorders such as blossom end rot (Pill and Lambeth, 1980). On the other hand, excess water may determine both a reduction in fruit quality and yield due to the fruit susceptibility to cracking (Peet and Willits, 1995) and a negative environmental impact, such as nitrogen leaching.

An estimate of crop water requirements should be the initial strategy in irrigation scheduling in order to achieve the best tomato yield and to limit groundwater contamination with nitrates; one approach is the indirect assessment of water evapotranspired by the crop (*ETc*) according to FAO guidelines (Doorenbos and Pruit, 1977; Allen et al., 1998) and multiplying potential evapotranspiration (*ET0*) with a crop coefficient (*kc*). The crop water requirement based on this approach is strictly dependent from the *kc* value used; indeed, an adequate estimate of this parameter is necessary, calibrated for the climate and crop-specific conditions.

A direct and so a more efficient approach to calculate *ETc*, compared to the method previously cited, is the calculation of a daily soil water balance to trigger irrigation according to effective soil water storage and water removed by the crop. Furthermore, a direct measurement of soil water tension could improve irrigation management, also ensuring a high level of automation (Leib et al., 2003).

Recent processing tomato hybrids have a determined growth that allows for the simultaneous maturity of all fruits; as the price of the marketable product is calculated on fresh fruit weight, it is possible to delay irrigation until crop maturity to exploit the full productivity of the crop (May and Gonzales, 1999). This can be achieved using fixed intervals (from two to six days) between irrigation supplies to reduce crop water stress and simplify the irrigation automation. However this method does not take into account the actual soil water content, and so an excess in water supply for the crop demand is easily reached without increment in fruit yield, with an increase in irrigation costs and an environmental risk because of chemical leaching.

In order to provide a more precise evaluation of water management, a long term study is necessary which also allows for a comparison between different strategies in terms of water scheduling.

The development and certification of site-specific guidelines for optimal timing and water requirements require extensive and expensive field experiments, taking into account all the possible combinations among crop yield responses and the amount of water supplied during the growth season.

Crop growth simulation models represent a valid tool to evaluate how different crop management systems and/or different pedo-climatic conditions can interact with crop production and thereby streamline the decision-making process. In the specific case of tomatoes, different crop simulation models have been used in field conditions. Erosion Productivity Impact Calculator (EPIC) model, (Cavero et al., 1998; 1999; Rinaldi et al., 2001), TOMGRO (Jones et al., 1991; Bertin and Gary, 1993) and CROPGRO (Messina et al., 2001; Koo, 2002; Ramirez et al., 2004; Rinaldi et al., 2007) are the most cited models in literature.
AQUACROP (Steduto et al., 2009; Raes et al., 2009), is a new mathematical crop model, developed for environments, as Mediterranean area, in which the water is the limiting factor for the crop yield, focusing the core of simulation on component linked to water and water use efficiency; therefore for the purpose of this research, AQUACROP was used.
The aims of this study are: i) to calibrate and validate the AQUACROP model for processing tomatoes in order to simulate adequately field-grown tomatoes under Mediterranean conditions; ii) to use the validated model to investigate different irrigation scheduling strategies from productive and economic perspectives.

2. MATERIALS AND METHODS

2.1 Model description

The AQUACROP model (Steduto et al., 2009; Raes et al., 2009) evolved from FAO Irrigation and Drainage Paper No. 33 "Yield Response to Water" (In: Doorenbos and Kassam, 1979), a key reference for estimating yield response to water.
According to the authors, this new model was built to reduce complexity as much as possible whilst maintaining an optimal balance between simplicity, precision and robustness.
In FAO Paper N° 33, the relationship that links crop productivity to the amount of water used is expressed by the following equation:

$$\left(\frac{Y_x - Y_a}{Y_x}\right) = k_y\left(\frac{ET_x - ET_a}{ET_x}\right) \qquad [1]$$

where Y_x e Y_a are the potential and the actual yield, respectively, ET_x e ET_a are the maximum and the actual evapotranspiration, respectively and k_y is the proportionality factor between the loss in crop productivity and the relative evapotranspiration abatement.

AQUACROP advances from the Eq. 1 by:

- dividing *ET* in soil evaporation (*E*) and crop transpiration (*Tr*), to avoid the confounding effect of the non-productive consumptive use of water (*E*); this is important especially during the crop cycle, in which the canopy doesn't cover the soil globally;
- obtaining biomass (*B*) from the product of water productivity (*WP*) and cumulated crop transpiration, expressing the final yield (*Y*) as the product of *B* and Harvest Index (*HI*); this partition allows to distinguish the functional relationships among biomass and the yield with the environment for both of them;
- normalizing *Tr* with reference evapotranspiration (*ET0*), to make the *B-Tr* relationship applicable to different climatic regimes, and running with daily time steps (either calendar or growing degree days), to more realistically account for the dynamic nature of water stress effects and crop responses.

Both Eq. (1) and the AQUACROP model are "water-driven" in their crop growth estimation. However, AQUACROP focuses more on the relationship between *B* and *Tr* rather than *Y* and *ET*, basing itself on the robustness of the biomass water productivity, also known as biomass water use efficiency *(WUE)* or water productivity coefficient *(WP).* A figure showing these evolutionary steps is shown in Fig. 1.
WP is the model's core, and similarly to other models there are sub-models: the soil, with its water balance; the crop, with its development, growth and yield; the atmosphere, with its thermal regime, rainfall, evaporative demand and CO_2 concentration; and the management, with its major agronomic practice such as irrigation and fertilization. AQUACROP flowchart is shown in Fig. 2.
The canopy development is expressed by the Canopy Ground Cover (*CC*), so not by the Leaf Area Index. *CC* drives three fundamental processes: leaf expansion; transpiration, regulated by stomatal conductance; senescence, caused by loss in transpiration and ability in assimilation. For each process is associated a curve of *Ks*, which magnitude is influenced by water depletion and by a shape factor of this curve. The roots have a development in depth, shape and water assimilation ability, based on soil limitation and in according with the canopy development.
The above biomass is calculated using the *WP*. This parameter, is "normalized" for the climate, or for the environment evapotranspiration request

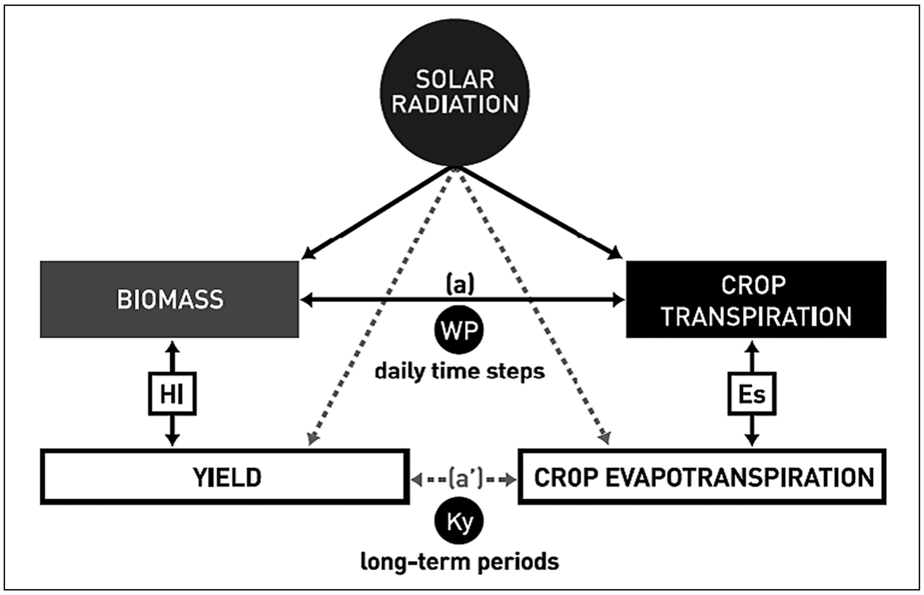

Fig. 1 - Graphic breakdown of the AQUACROP concept. From Steduto et al. (2009). For the acronyms, see text.
Fig. 1 - Schema concettuale del modello AQUACROP. Da Steduto et al. (2009). Per gli acronimi, vedere il testo.

(*ET0*; Steduto *et al*., 2007) and so it can be used in different climatic regions at different times. Moreover, it is expected that the normalization of *WP* for reference evapotranspiration (*ET0*) could be more robust than for saturation vapour pressure deficit (*VPD*) since, in arid environments, *VPD* could be more exposed to climate variability than *ET0*, as reported by Steduto and Albrizio (2005). This is due to strong link of *VPD* with both high air temperature and precipitation variability characterizing Mediterranean environments (Monteith, 1993).

The aerial biomass does not taking into account the partitioning among the different plant organs, excepted for fruits, grain or tubers, which subdivision occurs thanks to the Harvest Index (*HI*). This simplification excludes further source of uncertainty that it is still one of the crop phenomena hard to

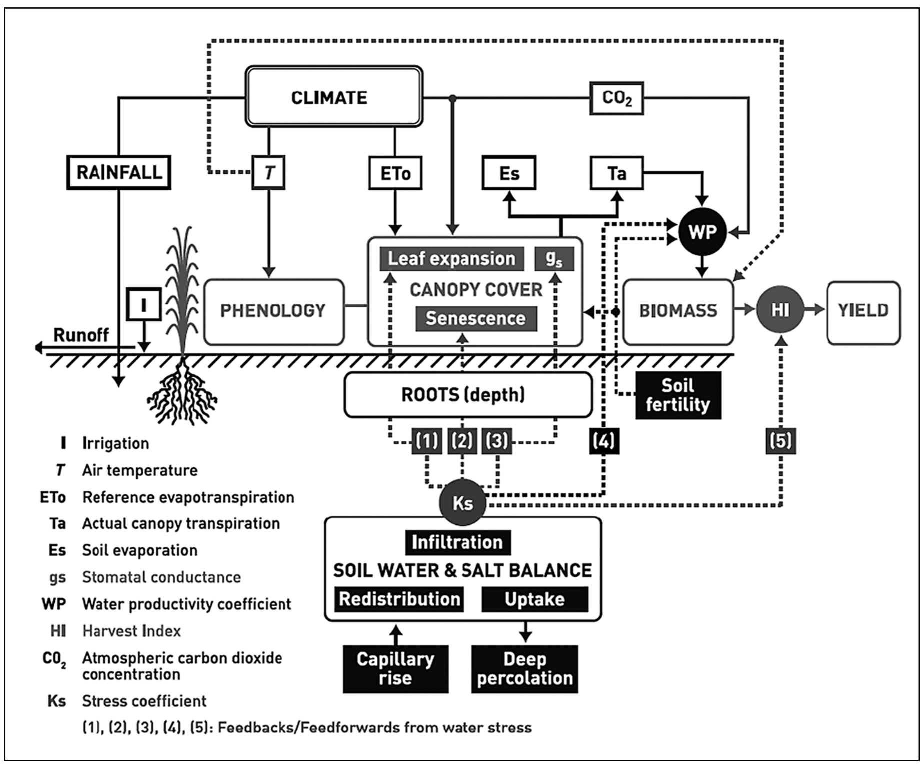

Fig. 2 - Flowchart of AQUACROP indicating the main components of the soil-plant-atmosphere continuum. From Steduto et al. (2009).
Fig. 2 - Diagramma di flusso del modello AQUACROP, con indicazione dei principali componenti del continuum *suolo-pianta-atmosfera. Da Steduto et al. (2009).*

simulate. The *HI* is modulated by water stress with negative or positive variations in *HI* values depending on the intensity, timing and duration of the stress. The environmental stresses are expressed through the stress indexes (*Ks*), specific for every factor that is at the crop growth basis, so leaf expansion, stomatal conductance and senescence.

Water flows in the soil are simulated with a "cascade movement", i.e., different soil layers are considered as reservoirs, whose maximum capability limit is expressed by the field capacity; if the water in a single layer overcomes this threshold, the excess falls into the layer below.

The limits of this approach are imputable to the impossibility to simulate the phenomenon of movements to the higher layer of the water; but the advantage of this approach is the computational rapidity, particularly appreciated in long term simulations.

2.2 Experimental data set

The data-set used for the calibration and validation of AQUACROP was derived from a field experiment carried out over three years (2002, 2003 and 2004) at the Research Unit experimental farm in Foggia (lat. 41° 8' 7" N; long. 15° 83' 5" E, alt. 90 m a.s.l.), Southern Italy. Daily weather data used for simulation (maximum and minimum temperatures, rainfall and solar radiation) were collected by the local meteorological station.

The soil is a silty-clay vertisol of alluvial origin, Typic Calcixeret (Soil Taxonomy 10th ed., USDA 2006), with the following characteristics: organic matter, 2.1%; total N, 0.122%; $NaHCO_3$ extractable P, 41 ppm; NH_4O Ac-extractable K_2O, 1598 ppm; pH (water), 8.3; field capacity water content, 0.396 m^3 m^{-3}; permanent wilting point water content, 0.195 m^3 m^{-3}, available soil water, 202 mm m^{-1}.

The climate is "accentuated thermo-Mediterranean" (Unesco-FAO classification), with temperatures below 0 °C in the winter and above 40 °C in the summer. Annual rainfall (average 550 mm) is mostly concentrated during the winter months and class "A pan" evaporation exceeds 10 mm day^{-1} in summer. Long-term seasonal (1 May-31 August) potential evapotranspiration (*ET0*) and rainfall of the processing tomato are of 690 and 120 mm, respectively.

For N fertilization, 100 kg of N ha^{-1} as ammonium nitrate (34.5%) were applied. Half of the fertilizer was spread prior to transplantation with the remainder applied at the first signs of fruit formation. The experimental design was a completely randomized block with four replications and with a plot size of 50 m^2 (5 m x 10 m). The tomato plants (hybrid PS 1296) were transplanted on 28 April 2002, 5 May 2003 and 18 May 2004 at a density of 3 plants m^{-2} using a twin row pattern. Irrigation was applied using a drip method: 359, 360 and 560 mm were used for the three years, respectively. Irrigation was driven, in according to the crop evapotranspiration (*ETc*), obtained by multiplying *ET0* with *kc*, this latter estimated in a previous research (Garofalo et al., 2011), refunding 100% of *ETc*, when it reached 30 mm. Common weed and pest control was carried out as required. At harvest (19 August in 2002, 21 August in 2003 and 7 September in 2004) the tomato fruits were counted and weighed. The total biomass (fruit and plant residues) was weighed both fresh and dried. Growth analysis was carried out during the crop cycle with a destructive method; two plants per plot were sampled at 2-week intervals, separating leaves, stems and fruits; green leaf area was measured with a LICOR-3000 leaf area meter to derive *LAI*. All biomass was subsequently dried at 65 °C for 48 hours.

Canopy cover (*CC*) was estimated from *LAI* using Beer's law (Eq. 2):

$$CC = 1 - e^{(-k*LAI_d + Cf)} \quad [2]$$

Where *k* is the light extinction coefficient (0.75), LAI_d is the green leaf area and *Cf* is the clumping factor, calculated with the following equation:

$$Cf = 0.75 + (0.25)*\left(1 - e^{(-0.35*LAI_d)}\right) \quad [3]$$

Volumetric soil water content (m^3 m^{-3}) was measured at the same sampling dates with the gravimetric method at depths of 0-0.2 and 0.21-0.4 cm and then multiplied for soil bulk density (1.20 kg dm^{-3}). From these values, soil moisture at 0-50 cm depth was then calculated to make comparisons with the outputs of the model. For further details on these experiments see Rinaldi et al. (2003), Rinaldi and Rana (2004) and Elia et al. (2006).

2.3 Model calibration and validation

The parameters for processing tomatoes were partly derived from measurements and partly calculated through continuous approximations using an iterative method, ceased only when the simulated values of some phenologic and productive variables become similar to the corresponding average values of previously observed data (Castrignanò et al., 1997). The parameters used for the calibration were flowering and maturity dates, yield at harvest, total dry matter, leaf area index and soil water content during the crop cycle. Since AQUACROP simulates the canopy development, using the *CC*, it is necessary to convert the *LAI* in *CC*, as reported in Eq. 2, for calibration, validation and data analysis.

The choice of parameters to calibrate was driven on the available data and on suggestion of AQUACROP authors. In fact, it has been preferred to base the calibration work, mainly changing the model parameters on the data collected during the experiment (phenology, *LAI*, *HI*, total dry matter, yield dry matter) and afterward the conservative crop parameters, until the lowest value of RMSE between simulated and observed data, was achieved.

Calibration was carried out for each of the three years, using a cross calibration method (Jones and Carberry, 1994) with a calibration for one year and validation using the remaining two years.

The calibration and validation processes were performed in two steps: firstly, the model was calibrated separately for each growing season to estimate the best values of crop parameters that fit the observed data in different years. Subsequently, the average crop parameter values obtained from each yearly calibration were used in the validation phase to give more robustness to the crop growth simulation compared to a calibration based on a single year.

To measure validation assessment, different statistical indices were used: Relative Root Mean Square Error (RRMSE) Modelling Efficiency, (ME) and Residual Mass Coefficient (RMC) indices, according to Loague and Green (1991). RRMSE gives a measurement (%) of the relative difference between simulated and observed data. The ME range is ≤ 1 (optimum = 1) and it compares modelling with experimental variability. A negative value of ME indicates that the modelling variability is greater than the experimental variability and that the simulation is therefore not satisfactory. For RMC the range is $-\infty \div 1$ and optimum value is 0; values greater than 0 indicate that the model tends to underestimate the measured data, while if RMC shows a negative value then the model tends to overestimate. Pearson's correlation coefficient also was used to measure the strength of the association between two variables. A positive correlation indicates that both variables increase or decrease together, whereas a negative correlation indicates that as one variable increases the other decreases and vice versa. The use of these index, is broadly reported by different authors (Confalonieri and Bechini, 2004; Donatelli et al., 1997; Garofalo et al., 2009; Rinaldi et al., 2007) when it is necessary to verify the robustness of the model, to simulate the crop growth in management and climatic condition, different to those used in calibration step.

After this process, average values of crop parameters were used for long term simulations.

2.4 Seasonal long-term simulation

For the long term simulation, daily climatic data from 1953 to 2006 were used: the data were recorded at the on-site agro-climatic station and provided daily maximum and minimum temperatures, rainfall, and *ET0* estimated with the Priestley-Taylor equation (Priestley and Taylor, 1972).

Transplanting time was set at 1st of May and the harvest was simulated by the model at fruit maturity. To evaluate the effects of irrigation water on tomato crop growth and yield we explored a wide range of seasonal water amounts (170, 270, 370, 470 and 570 mm) at a fixed time interval through two irrigation supplies (4 days). This irrigation planning criterion was selected to reflect the common practices adopted by farmers in the Capitanata region. As a result, 21 water applications covering the whole crop growth cycle were scheduled, with a fixed amount for each application equal to 8 (*I_170*), 13 (*I_270*), 17.6 (*I_370*), 22.4 (*I_470*) and 27.2 (*I_570*) mm. The choice of 570 mm as the maximum seasonal irrigation water follows the average irrigation amount used by farmers in Capitanata (Rinaldi and Rana, 2004). The lowest irrigation supplies (8 and 13 mm) are nevertheless feasible since the drip irrigation method also allows for limited water applications and evaporation losses are limited by the reduced percentage of wet soil below the emitter line.

This irrigation planning clearly does not follow the principles of sustainable irrigation, as it does not take into account the effective water soil content or the plant water conditions: as a result, excesses in water supply are frequent when using this criterion, with environmental and economic consequences. In order to investigate the growth and productivity of processing tomatoes with irrigation management based on soil water content, different levels of deficit irrigation were also simulated. The model was set to apply irrigation automatically every time the soil water depletion (*WD*) reached 30, 50 and 70 mm, providing 25 (*WD_30*), 40 (*WD_50*) and 55 (*WD_70*) mm of water, respectively. Moreover, in order to try to reduce the seasonal water amount, the same levels of deficit irrigation were simulated, stopping the irrigation 15 days before fruit maturity;

this can be seen in the *WDS_30*, *WDS_50* and *WDS_70* scenarios.
To evaluate the most profitable irrigation management method, a simple economic analysis was performed, considering the price of tomatoes, water prices and fixed production costs. The net income for the farmer (€ ha^{-1}) was calculated as the difference between the economic yield value and the crop production cost, according to the costs and prices of the processing tomatoes grown on the Capitanata Plain during 2009 (Tab. 1). In order to provide information for other locations where the water prices are lower than in Capitanata, a 20% reduction in irrigation water costs was considered in the analysis; on the other hand, a 20% increase in water costs was also evaluated to predict a low availability for general irrigation water.
For the agronomic and economic evaluation of the tomato crop, we used the model output of:
(i) total plant dry matter (*TDM*, kg ha^{-1});
(ii) dry fruits biomass at harvest (*DFM*, kg ha^{-1}) and then fresh fruit biomass was derived using an average dry matter fruit contento of 5.5% (*FDM*, kg ha^{-1});
(iii) water use efficiency for total dry matter (*WUE*, *TDM*/water transpired, kg m^{-3});
(iv) fresh and dry fruit water use efficiency (*WUEf* and *WUEd*, kg m^{-3});
dividing *TDM* and the fresh and dry fruit with the irrigation water amount:
(v) the irrigation water use efficiencies (*IWUE*, *IWUEf* and *IWUEd*, kg m^{-3});
(vi) soil water content (m^3 m^{-3}) for the 0-0.5 m soil depth (m^3 m^{-3});

Costs and prices	**Values**
**Base production cost (€ ha^{-1})*	5,400.00
Price of harvest product (€ t^{-1} of fresh fruit)	82.00
***Irrigation water cost (€ mm^{-1}):*	
< 205 mm	1.2
205-250 mm	1.8
250-300 mm	2.4
> 300 mm	3.6

*Considering both N price and its application cost and water application cost.
**The water cost is taken from "Consorzio per la Bonifica della Capitanata, Foggia".

Tab. 1 - Prices and costs of processing tomatoes cropped in Southern Italy (2009 season).
Tab. 1 - Prezzi e costi del pomodoro da industria coltivato in Sud Italia (stagione 2009).

(vii) production cost and net return (€ ha^{-1}). Frequency distributions and cumulated probability functions were also estimated for the 54 yearly simulation outputs.

3. RESULTS AND DISCUSSION

3.1 Model calibration

Tab. 2 shows the crop file parameters that were changed to obtain the best fit between observed data and model simulations for tomato growth during the crop cycle, based on every experimental year and then averaged.
Maximum canopy cover is set after 1,298 *GDD* (base temperature equal to 5 °C), with a difference among years that is particularly evident between the first two years and the third year, with a gap of about 200 *GDD* for the latter. The maximum value for canopy cover was 86% and very close over the three years. The *GDD* necessary to ensure the beginning of the flowering stage were different over the years, with an average value of 691, but with a standard deviation of 273 *GDD*. Finally, the thermal time necessary to reach fruit maturity was 2,022 with a very small standard deviation over the years of 98 *GDD*.
The calibration study to evaluate the response of the processing tomato to water stress used the same parameters as those for water depletion, starting with canopy expansion for stomatal closure and early senescence (Tab. 2). The *WP* normalized for *ET0* proved to be similar for 2003 and 2004 (18 g m^{-2}), but greater in 2002 (19.5 g m^{-2}). Fig. 3 shows the good fit between simulated and observed data for the three years after calibration.
For the *HI*, the mean value deriving from the calibration for each year was 61%, with a standard deviation equal to 2.5%; the adjustment for *WP* was also different, as it was higher in the first than in the second and third years. Despite in the model the effect of water stress on *HI* variation is reported as discrete value (none, small, moderate, strong, very strong), *HI* changing during pollination stress are driven by a linear equation that takes into account the soil water depletion. *HI* adjustment, as result of water stress during yield formation, is given multiplying reference *HI* for a factor deriving from *Ks* for stomatal closure and by a crop parameter that can vary from 1 (strong effect) to 20 (small effect), depending with crop and the literal value chosen.
The crop transpiration coefficient (*kc*) at full canopy cover was 1.13 on average, whereas the maximum water extraction was 15.3 mm; for both parameters, calibration with the data of 2002

Year used for calibration			2002	2003	2004	Mean
	Parameter	Units				
Growth	Initial canopy cover	%	0.67	0.67	0.67	0.67
	Maximum canopy cover	%	87	85	85	86
	Canopy growth	*% °C day $^{-1}$*	0.597	0.630	0.536	0.588
	Canopy decline	*% °C day $^{-1}$*	0.17	0.38	0.31	0.29
	Crop Water Productivity	*g m^{-2}*	19.5	18	18	18.5
	Reference Harvest Index	%	63	60	58	61
	Adjustment for yield formation	*% of HI*	100	85	85	90
	Base Temperature	*°C*	5.0	5.0	5.0	5.0
	Upper Temperature	*°C*	30.0	30.0	30.0	30.0
Root	Maximum rooting depth	*m*	0.80	0.80	0.80	0.80
	Average root zone expansion	*cm day $^{-1}$*	1.5	1.0	1.0	1.2
Transpiration	ET crop coefficient at full canopy		1.20	1.10	1.10	1.13
	Reduction of *kc* with age	*% day $^{-1}$*	0.15	0.15	0.15	0.15
	Maximum root extraction	*mm day $^{-1}$*	16.4	14.8	14.8	15.3
****Water Stress***	Canopy expansion *Upper*		0.25	0.25	0.25	0.25
	Canopy expansion *Lower*		0.60	0.60	0.60	0.60
	Stomatal closure		0.50	0.65	0.65	0.60
	Early canopy senescence		0.65	0.70	0.70	0.68
	Reduction in *HI* after *Failure in pollination*		moderate	small	small	small
	Reduction in *HI* after *Stomatal closure*		moderate	strong	strong	strong
Phenology	Max Canopy	*GDD*	1240	1223	1430	1298
	Flowering	*GDD*	472	603	999	691
	Flowering duration	*GDD*	748	793	717	753
	Length building up *HI*	*GDD*	904	1151	932	996
	Senescence	*GDD*	1357	1751	1510	1522
	Maturity	*GDD*	2012	2125	1930	2022

*Soil water depletion fraction at which water stress on a specific plant process starts.

Tab. 2 - AQUACROP model crop parameters for processing tomatoes (hybrid PS 1296).
Tab. 2 - Parametri colturali del modello AQUACROP per il pomodoro da industria (ibrido PS 1296).

suggested higher values than those of the other two years. The maximum root length was the same for all three years, with 90% of soil water extracted in the first 0.6 m.

Crop simulation models are exemplifications, though with a good approximation, of complex processes that occurs in the biological systems. The crop response to different climatic condition, determines a behaviour that can differ among years, that is not so easy to contain in a single parameterized value; this explains the slight variation in some of the calibrated values among years, and so a cross calibration was necessary to evaluate if the crop parameters calibrated for one year are suitable for the remaining years, or if average values are more suitable.

Fig. 4 shows that for tomato dry fruit yield a good "simulated vs. measured" fit was achieved after calibration; calibration for 2002 and 2003 had a good response also in term of soil water content, with a good fit between observed and simulated data, whereas, in 2004, discrepancy between model output and experimental data was observed, especially at lowest value of *SWC*. However, *SWC* is a parameter not so easy to fit with a simulation model, especially if the cascade approach is used for soil water balance calculation.

3.2 Model validation

The climatic behaviour for the three years, from 15 April to 31 August, are shown in Fig. 5. These years were characterized by different results for temperature, rainfall and *ET0*. In fact, during the first part of the crop cycle (50 days after transplanting, DAT), the average temperature recorded in 2003 was about 3°C per day higher than in 2004. This gap was also maintained during the second part of the cycle (50-100 DAT), whereas in the final part of the growing season, the average

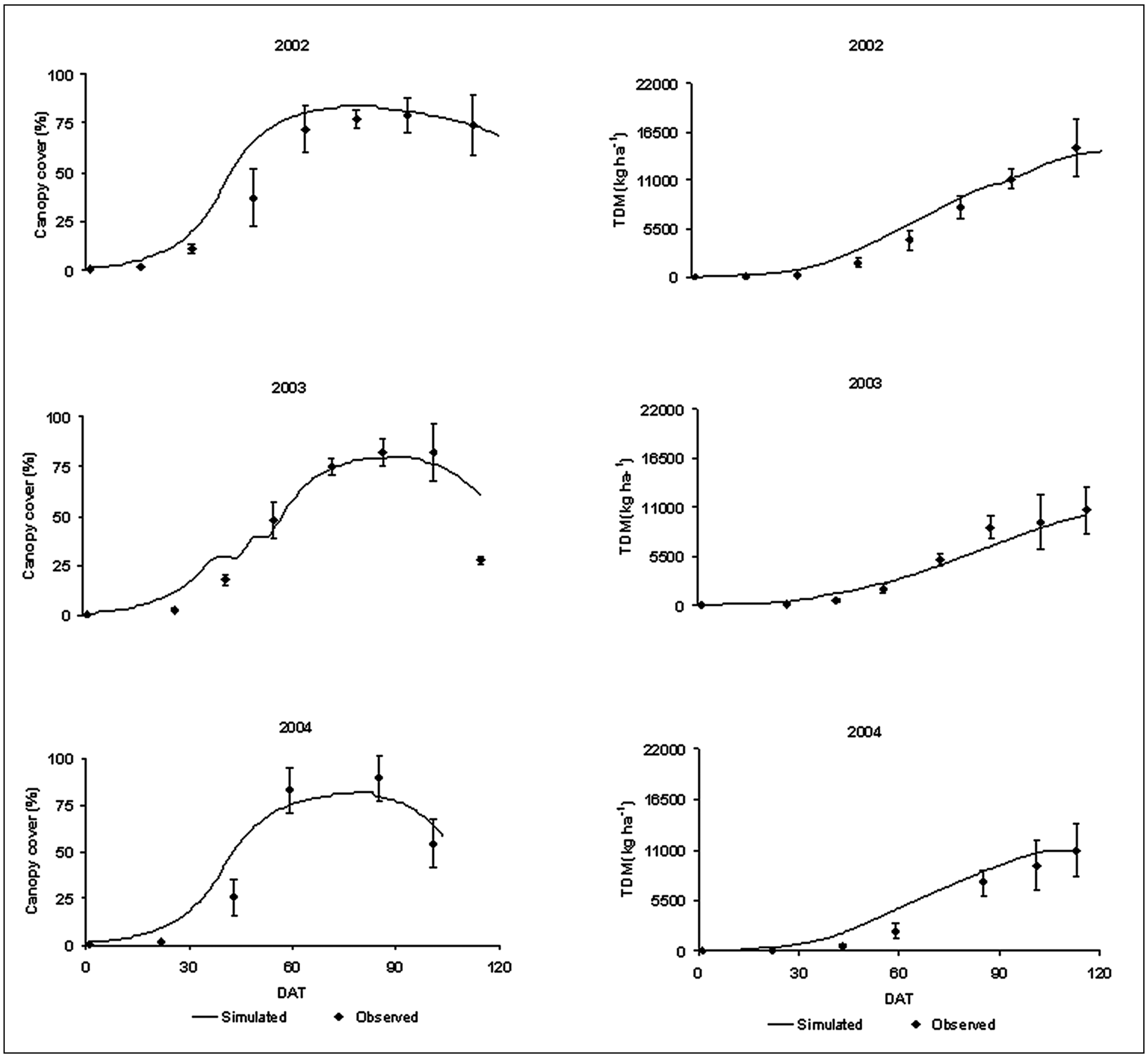

Fig. 3 - Comparison of canopy cover (on the left) and total dry matter (on the right) during crop growing season between simulated (continuous line) and observed (rhombus) values, after calibration, carried out for each experimental year. The bars indicate the standard deviation for the observed values. DAT = Days after transplanting.

Fig. 3 - Confronto della percentuale di copertura vegetale (sinistra) e sostanza secca totale (destra) durante la stagione di crescita tra valori simulati (linea continua) e osservati (rombi), dopo la calibrazione condotta per ciascun anno sperimentale. Le barre indicano la deviazione standard per i valori osservati. DAT = Giorni dopo il trapianto.

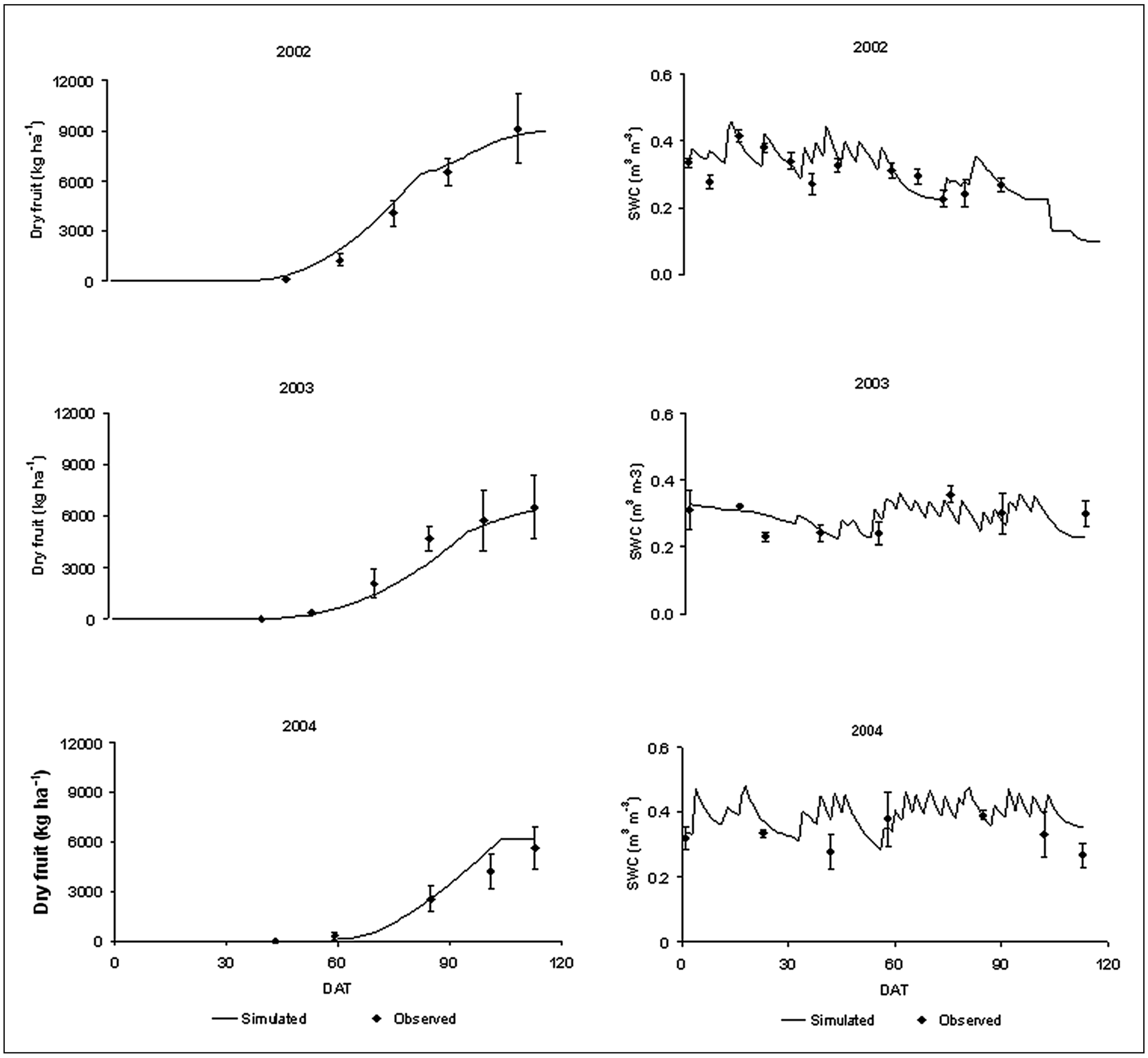

Fig. 4 - Comparison of dry fruit matter (on the left) and soil water content (0-50 cm depth, on the right), during crop growing season between simulated (continuous line) and observed (rhombus) values after calibration, carried out for each experimental year. The bars indicate the standard deviation for the observed value.

Fig. 4 - Confronto della produzione di sostanza secca dei frutti (sinistra) e del contenuto idrico del suolo (profondità 0-0.5 m, a destra) durante la stagione di crescita tra valori simulati (linea continua) ed osservati (rombi) dopo la calibrazione condotta per ciascun anno sperimentale. Le barre indicano la deviazione standard per i valori osservati.

temperature was similar for both years (Fig. 5a). 2002 was characterized by temperature levels between those of the other years during the first and the second part of the growing season, but which were lower during the third part of the crop cycle.

Rainfall was very scarce throughout 2003 (84 mm as cumulated rainfall), whereas at the end of the crop cycle in 2002 and 2004 the accumulated rainfall was very similar (303 mm), even if it was different in the growing season (Fig. 5b). Finally, the *ET0* recorded during the tomato growing season showed an extremely differing pattern over the three years; 2003 showed greater values of *ET0* when compared with those of 2002 and 2004, with a seasonal *ET0* of 673, 775 and 553 mm for 2002, 2003 and 2004 respectively (Fig. 5c). This climatic variability and the different behaviour of processing tomatoes over the years can be considered an effective analysis in testing the robustness of the model.

In Tab. 3 the main statistical indices used to evaluate the accuracy of the model are shown. It is possible to observe how each calibration, based on every year, had both strong and weak points. In fact, calibration carried out in 2002 seems to have been the worst, at least when considering the validation mean indices. Average RRMSE were 48.5%, whereas the validation index using parameters from the 2003 and 2004 calibrations were 41.5% and 30.4% for 2003 and 2004 respectively. Moreover, the ME index using the crop parameters calibrated in 2002 showed the lowest value in the validation phase (0.43), if compared with 2003 (0.53) and 2004 (0.71). Calibration from 2002 and 2003 showed an overestimation of simulated compared with observed data for all four output variables, whereas calibration from 2004 was more balanced with an average RMC of 0.16. The RRMSE, ME and RMC were better from simulations using the average crop values of the previous calibrated years than the values obtained from the mean of each year (except for the *SWC*), as can be seen in Tab. 3. In particular, the average RRMSE index gave fair values (28.7%), the average ME showed a good response to the model (0.68) and the RMC indicated that the model gave a very slight over-estimation (-0.02).

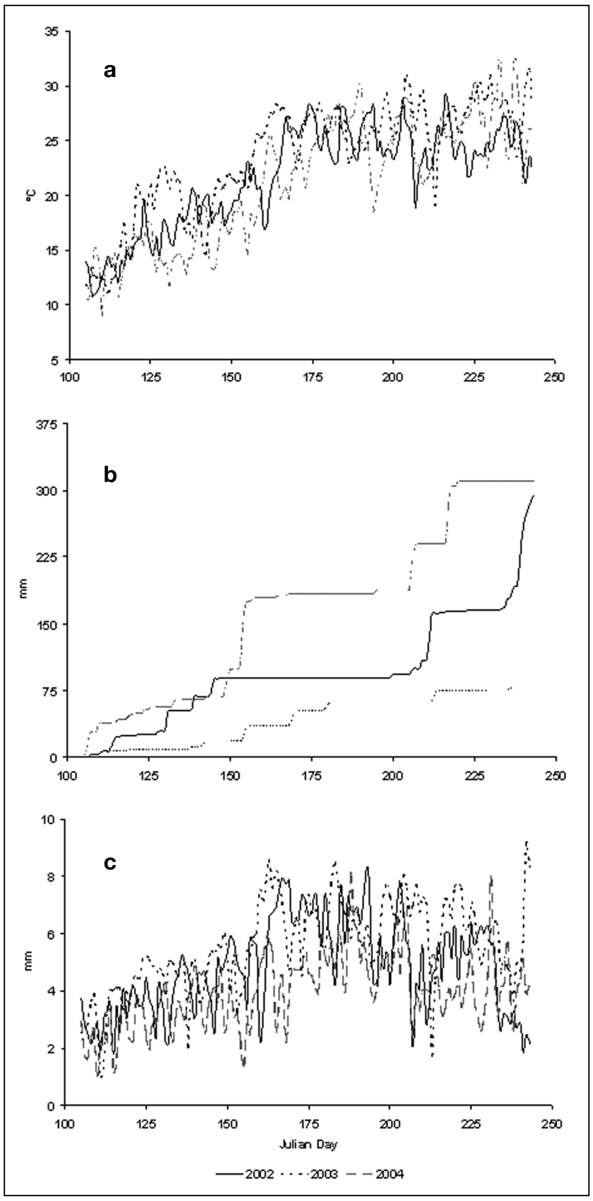

Fig. 5 - Daily mean temperature (a), cumulated rainfall (b) and daily ET0 (c), recorded during the tomato crop growing season for the three experimental years in Foggia.
Fig. 5 - Temperatura media giornaliera (a), pioggia cumulata (b) ed ET0 giornaliera (c), registrati durante la stagione di crescita del pomodoro nei tre anni sperimentali a Foggia.

Analysing the crop output variables individually, the best result was obtained for the canopy cover (*CC*), with a value of 22.6%, 0.92 and -0.009 for RRMSE, ME and RMC, respectively. For the total plant dry matter (*TDM*), the model showed a good response in terms of ME (0.92), a fairly good RRMSE (28.8%) and an optimum RMC (0.01). For fruit dry matter (*FDM*), RMSE was not very good, but considering the ME and RMC indices, we can consider the AQUACROP model valid also for fruit growth simulation. The same consideration can be made for the soil water content (*SWC*), with RRMSE, and RMC indices which were very close to optimum values. A visual judgement can be made from Fig. 6, where the linear regressions between simulated and observed values for the same output for all experimental years are shown. Consequently, this parameterization can be considered more suitable for use in long-term simulations.

A comparison between the robustness of AQUACROP and other models, to simulate tomato crop, can be done using the data reported by Rinaldi et al. (2007); in fact, CROPGRO model was calibrated and validated for tomato, with the same experimental data Comparing the validation indexes emerged as, AQUACROP had a slight advantage on CROPGRO, in term of *TDM*, *FDM*, canopy development and *SWC* when average values of crop parameters calibrate for each year were used.

3.3 Seasonal analysis: yield

A consistent increase in processing tomato productivity was reached in the simulation varying the seasonal water amount from 170 to 370 mm and using fixed intervals between irrigation times, with a fresh fruit yield of 84 and 123 t ha^{-1}, respectively. Using the soil water depletion criterion for automatic irrigation management, the yield was 117 t ha^{-1}, on average, with the highest values for *WD_30* and *WDS_30* (122 t ha^{-1}) and the lowest values for *WD_70* and *WDS_70* (112 t ha^{-1}).

Significant increases in fruit productivity (in

Variable	Year used for calibration	n	Observed mean	Simulated mean	Diff. (%)	RRMSE[a] (%)	ME[b]	RMC[c]	r[d]
	2002								
TDM[e] ***(kg ha^{-1})***		15	4454	6268	40.7	60.5	0.61	-0.41	0.95
CC[f] ***(%)***		13	43.3	47.6	10.1	29.1	0.87	-0.10	0.94
FDM[g] ***(kg ha^{-1})***		11	2912	4668	60.3	92.5	-0.25	-0.60	0.86
SWC[h] ***(m^3 m^{-3})***		14	0.32	0.32	10.1	11.8	0.38	0.00	0.67
					30.3	*48.5*	*0.40*	*-0.28*	*0.86*
	2003								
TDM[e] ***(kg ha^{-1})***		15	4679	5619	20.1	39.8	0.86	-0.20	0.94
CC[f] ***(%)***		13	41.0	54.8	33.7	51.1	0.63	-0.34	0.89
FDM[g] ***(kg ha^{-1})***		11	3362	4395	30.7	60.3	0.52	-0.31	0.81
SWC[h] ***(m^3 m^{-3})***		18	0.32	0.35	7.5	15.0	0.11	-0.08	0.60
					23.0	*41.5*	*0.53*	*-0.23*	*0.81*
TDM[e] ***(kg ha^{-1})***	*2004*	16	4757	4029	-15.3	30.9	0.91	0.15	0.99
CC[f] ***(%)***		14	41.9	42.6	1.6	16.4	0.96	-0.02	0.98
FDM[g] ***(kg ha^{-1})***		11	3674	1773	-51.7	63.5	0.38	0.52	0.91
SWC[h] ***(m^3 m^{-3})***		18	0.31	0.32	3.5	10.9	0.58	-0.03	0.85
					-15.5	*30.4*	*0.71*	*0.16*	*0.93*
	mean								
TDM[e] ***(kg ha^{-1})***		23	4633	4609	-0.5	28.9	0.92	0.01	0.96
CC[f] ***(%)***		20	42,0	46,0	9.4	22.6	0.92	-0.09	0.97
FDM[g] ***(kg ha^{-1})***		16	3314	3036	-8.4	48.7	0.67	0.08	0.84
SWC[h] ***(m^3 m^{-3})***		25	0.32	0.34	6.1	14.5	0.19	-0.06	0.61
					1.7	*28.7*	*0.68*	*-0.02*	*0.85*

[a] Relative Root Mean Square Error; [b] Modelling Efficiency; [c] Residual Mass Coefficient; [d] Pearson's correlation coefficient; e Total Dry Matter; f Canopy Cover; [g] Fruit Dry Matter; h Soil Water Content 0-0.5 m depth.

Tab. 3 - Statistical indices of comparison of simulated vs. observed values of tomato in the cross calibration-validation phase, using one year for calibration and the remaining two years for validation.
Tab. 3 - Indici statistici del confronto tra valori simulati vs. osservati del pomodoro nella fase di calibrazione-validazione incrociata, usando un anno per la calibrazione e gli altri due per la validazione.

comparison to the less irrigated regime scenario) were obtained with a seasonal water supply of 270 mm; in the most irrigated scenarios (470 and 570 mm), the yield proved to be very close (124 t ha^{-1}) to that obtained with the intermediate scenario; these values are also close to those obtained with *WD_30* and *WDS_30*, but the seasonal water amount was lower than that in the more irrigated scenarios; in fact, the water applied by AQUACROP using this strategy was 311, 267, 239, 290, 245 and 216 mm for *WD_30*, *WD_50*, *WD_70*, *WDS_30*, *WDS_50* and *WDS_70*, respectively. Therefore, despite such notable differences in irrigation water supply between the *I_370* and *I_570* scenarios (and between the *I_570* and scenarios based on water depletion), the increase in *TDM* and *DFM* was negligible.

Cumulative probability density functions (Fig. 7a) showed how the tomato yield response to irrigation at fixed times determined different paths based on different water amounts. Indeed, the curve pattern for *I_170* has the lowest values and a large variability; *I_270* showed intermediate behaviour, while the other three irrigation regimes overlapped completely. This tomato productivity response indicates that using fixed turns at low water input, yield variability is not controlled and the yield is largely rainfall-dependent. On the contrary, at high water input, the yield is more stable over the years but there is an increased probability of large amounts of water and nutrients supplies being leached below the root zone, with no benefit in terms of fruit productivity, net income, water and environmental conservation.

Yearly variability, in terms of tomato productivity, decreased in the irrigation scenarios based on soil water content; indeed, the probability curves for the fresh fruit yield were contained in a difference between the highest and the lowest value equal to 26, 28 and 31 t ha^{-1}, for *WD_30*, *WD_50* and *WD_70*, respectively (Fig. 8a).

As regards water use efficiency (*WUE*, 2.58 kg of total dry matter produced per m^3 of transpired water as a mean value) resulted very similar in all water regimes and treatments (Tab. 4), this is due to the *"water productivity"* parameter implemented in the AQUACROP model, whose normalization for the *ET0* also allows for a greater stability of *WUE* under different climatic and management conditions. Thus, differences in crop growth and productivity are exclusively based on the water transpired by the crop. The same considerations can be made for the *WUEd*, since this value ranged from 1.35 to 1.66 kg m^{-3} for the *I_170* and *WD* (mean value) treatments, respectively. Applying irrigation strategies to fixed time intervals (the strategy widely applied by local farmers), the model simulated large differences in water lost through drainage, among the water regimes. In *I_170* and *I_270*, the amount of drained water was 40 and 61 mm, respectively, with a yearly variability of 56%. In *I_370*, *I_470* and *I_570* the model simulated drainage of 115, 209 and 307 mm, respectively. Variability over the years decreased from 42.2% observed in *I_370* to 19% in *I_570*. Moreover, for the first three water regimes, the water drained was 31% of the seasonal water applied, whereas this value reached 44% and up to 51% in *I_470* and *I_570* respectively. These results for drained water, accompanied by a similar *WUE* value for all water regimes, explained the similar results in terms of tomato yield for the *I_370*, *I_470* and *I_570* irrigation regimes. Obviously, when considering only water supplied by irrigation, the efficiency in converting water into dry biomass is heavily affected by drained water. On the other hand, the *IWUEd* showed a clear decline, ranging from 2.74 in *I_170* to 1.22 kg m^{-3} in *I_570*. *IWUEf* was 38.4 kg m^{-3} on average, with the two extremes

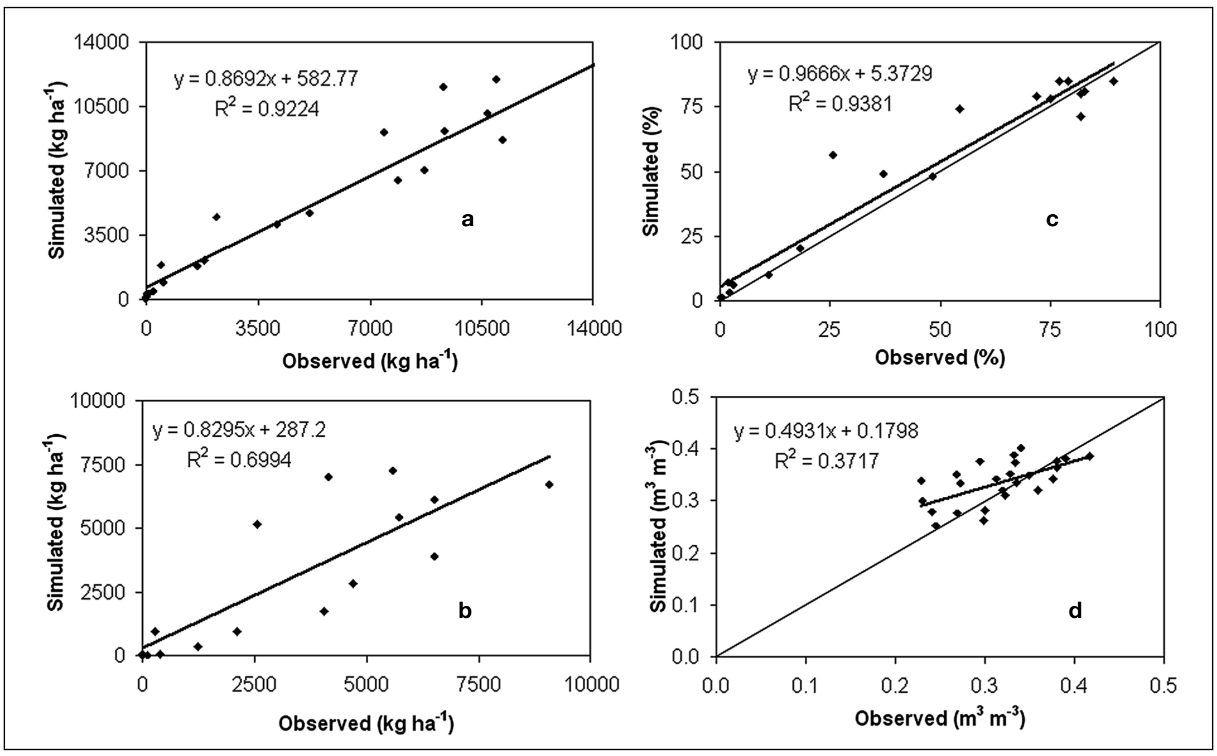

Fig. 6 - Linear regressions between simulated and observed value, recorded during growing season for total plant dry matter yield (a), dry fruit matter yield (b), canopy cover (c) and soil water content (d) for all three experimental years.

Fig. 6 - Regressioni lineari tra valori simulati ed osservati, registrati durante la stagione di crescita per la produzione di sostanza secca totale (a), sostanza secca dei frutti (b), frazione di copertura vegetale (c) e contenuto idrico del suolo (d), per tutti i tre anni di esperimento.

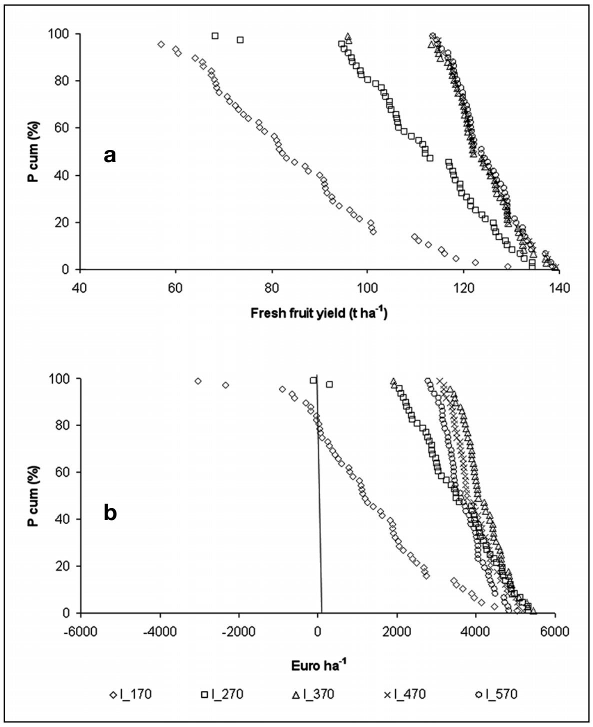

Fig. 7 - Cumulative probability, using a long-term simulation (54 years), to exceed a fresh fruit tomato yield value (a) and net income value (b), for fixed time irrigation scenarios. (P cum = cumulated probability).
Fig. 7 - Probabilità cumulata, usando una simulazione di lungo termine (54 anni), di superare un valore di produzione di bacche fresche di pomodoro (a) e di reddito netto (b), per gli scenari a turno fisso di irrigazione (P cum = probabilità cumulata).

equal to 54.9 and 24.3 kg m^{-3} in *I_170* and *I_570*, respectively. When compared to the more irrigated fixed turn strategy, the greater standard deviation in *IWUEf* for *WD* water regimes (Tab. 4) is due to the extreme variability of water amounts supplied in *WD* scenario irrigation, guaranteeing the same level of yield over the years. On the contrary, in fixed turn scenarios, the yield was similar (due to water lost in percolation, with no benefit in fruit improvement) with the same level of water applied by irrigation; this explains the lower variability in *IWUEf*.
The amount of percolated water in the *WD* water regimes was extremely reduced, with a mean value of 8.5 mm and a gap between the extreme values of only 5.6 mm. *IWUEd* was greater in *WDS_70* (3.1 kg m^{-3}) than in *WDS_30* (2.3 kg m^{-3}); similarly, the *IWUEf* values were 61.2 kg m^{-3} and 45.3 kg m^{-3} for *WDS_70* and *WDS_30*, respectively, with differences less than those found in water regimes based on fixed times (Tab. 4).
Standard deviation values of crop yield (Tab. 4), highlighted how irrigation management has an important role in stabilizing the yearly variability of fruit yield in processing tomatoes. Therefore, in any forecast of optimal water supply, it is possible to obtain a reasonable production assessment, independently of climatic conditions. The range of variation in terms of fresh fruit was, for instance, about 19.9 t ha^{-1} in the *I_170* scenario and only 6.9 t ha^{-1} in the *I_470* and *I_570* scenarios on average. Irrigation scheduling based on actual water soil content (actual crop water requirements) showed two important advantages if compared with the "fixed times" criterion: 1) a reduction in irrigation water applied at the same fruit yield level (from 19% to 47%) and 2) a reduction in the variability of the fruit yield (from 6% to 11%) (Hartz, 1993; Imtiyaz et al., 2000).

3.4 Seasonal analysis: profitability

The net income of different simulated water regimes are shown in Fig 7b and Fig. 9b. The lowest irrigation regime (170 mm) provided adequate incomes for farmers, since the average value was 1,280 € ha^{-1}. However, this indicated significant variability over the years (as underlined by standard deviation) and did not guarantee adequate or positive income in all the

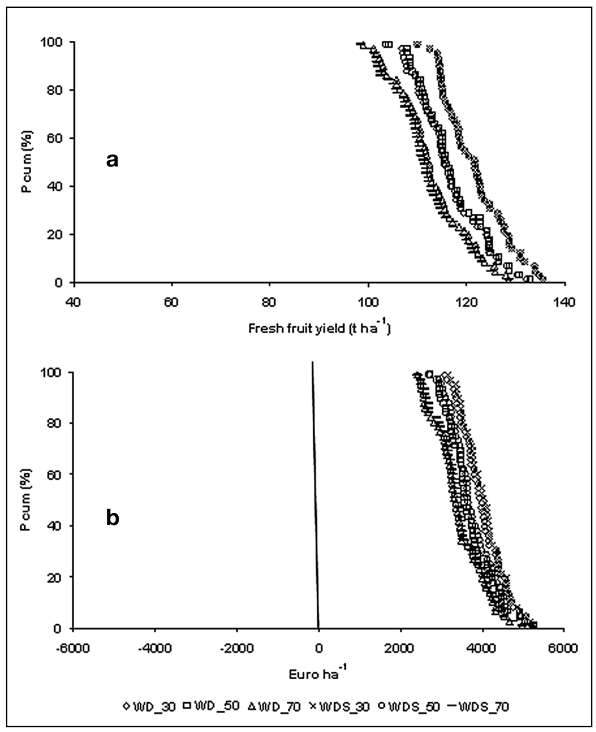

Fig. 8 - Cumulative probability, using a long-term simulation (54 years), to exceed a fresh fruit tomato yield value (a) and net income value (b), for soil water depletion scenarios. (P cum = cumulated probability).
Fig. 8 - Probabilità cumulata, usando una simulazione di lungo termine (54 anni), di superare un valore di produzione di bacche fresche di pomodoro (a) e di reddito netto (b), per gli scenari a ripristino del consumo idrico del suolo (P cum = probabilità cumulata).

Scenarios	TDM (t ha^{-1})	FDM (t ha^{-1})	FFM (t ha^{-1})	WUE (kg m^{-3})		IWUE (kg m^{-3})			Net income (€ ha^{-1})	Net income (+20%) (€ ha^{-1})	Net income (-20%) (€ ha^{-1})
				° TDM	FDM	TDM	FDM	FFM			
I_170	7.9 ± 1.8	4.7 ± 1.2	83.9 ± 19.9	2.31 ± 0.52	1.35 ± 0.34	4.66 ± 0.98	2.74 ± 0.65	54.87 ± 13.01	1,280 ± 1,714	1,239 ± 1,709	1,320 ± 1,719
I_270	10.3 ± 1.2	6.2 ± 0.8	112.2 ± 14.2	2.51 ± 0.47	1.52 ± 0.29	3.81 ± 0.45	2.31 ± 0.29	46.16 ± 5.83	3,422 ± 1,121	3,347 ±1,120	3,497 ± 1,122
I_370	11.2 ± 0.7	6.8 ± 0.5	123.3 ± 8.3	2.58 ± 0.44	1.57 ± 0.27	2.04 ± 0.02	1.85 ± 0.12	37.03 ± 2.48	4,011 ± 729	3,872 ± 743	4,151 ± 717
I_470	11.3 ± 0.6	6.9 ± 0.4	124.4 ± 6.7	2.59 ± 0.44	1.58 ± 0.27	2.41 ± 0.13	1.47 ± 0.08	29.42 ± 1.59	3,745 ± 628	3,533 ± 646	3,957 ± 612
I_570	11.4 ± 0.6	6.9 ± 0.4	124.9 ± 6.6	2.59 ± 0.46	1.58 ± 0.28	2.00 ± 0.11	1.22 ± 0.06	24.34 ± 1.29	3,420 ± 523	3,137 ± 523	3,704 ± 523
WD_30	11.1 ± 0.6	6.8 ± 0.4	121.8 ± 6.6	2.67 ± 0.42	1.63 ± 0.26	3.72 ± 0.94	2.27 ± 0.57	45.35 ± 11.49	4,094 ± 530	3,994 ± 531	4,192 ± 525
WD_50	10.6 ± 0.6	6.5 ± 0.4	116.5 ± 6.8	2.74 ± 0.43	1.67 ± 0.26	4.13 ± 1.00	2.52 ± 0.61	50.43 ± 12.19	3,779 ± 573	3,702 ± 575	3,855 ± 567
WD_70	10.2 ± 0.6	6.2 ± 0.4	121.8 ± 7.3	2.73 ± 0.43	1.67 ± 0.26	4.51 ± 1.32	2.75 ± 0.80	55.01 ± 16.07	3,467 ± 619	3,402 ± 619	3,532 ± 613
WDS_30	11.1 ± 0.6	6.8 ± 0.4	116.5 ± 6.6	2.68 ± 0.42	1.63 ± 0.26	4.00 ± 0.97	2.41 ± 0.59	48.77 ± 11.89	4,137 ± 514	4,049 ± 512	4,227 ± 514
WDS_50	10.6 ± 0.6	6.5 ± 0.4	112.1 ± 6.8	2.74 ± 0.43	1.67 ± 0.26	4.55 ± 1.18	2.77 ± 0.72	55.48 ± 14.44	3,843 ± 566	3,779 ± 567	3,905 ± 561
WDS_70	10.2 ± 0.7	6.2 ± 0.4	116.8 ± 7.3	2.73 ± 0.43	1.67 ± 0.26	5.02 ± 1.54	3.06 ± 0.94	61.23 ± 18.77	3,509 ± 616	3,452 ± 617	3,565 ± 612

°TDM = Total plant dry matter at harvest; FDM = Fruit dry matter at harvest; FFM = Fresh fruit at harvest; WUE = Water use efficiency; IWUE = Irrigation water use efficiency.

Tab. 4 - Yield and economic results of simulation (seasonal analysis over 54 years) of field-tomatoes with the AQUACROP model. The last two columns refer to a variation of water cost equal to ±20% with respect to the cost shown in Table 1.
Tab. 4 - Produzione della simulazione (analisi stagionale di 54 anni) del pomodoro da industria condotta con il modello AQUACROP. Le ultime due colonne si riferiscono alla variazione del costo dell'acqua irrigua pari a ±20% rispetto al costo riportato in Tabella 1.

simulated years. Increasing the water supply by 100 mm, in comparison to *I_170*, produced a notable increase in income (3,422 € ha^{-1}). With a seasonal irrigation volume of 270 mm, it is possible to note a good compromise between saving water and economic gain, even if there were oscillations of 33% in terms of net income during the different growing years (underlined by the high standard deviation (± 1,162 € ha^{-1}).
The greatest net income was obtained with seasonal water amounts of 370 mm, resulting in 4,011 € ha^{-1}, with an annual variability of 18%. Net incomes, slightly lower if compared with *I_370*, were obtained in the *I_470* scenario, with values of 3,745 € ha^{-1}, even if the oscillation was only 729 € ha^{-1} (17%). With irrigation over 470 mm the net income decreased to the same level obtained in the *I_*270 scenario, but with less yearly variability (3420 € ha^{-1}, Fig. 9b).
WD treatments allowed for adequate fresh fruit yield, water saving, a net income comparable with that obtained with irrigation at fixed times, but above all, a stable profitability over the years. In fact, the *WD_30* and *WDS_30* scenarios, requiring 311 and 290 mm of seasonal water respectively, ensured a net income equal to 4,137 and 4,094 € ha^{-1}, respectively, greater than *I_370* by about 100 € ha^{-1}, and with oscillations over the years of less than 200 € ha^{-1} (Fig 8b and Fig. 10b).
All these observations are summarized by the cumulative probability density functions for net income, considering the actual cost of water irrigation. Indeed, Fig. 7b underlines how the probability of obtaining a positive income is more than 80% for *I_170*. The probability curves for the *I_370*, *I_470* and *I_570* scenarios showed a fairly stable net income considering that the average gap between a probability level 50 and 75% is only 273 € ha^{-1}.
From an analisys of probability density functions in *WD* scenarios when compared to fixed turn scenarios, the advantages of the former are clear both in terms of net income (2,400 € ha^{-1} was the lowest simulated income for all scenarios) and stability: considering all *WD* scenarios, the range between the probability level of 50 and 75% is 305 € ha^{-1}, whereas using fixed turns, this range was 512 € ha^{-1} (Fig. 8b).
Evaluating a scenario of changing water costs, a reduction of the cost by 20% provided no benefit in terms of net income in the *I_170* scenario, since the average value remained very close to that with the present cost of water (Fig. 9a); a slight increase of net income was observed in the *I_370* and *I_470* scenarios, resulting in an average increase of 4.6%. In

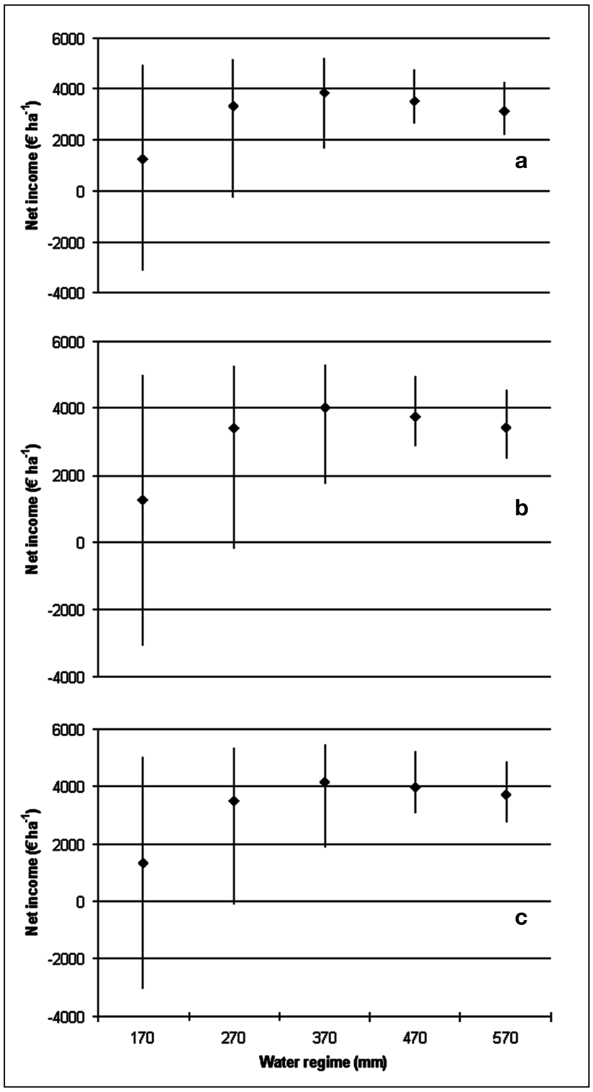

Fig. 9 - Net income for simulated processing tomatoes for fixed time irrigation scenarios, considering an increase of 20% in water cost (a), real water cost (b) in 2010 in Capitanata and a reduction of 20% in water cost (c). The symbols represent average values (54 years), the bars represent the maximum and minimum values.
Fig. 9 - Reddito netto simulato per il pomodoro da industria negli scenari irrigui a turno fisso, considerando un aumento del 20% del costo dell'acqua irrigua (a), il suo costo reale (b) nel 2010 in Capitanata e una sua diminuzione del 20% (c). I simboli rappresentano i valori medi (54 anni), le barre indicano i valori massimi e minimi.

the *I_570* scenario, the net income increased from 3,420 to 3,704 € ha^{-1}. The lowest increase was recorded for *I_270*, since the difference in terms of net income was only 2.2%.
An increase in the cost of water could be adopted as a policy to ensure "water saving", encouranging farmers to reduce the amount of water applied to tomatoes. However, in the case of farmers with water regimes of *I_470* and *I_570*, a reduction in net income of 6% and 8% respectively was noted (Fig. 9c). In *WD* scenarios, the differences in net income as a consequence of variations to the cost of water were limited to a few percentage points (Fig. 10a and 10c), with the greatest difference recorded

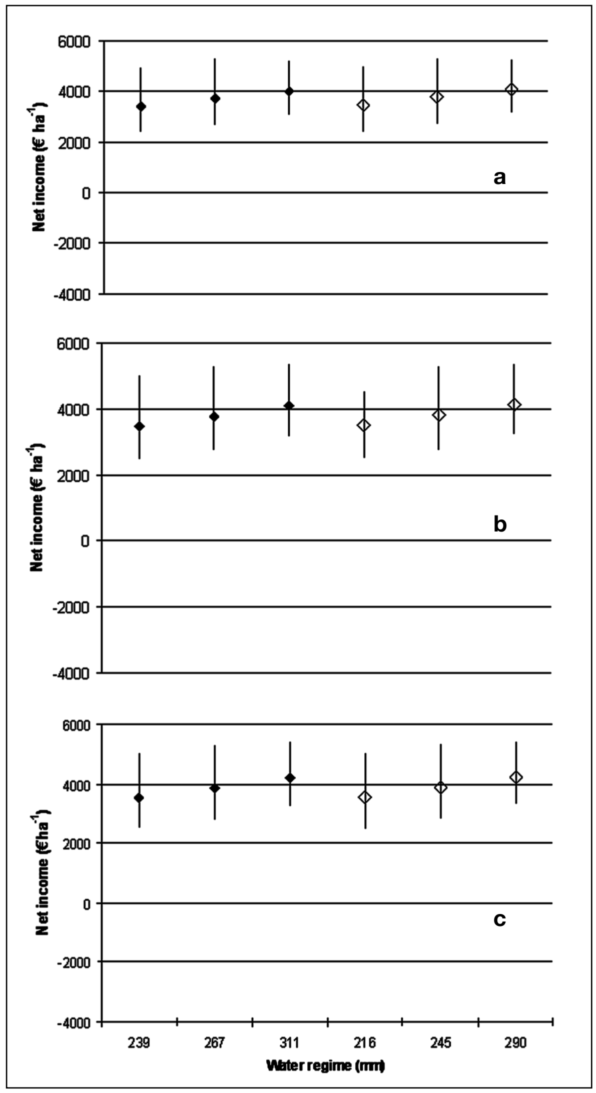

Fig. 10 - Net income for simulated processing tomatoes in soil water depletion scenarios, considering an increase of 20% in water cost (a), real water cost (b) in 2010 in Capitanata and a reduction of 20% in water cost (c). The symbols represent average values (54 years; full rhombus is WD; empty rhombus is WDS), the bars represent the maximum and minimum values.
Fig. 10 - Reddito netto simulato per il pomodoro da industria negli scenari irrigui a ripristino del consumo idrico del suolo, considerando un aumento del 20% del costo dell'acqua irrigua (a), il suo costo reale (b) nel 2010 in Capitanata e una sua diminuzione del 20% (c). I simboli rappresentano i valori medi (54 anni; i rombi pieni sono per gli scenari WD; i rombi vuoti sono per gli scenari WDS), le barre indicano i valori massimi e minimi.

in the *WD_30* scenario (± 2.4%) and the lowest in the *WDS_70* scenario (± 1.6%).

4. CONCLUSIONS

From this study emerged the capability of crop model simulation to support crop management (especially in environments with scarce water availability) in order not only to save water but also to ensure an adequate net income for farmers.

Two principal aims were reached during this study. The first was to obtain, after cross/validation, the tomato crop parameters for AQUACROP in a typical Mediterranean environment, providing average values for the main input required by the model, also suggesting the possible range values that could give a better fit for a wide range of management or climatic conditions. Some of these parameters proved to be more conservative compared to others, especially as regards as crop response to water stress, whereas parameters linked to canopy and crop growth were more sensitive to yearly variability.

The second objective achieved during this study was to find a strategy to optimize irrigation water management based on long-term simulations with AQUACROP.

Irrigation based on fixed times showed some negative aspects; in particular, high yield variability over the years at low irrigation regimes and large amounts of drained water below root zone at high irrigation regimes.

On the other hand, irrigation based on actual soil water content has the important and positive advantages of both increasing net income and, at the same time, using irrigation water in a more sustainable way, taking into account climatic variability and water actually used by the crop, thus preserving this resource and, more generally, natural ecosystems.

Consequently, even if adopting this strategy may set difficulties in any large-scale application due to the cost (soil moisture sensors, automation) and traditional approach of farmers, we believe that it could be the best approach for irrigated agriculture.

Finally, we can conclude that a 20% increase in water costs will not reduce farmers net incomes but will stimulate them to make better use of irrigation water. However, this could be seen more as an opportunity for water distribution organizations to invest in technical support for farmers themselves by changing, for example, irrigation strategies to those based on soil water status rather than at fixed times.

ACKNOWLEDGMENTS

This study was partly supported by the Italian Ministry of Agriculture and Forestry Policies under contracts n. 209/7393/05 and n. 8373/7303/09 (AQUATER Project, Co-ordinator: Dr. M. Rinaldi) and, partly, by the Italian Ministries of Finance and Economy, of Education, University and Research, for the Environment and Territory, of Agricultural, Food and Forestry Policies, contract N. 285 – 20/02/2006 (CLIMESCO Project, Coordinator: Dr. D. Ventrella).

REFERENCES

Allen R.G., Pereira L.S., Raes D., Smith M., 1998. Crop evapotranspiration: Guidelines for computing crop water requirements. Irr & Drain Paper 56. UN-FAO, Rome, Italy, 15 pp.

Bertin N., Gary C., 1993. Tomato fruit-set: a case study for validation of the model TOMGRO. Acta Hortic. 328:185-193.

Castrignanò A., Di Bari V., Stelluti M., 1997. Evapotranspiration predictions of CERES-Sorghum model in Southern Italy. Eur J Agron. 6:265-274.

Cavero J., Plant R.E., Shennan C., Friedman D.B., Williams J.R., Kiniry J.R., Benson V.W., 1999. Modeling nitrogen cycling in tomato-safflower and tomato-wheat rotations. Agr Syst, 60:123-135.

Cavero J., Plant R.E., Shennan C., Friedman D.B., Williams J.R., Kiniry J.R., Benson V.W., 1998. Application of EPIC model to nitrogen cycling in irrigated processing tomato under different management system. Agr Syst, 56:391-414.

Confalonieri R., Bechini L., 2004. A preliminary evaluation of the simulation model CropSyst for alfalfa. Eur JAgron, 21:223-237.

Donatelli M., Stöckle C.O., Ceotto E., Rinaldi M., 1997. Evaluation of CropSyst for cropping systems at two locations of northern and southern Italy. Eur J Agron. 6:35-45.

Doorenbos J., Kassam A.H., 1979. Yield response to water. U.N. Food and Agriculture

Doorenbos J., Pruitt W.O., 1977. Crop water requeriments. Irr & Drain Paper 24. UN-FAO, Rome, Italy.

Elia A., Trotta G., Convertini G., Vonella A.V., Rinaldi M., 2006. Alternative fertilization for processing tomato in Southern Italy. Acta Hortic. 700:261-265.

FAO - UNESCO (1963) Bioclimatic map of the Mediterranean Zone, explanatory notes. Paris, France.

Faostat, 2009. HYPERLINK "http://faostat.fao.org/" http://faostat.fao.org/

Garofalo P., Vonella A.V., Maddaluno C., Rinaldi M., 2011. Verifica dei coefficienti coltrali (kc) su colture erbacee in una pianura del Sud Italia. In: Atti del XIV Convegno Nazionale di Agrometeorologia "Agrometeorologia per l'azienda agraria", Bologna, Giugno 7-9, 17-18.

Garofalo P., Di Paolo E., Rinaldi M., 2009. Durum wheat (Triticum durum Desf.) in rotation with the faba bean (Vicia faba var minor L.). A long-term simulation case-study. Crop Pasture Sci. 60:240-250.

Hartz T.K., 1993. Drip-irrigation scheduling for fresh-market tomato production. Hort Sci. 28:35-37

Imtiyaz M., Mgadla N.P., Chepete B. and Manase S.K., 2000. Response of six vegetable crops to irrigation schedules. Agric Water Manage 45:331-342.

ISTAT, 2009. http://agri.istat.it

Jones P.N., Carberry P.S., 1994. A technique to develop and validate simulation models. HYPERLINK "http://www.sciencedirect.com/science/journal/0308521X" Agr Syst. 46:427-442.

Jones J.W., Dayan E., Allen L.H., Van Keulen H., Challa H., 1991. A dynamic tomato growth and yield model (TOMGRO). Trans ASAE 34:663-672.

Koo J., 2002. Modeling the impacts of climate variability on tomato disease management and production. Ph.D. Thesis. University of Florida, USA, 220 pp.

Leib B.G., Jabro J.D., Matthews G.R., 2003. Field Evaluation and Performance Comparison of Soil Moisture Sensors. Soil Sci. 168:396-408.

Loague K., Green R.E., 1991. Statistical and graphical methods for evaluating solute transport models: overview and application. J Contam Hydrol. 7:51-73.

May D.M., Gonzales L., 1999. Major California processing tomato cultivars respond differently in yield and fruit agricultural quality to various level of moisture stress. Acta Hortic. 487:525-529.

Messina C.D., Jones J.W., Hansen J.W., 2001. Understanding ENSO effects on tomato yields in Florida: a modelling approach. In: Proceedings of the Second International Symposium Modelling Cropping Systems, Florence, Italy, July 16-18, 155-156.

Montheith J.L., 1993. The exchange of water and carbon by crops in a Mediterranean climate. Irrigation Sci. 14:85-91.

Peet M.M., Willits D.H., 1995. Role of excess water in tomato fruit cracking. Hortic Sci. 30:65-68

Pill W.G., Lambeth V.N., 1980. Effects of soil water regime and nitrogen from on blossom-end rot, yield, water relations, and elemental composition of tomato. J Am Soc Hortic Sci. 105:730-734

Priestley C.H.B., Taylor R.J., 1972. On the assessment of surface heat flux and evaporation using large-scale parameters. Mon Weather Rev. 100:81-92.

Raes D., Steduto P., Hsiao T.C., Fereres E., 2009. AQUACROP - The FAO crop model for predicting yield response to water: II. Main algorithms and software description. Agron J. 101:438-447

Ramirez A., Rodriguez F., Berenguel M., Heuvelink E., 2004. Calibration and validation of complex and simplified tomato growth models for control purposes in the southeast of Spain. Acta Hortic. 654:147-154.

Rana G., Rinaldi M., Introna M., Ciciretti L., 2000. Determinazione sperimentale dei consumi idrici del pomodoro da industria in Capitanata. In: Atti Convegno Pom B19. Gutenberg, Salerno, 99-106.

Rinaldi M., Ventrella D., Gagliano C., 2007. Comparison of nitrogen and irrigation strategies in tomato using CROPGRO model. A case study from Southern Italy. Agr Water Manage. 87:91-105.

Rinaldi M., Trotta G., Convertini G., Vonella A.V., Elia A., 2004. Fertilizzanti azotati alternativi su pomodoro da industria. L'Informatore Agrario. 11:65-68.

Rinaldi M., Rana G., 2004. I fabbisogni idrici del pomodoro da industria in Capitanata. Ital J Agrometeorol. 1:31-35.

Rinaldi M., Trotta G., Convertini G., Vonella A.V., Elia A., 2003. Impiego su pomodoro da industria di fertilizzanti azotati alternativi. L'Informatore Agrario 11:75-78.

Rinaldi M., Di Paolo E., Colucci R., Di Lena B., 2001. Validation of EPIC model in simulating tomato field crop in Italian environments. In: Proceedings of the Second International Symposium Modelling Cropping Systems, Florence, Italy, July 16-18, pp. 167-168.

Scholberg J.M.S., Boote K.J., Jones J.W., McNeal B.L., 1997. Adaptation of the CROPGRO model to simulate the growth of field-grown tomato. In M.J. Kropff, et al. (ed.) System Approaches for Agricultural Development: Application of Systems Approaches at the Field Level. Kluwer Academic Publishers, Dordrecht, The Netherlands, pp. 133-151.

Steduto P., Hsiao T.C., Fereres E., 2007. On the conservative behaviour of biomass water productivity. Irrig Sci. 25:89-207.

Steduto P., Hsiao T.C., Raes D., Fereres E., 2009. AQUACROP - The FAO Crop Model to Simulate Yield Response to Water: I. Concepts and Underlying Principles. Agron J. 101:426-437.

Steduto P., Albrizio R., 2005. Resource use efficiency of field grown sunflower, sorghum, wheat and chickpea. II. Water use efficiency and comparison with radiation use efficiency. Agr Forest Meteorol. 130:269-281.

USDA (2006) 'Keys to Soil Taxonomy.' 10th edn, pp. 333. Available at: ftp://ftp-fc.sc.egov.usda.gov/NSSC/Soil_Taxonomy/keys/keys.pdf.

Waister P.D., Hudson J.P., 1970. Effects of soil moisture regimes on leaf water deficit, transplantation and yield of tomatoes. Hort Sci. 45:359-370.